

Triangular-Reference Schrödinger Bridges for Time Series Generation

Gabriele Bocchi*

Abstract

We introduce *Triangular-Reference Schrödinger Bridges for Time Series (TR-SBTS)*, a conservative extension of the SBTS framework in which the Brownian reference is replaced by an intervalwise frozen, possibly degenerate diffusion reference, triangular across a hierarchy of latent volatility levels. The construction is a single entropy projection on the augmented state space, with the variational constraint imposed jointly across time and the latent levels and unfolded hierarchically by the disintegration of relative entropy. The variational core of SBTS is preserved: the entropy minimiser is the h -transform of the reference, and on each frozen interval the optimal dynamics admit a logarithmic-gradient drift formula on the affine leaves of the active covariance directions, valid even when the frozen covariance is rank-deficient. We establish stability of the frozen approximation and convergence of the corresponding regularised kernel estimators. The construction is realised through a finite-dimensional conditioning map assembled from three complementary reductions of the past—a block PCR summary, a reference-aware Mahalanobis kernel on past increments induced by the runtime frozen covariance cumulants, and a past-window WLS drift regressor under the same reference metric—together with a coupled state-covariance bridge step in which each latent level produces a dynamic reference for the level above, summarised by a covariance descriptor; the construction is evaluated on numerical experiments.

1 Introduction

The generation of realistic synthetic time series is a central problem in modern data-driven modelling. Sequential data appear in finance, energy, climate, health care, audio and video processing, and many other domains in

**Arakne S.r.l., Roma.* E-mail: gabriele.bocchi@arakne.it.

which one wants to reproduce not only static distributions, but also temporal dependence, cross-sectional dependence, and pathwise variability. In finance, synthetic trajectories are used for stress testing, risk measurement, scenario generation, data augmentation, and the assessment of downstream decision rules, including hedging and forecasting procedures. These applications are particularly demanding: a useful generator should reproduce marginal laws, dependence across time, correlation across components, volatility clustering, tail behaviour, and, when relevant, abrupt regime changes.

Classical parametric models provide interpretable dynamics, but their calibration can be delicate and the resulting synthetic paths are exposed to model misspecification. This has motivated the development of data-driven generative models. General-purpose generative modelling includes likelihood-based models, variational autoencoders, normalising flows, generative adversarial networks, score-based models, diffusion models, and optimal-transport-based approaches; see, among many others, [13, 3, 19, 17, 23, 16, 4]. For time series, additional structure is needed: matching one-time marginals, or even a static joint distribution, is not enough if the sequential and causal structure is lost. This has led to specialised architectures and metrics, including TimeGAN [26], QuantGAN [24], COT-GAN [25], conditional-loss Euler generators [18], signature-based methods [5, 8], and neural-SDE or functional-data approaches [9].

Schrödinger bridge methods provide a particularly natural framework for this problem. The classical Schrödinger bridge problem seeks the probability law on path space which is closest, in relative entropy, to a reference path measure while satisfying prescribed marginal constraints. It can be viewed as an entropic version of optimal transport and, in diffusion settings, it admits a stochastic-control interpretation: the optimal law is obtained by adding a drift to the reference dynamics, with the energy of the control measured by relative entropy. This point of view combines probabilistic structure, variational interpretability, and a constructive generative mechanism. It is also connected to computational approaches based on entropic optimal transport, Sinkhorn-type algorithms, iterative proportional fitting, and more recent Schrödinger-bridge matching methods; see for instance [21, 11, 12, 7, 4, 6, 14].

The Schrödinger Bridge for Time Series (SBTS) framework introduced in [15] adapts this idea to sequential data. Instead of imposing only two endpoint marginals, SBTS constrains the full joint law of the observations on a fixed time grid. Starting from a Brownian reference, it searches for the path measure closest to the reference law, in relative entropy, whose finite-dimensional distribution at the observation dates matches the empirical time-series law. The minimiser is a controlled diffusion with path-dependent

drift. This drift can be represented through backward Schrödinger potentials and estimated from data by kernel regression or neural methods. In this way, SBTS directly targets the joint time-series distribution while still producing a continuous-time interpolation between observed dates.

Subsequent works have clarified both the empirical strengths and the limitations of this approach. The systematic evaluation in [1] benchmarks SBTS against state-of-the-art time-series generators and studies its performance through metrics designed to test marginal fidelity, temporal dependence, and statistical robustness. These results support SBTS as a competitive and robust time-series generator, but they also point to practical issues that become important in longer or higher-dimensional settings: kernel bandwidth selection, conditioning dimension, hyperparameter calibration, and the fact that the Brownian reference imposes a fixed quadratic variation. The last point is especially relevant for financial time series, where stochastic volatility, rank-deficient covariance structures, and correlated noise are part of the phenomenon one wants to reproduce rather than secondary modelling details.

Two recent developments address these limitations in different directions. The jump-diffusion extension of [22] replaces the purely continuous Brownian reference by a reference process with a compound Poisson component. The corresponding bridge is formulated on càdlàg path space and learns both a drift and a jump intensity, allowing the generated paths to capture heavy tails, abrupt moves, and regime changes. A different and complementary development is the Schrödinger–Bass Bridge for Time Series (SBBTS) of [2]. It extends the Schrödinger–Bass framework from a two-marginal setting to full time-series distributions and optimises jointly over drift and volatility. This gives a powerful framework for learning stochastic volatility and correlation structures that cannot be captured by a Brownian-reference SBTS model.

The present work follows a conservative extension of SBTS: the relative-entropy backbone of SBTS is preserved and the reference law is modified. The Brownian reference on the observed process is replaced by an adapted triangular reference on an augmented state

$$Z = (Z^0, Z^1, \dots, Z^L),$$

where Z^0 denotes the principal time series, such as prices or returns, and the lower components Z^1, \dots, Z^L represent volatility or covariance descriptors constructed on the coarse observation grid.

The resulting model is still an SBTS model in its variational core. Given the joint coarse-grid law

$$\mu = \mathcal{L}(Z_{t_0}, \dots, Z_{t_N}),$$

we look for the path law closest in relative entropy to the reference while matching this joint law. The constraint is therefore joint both across time and across the augmented levels. The novelty lies in the reference: on each coarse interval $(t_i, t_{i+1}]$, its transition kernels are adapted to the common coarse past

$$\mathcal{G}_i := \sigma(Z_{t_0}, \dots, Z_{t_i})$$

and triangular across the levels. After ordering the components from the deepest volatility descriptor to the observed process, each level is generated conditionally on the common past and on the lower-level components already constructed.

This triangular structure is not a separation of the target constraint into independent marginal problems. The target remains the joint law of the whole augmented vector. Rather, the chain rule for relative entropy gives a conditional representation of the joint entropy cost. In the simplest two-level notation,

$$H(P^{X,Y} | R^{X,Y}) = H(P^Y | R^Y) + \mathbb{E}_{P^Y} [H(P^{X|Y} | R^{X|Y})].$$

Thus the augmented bridge can be read, and implemented, in a bottom-up way: one starts from a deepest descriptor for which a stable reference is available, then constructs each higher component conditionally on the common past and on the lower-level environment. The final price bridge is the top component of this single augmented entropy projection.

Conditionally on the coarse past and on the lower-level descriptors, the reference dynamics on each interval are frozen Gaussian martingales, possibly with degenerate covariance. Equivalently, the reference is obtained by concatenating Gaussian transition kernels on the affine leaves generated by the active covariance directions. This keeps the model explicit while allowing the reference covariance to encode volatility information learned from high-frequency data or supplied by an auxiliary procedure. In this sense, high-frequency observations are not used to refine the output grid itself; they are used to enrich the coarse-grid state by adding realised covariance and higher-order volatility descriptors.

We call the resulting problem the Triangular-Reference Schrödinger Bridge for Time Series, abbreviated TR-SBTS. Under the finite-entropy condition

$$\mu \ll \mu_T^R, \quad H(\mu | \mu_T^R) < \infty,$$

where μ_T^R is the coarse-grid law induced by the triangular reference, the

entropy minimiser is the usual h -transform

$$\frac{dP^*}{dR} = \frac{d\mu}{d\mu_T^R}(Z_{t_0}, \dots, Z_{t_N}),$$

and the value of the problem is $H(\mu \mid \mu_T^R)$. Locally, on each frozen interval, the optimal dynamics are described by backward heat potentials on the corresponding affine diffusive leaf. This yields the degenerate analogue of the classical SBTS heat-drift formula.

A second point developed in the paper is the relation between the frozen reference and an underlying continuous-time formulation, in which the latent volatility varies continuously: refining the volatility grid recovers this continuous limit, with the approximation error expressed at the level of cumulative covariances on the active diffusive leaf. Consistency along refining grids follows from finite entropy of the constraint with respect to the triangular reference, together with continuity of the latent covariance descriptors.

The statistical part of the paper studies how the local conditional objects entering the heat potentials can be estimated from data, using regularised kernel estimators and finite-dimensional causal summaries of the past. We prove rigorous convergence of the resulting estimators for the heat potentials, the drifts, and the induced transition kernels, providing explicit consistency guarantees for the full approximation chain.

At the numerical level, the conditioning past is reduced to a finite-dimensional summary via three complementary strategies. The first is block PCR, projecting positions and increments onto the empirical active directions of the observed paths. The second is the reference-aware local Mahalanobis kernel on past increments induced at runtime by the frozen covariance cumulants, a second-moment statistic that compares each historical increment to its runtime counterpart in the reference geometry. The third is a past-window WLS drift regressor under the same reference metric, producing a fixed-dimensional first-order summary of the trend over the past window whose output dimension does not grow with the memory length. Combined with a strong present anchor in normalised coordinates, these reductions yield a three-estimator architecture (present anchor, past-drift regressor, present/near-future volatility descriptor) that has proved stable and reliable in practice. The effective projection dimensions and memory lengths are selected by statistical validation, keeping each reduction data-driven; separate reductions for position-type and increment-type variables provide a more flexible, cylinder-like representation than a single global linear subspace. The construction is then evaluated on numerical experiments (Section 6).

The paper is organised as follows. Section 2 formulates the SBTS entropy projection at the level of an arbitrary reference law and proves the variational identification of the minimiser. Section 3 specialises this projection to the intervalwise frozen Gaussian reference, derives the local backward representation on possibly degenerate affine leaves and the corresponding logarithmic-gradient drift formula, and records (in Subsection 3.2) the sense in which this reference is itself an approximation of an ideal volatility-informed reference, proves the corresponding cumulant-based stability result, and exposes the joint and hierarchical structure inherent in the construction. Section 4 develops the statistical approximation of the backward potentials and proves convergence of the estimated drifts. Section 5 describes the implementation: finite-dimensional conditioning variables, the three complementary reductions of the past (block PCR, reference-aware Mahalanobis kernel, past-window WLS drift regressor), empirical kernel weights, the covariance-descriptor database, and the coupled state–covariance generation pipeline. Section 6 reports the numerical experiments used to evaluate the construction. Appendix A contains the detailed proof of the statistical approximation theorem. Appendix B describes the predictive scoring procedure used for validation.

2 Reference-based SBTS entropy projection

We first isolate the basic variational block used in the sequel: the entropy minimisation on path space under a finite-dimensional constraint at the observation times, with respect to an arbitrary reference law. The result is purely variational and requires almost no structure of the reference. The only standing assumption is that the constraint has finite relative entropy with respect to the reference grid law. Specific instantiations of this block, in particular the triangular intervalwise frozen Gaussian reference that supports the hierarchical construction described in the introduction and that is used to extract explicit drift formulas in the remainder of the paper, are obtained by specialising the choice of reference.

Let

$$0 = t_0 < t_1 < \dots < t_N = T, \quad \Omega := C([0, T]; \mathbb{R}^d),$$

and let $X = (X_t)_{0 \leq t \leq T}$ be the canonical process on Ω , with canonical filtration $\mathcal{F} = (\mathcal{F}_t)_{0 \leq t \leq T}$. We denote by

$$\Pi : \Omega \rightarrow (\mathbb{R}^d)^{N+1}, \quad \Pi(\omega) := (X_{t_0}(\omega), \dots, X_{t_N}(\omega))$$

the observation map at the coarse times.

Let $R \in \mathcal{P}(\Omega)$ be an arbitrary reference probability law on path space, and denote by

$$\mu_T^R := R \circ \Pi^{-1}$$

its joint law on the coarse grid. Let $\mu \in \mathcal{P}((\mathbb{R}^d)^{N+1})$ be a target law on the same grid, and assume

$$\mu \ll \mu_T^R, \quad H(\mu \mid \mu_T^R) < \infty. \quad (1)$$

We refer to the entropy minimisation problem

$$V(\mu) := \inf \left\{ H(P \mid R) : P \in \mathcal{P}(\Omega), P \circ \Pi^{-1} = \mu \right\} \quad (2)$$

as the *reference-based SBTS entropy projection* associated with the reference R and the constraint μ . The following theorem identifies its value and unique minimiser in closed form, under no structural assumption on R beyond (1).

Theorem 1 (Variational identification of the entropy projection). *Under assumption (1), set*

$$G := \frac{d\mu}{d\mu_T^R}.$$

Then the following statements hold.

(i) *The value of problem (2) is*

$$V(\mu) = H(\mu \mid \mu_T^R).$$

(ii) *There exists a unique minimiser $P^* \in \mathcal{P}(\Omega)$, given by the h-transform*

$$\frac{dP^*}{dR} = G(\Pi), \quad P^* \circ \Pi^{-1} = \mu.$$

(iii) *The density process of P^* with respect to R is the positive R -martingale*

$$M_t := E_R[G(\Pi) \mid \mathcal{F}_t], \quad 0 \leq t \leq T,$$

so that $M_T = dP^/dR$ and $P^* = M_T R$.*

Proof. Set

$$G := \frac{d\mu}{d\mu_T^R}, \quad P^* := G(\Pi) R.$$

Since $E_R[G(\Pi)] = 1$, the measure P^* is well defined. For every bounded measurable $\varphi : (\mathbb{R}^d)^{N+1} \rightarrow \mathbb{R}$,

$$E_{P^*}[\varphi(\Pi)] = E_R[G(\Pi)\varphi(\Pi)] = \int_{(\mathbb{R}^d)^{N+1}} \varphi(\mathbf{x}) \mu(d\mathbf{x}),$$

hence $P^* \circ \Pi^{-1} = \mu$, so P^* is feasible. Moreover,

$$H(P^* | R) = E_R[G(\Pi) \log G(\Pi)] = H(\mu | \mu_T^R),$$

so

$$V(\mu) \leq H(\mu | \mu_T^R).$$

Now let P be any feasible probability measure. If $H(P | R) = \infty$, there is nothing to prove. Assume then that $H(P | R) < \infty$, and write

$$L := \frac{dP}{dR}.$$

Since $P \circ \Pi^{-1} = \mu$, one has

$$E_P[\log G(\Pi)] = \int_{(\mathbb{R}^d)^{N+1}} \log G(\mathbf{x}) \mu(d\mathbf{x}) = H(\mu | \mu_T^R),$$

and

$$E_P[\log L] = H(P | R).$$

Finally,

$$1 = E_R[G(\Pi)] = E_P\left[\frac{G(\Pi)}{L}\right] = E_P[\exp(\log G(\Pi) - \log L)].$$

By Jensen's inequality,

$$1 \geq \exp(E_P[\log G(\Pi) - \log L]) = \exp\left(H(\mu | \mu_T^R) - H(P | R)\right),$$

and therefore $H(P | R) \geq H(\mu | \mu_T^R)$. This proves $V(\mu) = H(\mu | \mu_T^R)$. If equality holds, then equality holds in Jensen's inequality. Since the exponential function is strictly convex, there exists a constant $c \in \mathbb{R}$ such that

$$\log G(\Pi) - \log L = c \quad P\text{-a.s.}$$

Taking expectation under P , and using the equality of the two entropies, yields $c = 0$. Hence $L = G(\Pi)$ P -a.s. and $P = P^*$, proving uniqueness. The martingale representation in (iii) is immediate from the definition $M_t = E_R[G(\Pi) | \mathcal{F}_t]$. \square

Remark 2 (Controlled-diffusion form under Léonard’s condition (U)). *Theorem 1* requires no regularity of R beyond a measurable structure on path space; the optimal law is identified abstractly as an h -transform. When the reference additionally satisfies the uniqueness condition (U) of Léonard [20], the optimal law P^* admits an explicit semimartingale description: it is a controlled diffusion with respect to the predictable bracket of R , and there exists an adapted process β^* defined P^* -a.s. such that

$$P^* \in MP(\widehat{B}^*, A), \quad \widehat{B}_t^* := \int_{[0,t]} A(ds) \beta_s^*,$$

where A denotes the predictable R -bracket of the canonical process. Moreover the relative entropy splits as

$$H(P^* | R) = H(P_0^* | R_0) + \frac{1}{2} E_{P^*} \left[\int_{[0,T]} \beta_t^* \cdot A(dt) \beta_t^* \right],$$

where $P_0^* := P^* \circ X_0^{-1}$ and $R_0 := R \circ X_0^{-1}$. This follows from Theorems 2.1 and 2.3 of [20] applied to the pair (P^*, R) with zero reference drift. We use this representation only from Section 3 onward, to extract the explicit local drift on each frozen interval.

Remark 3 (Triangular references satisfy condition (U)). *The hierarchical, triangular reference described in the introduction and deployed in the rest of the paper falls within the class covered by Remark 2. On each coarse interval the reference is Gaussian conditional on the coarse past and on the latent volatility level, and the latent level is itself, recursively, the output of a reference whose conditional density depends only on its own lower-level environment. As long as the maps that translate latent levels into intervalwise covariances are deterministic, the joint reference density factorises into a finite product of explicit conditional Gaussians. The associated stochastic integrals are then finite and explicitly computable, and condition (U) of [20] is satisfied. The explicit drift identification of Section 3 is built on this representation.*

3 Exact intervalwise dynamics and drift formula

Theorem 1 identifies the minimiser abstractly as an h -transform of the reference law. From this point onward we work with the specific instantiation alluded to in Remark 3: a reference that is intervalwise frozen Gaussian along the coarse grid, possibly with degenerate covariances. Conditionally

on a realisation y of the latent volatility environment Y of Section 3.2 below, the frozen intervalwise covariances are deterministic; the entire description that follows is to be read as conditioned on (X_0, \dots, X_{t_N}, y) , i.e. on the past path and on the latent realisation that fixed the intervalwise references. We collect the corresponding setup here.

Intervalwise frozen Gaussian reference. Let $m_0 \in \mathcal{P}(\mathbb{R}^d)$, and for each $i = 0, \dots, N - 1$, let

$$\sigma_i : (\mathbb{R}^d)^{i+1} \times \mathcal{Y} \rightarrow \mathbb{R}^{d \times d}$$

be a Borel map, where \mathcal{Y} is the latent state space of Section 3.2. For $\mathbf{x}_i = (x_0, x_1, \dots, x_i) \in (\mathbb{R}^d)^{i+1}$ and a latent realisation $y_{i+1} \in \mathcal{Y}$ that determines the intervalwise reference on $(t_i, t_{i+1}]$, set

$$a_i(\mathbf{x}_i, y_{i+1}) := \sigma_i(\mathbf{x}_i, y_{i+1})\sigma_i(\mathbf{x}_i, y_{i+1})^\top \in \mathbb{S}_+^d.$$

We consider the reference law $R \in \mathcal{P}(\Omega)$ under which $X_0 \sim m_0$ and, for each $i = 0, \dots, N - 1$, conditionally on $(X_0, X_{t_1}, \dots, X_{t_i}, y_{i+1})$ the process on $(t_i, t_{i+1}]$ evolves as

$$dX_t = \sigma_i(X_0, X_{t_1}, \dots, X_{t_i}, y_{i+1}) dW_t^R, \quad t \in (t_i, t_{i+1}],$$

for some Brownian motion W^R . Equivalently, X is an R -martingale with predictable bracket

$$[X, X](dt) = A(dt), \quad A(dt) = a_i(X_0, X_{t_1}, \dots, X_{t_i}, y_{i+1}) dt \quad \text{on } (t_i, t_{i+1}].$$

The reference R is explicitly obtained by concatenating the Gaussian transition kernels associated with these frozen intervalwise diffusions, conditioned on the latent realisations $(y_{i+1})_{i=0}^{N-1}$. In particular, R satisfies condition (U) of Léonard [20] conditionally on the latent realisation, so that Remark 2 applies and the optimal law P^* of Theorem 1 admits an adapted drift correction β^* with respect to the predictable bracket A . The conditioning on the future latent value y_{i+1} is consistent because that value has already been realised in the triangular construction (the lower latent layer is generated first and then fed upstream); from the point of view of the upper-layer entropic problem on $(t_i, t_{i+1}]$, y_{i+1} is a known parameter of the intervalwise reference. We assume throughout this section that the target law $\mu \in \mathcal{P}((\mathbb{R}^d)^{N+1})$ has first marginal m_0 and satisfies the finite-entropy condition (1) conditionally on the latent realisation. The remainder of this section localises the description of β^* on a single frozen interval and extracts a closed-form drift formula whose logarithmic-gradient structure is read off from the corresponding backward heat potential.

3.1 Intervalwise backward representation on frozen diffusive leaves

We now turn to the second step of the exact backbone, namely the backward intervalwise structure. Remark 2 only guarantees the existence of an intrinsic drift correction for the optimal law under condition (U), without identifying it explicitly. The purpose of the next lemma is to extract this correction in closed form on a single frozen interval, under a simplified reference law with fixed diffusion coefficient.

Before stating the result, we introduce the intrinsic geometry associated with a frozen degenerate diffusion.

Let $A \in \mathbb{S}_+^d$, let

$$r := \text{rank}(A), \quad \lambda_1, \dots, \lambda_r > 0, \quad q_1, \dots, q_r \in \mathbb{R}^d$$

be the strictly positive eigenvalues of A and associated orthonormal eigenvectors, and set

$$E_A := \text{Span}\{q_1, \dots, q_r\}.$$

For every $x \in \mathbb{R}^d$, we define the *affine diffusive leaf through x* by

$$\mathcal{L}_A^x := x + E_A.$$

This is the affine subspace on which a diffusion with covariance matrix A , started from x , evolves.

We denote by ℓ_A^x the canonical Lebesgue measure on \mathcal{L}_A^x , defined as the push-forward of the Lebesgue measure on \mathbb{R}^r under the map

$$\Xi_x : \mathbb{R}^r \rightarrow \mathcal{L}_A^x, \quad \Xi_x(\xi) := x + \sum_{i=1}^r \xi_i q_i.$$

Equivalently, for every nonnegative Borel function φ on \mathcal{L}_A^x ,

$$\int_{\mathcal{L}_A^x} \varphi(z) d\ell_A^x(z) = \int_{\mathbb{R}^r} \varphi\left(x + \sum_{i=1}^r \xi_i q_i\right) d\xi.$$

Since A is invertible on E_A , we denote by

$$A_{E_A}^{-1} : E_A \rightarrow E_A$$

the inverse of the restriction of A to E_A . Explicitly,

$$A_{E_A}^{-1} v = \sum_{i=1}^r \lambda_i^{-1} \langle v, q_i \rangle q_i, \quad v \in E_A.$$

For $S \leq t < T$ and $y, z \in \mathcal{L}_A^x$, we define the intrinsic heat kernel associated with A by

$$p_A(t, y; T, z) := \frac{1}{(2\pi(T-t))^{r/2} \prod_{i=1}^r \lambda_i^{1/2}} \times \exp\left(-\frac{1}{2(T-t)} \langle A_{E_A}^{-1}(z-y), z-y \rangle\right).$$

Equivalently,

$$p_A(t, y; T, z) = \frac{1}{(2\pi(T-t))^{r/2}} \prod_{i=1}^r \lambda_i^{-1/2} \exp\left(-\frac{1}{2(T-t)} \sum_{i=1}^r \frac{\langle z-y, q_i \rangle^2}{\lambda_i}\right).$$

Given a nonnegative Borel function $g : \mathcal{L}_A^x \rightarrow [0, \infty]$, we define its backward heat propagation by

$$(P_{t,T}^A g)(y) := \int_{\mathcal{L}_A^x} p_A(t, y; T, z) g(z) d\ell_A^x(z), \quad (t, y) \in [S, T) \times \mathcal{L}_A^x,$$

whenever the integral is finite.

We say that a nonnegative Borel function $g : \mathcal{L}_A^x \rightarrow [0, \infty]$ is (A, S, T, x) -admissible if

$$(P_{t,T}^A g)(y) < \infty \quad \forall (t, y) \in [S, T) \times \mathcal{L}_A^x. \quad (3)$$

We also denote by $\mathcal{M}_+^{\text{loc}}(\mathcal{L}_A^x)$ the cone of positive Radon measures on \mathcal{L}_A^x , that is, positive locally finite Borel measures on \mathcal{L}_A^x . Whenever convenient, such measures are identified with Borel measures on \mathbb{R}^d supported on \mathcal{L}_A^x , by extension by zero outside \mathcal{L}_A^x .

Lemma 4 (Controlled diffusion induced by a terminal martingale density on one frozen interval). *Let $0 \leq S < T$, let $x \in \mathbb{R}^d$, and let*

$$(\Omega, \mathcal{G}, (\mathcal{G}_t)_{t \in [S, T]}, \mathbb{Q})$$

support a d -dimensional Brownian motion W . Let $\sigma \in \mathbb{R}^{d \times d}$, set

$$A := \sigma \sigma^\top \in \mathbb{S}_+^d, \quad X_t := x + \sigma(W_t - W_S), \quad t \in [S, T].$$

Let $r := \text{rank}(A) \geq 1$, and let $q_1, \dots, q_r \in \mathbb{R}^d$ be orthonormal eigenvectors of A associated with its strictly positive eigenvalues $\lambda_1, \dots, \lambda_r > 0$.

Let

$$f : \mathcal{L}_A^x \rightarrow [0, \infty]$$

be a Borel measurable function, identified throughout with its extension by zero outside \mathcal{L}_A^x . Assume that

$$\mathbb{E}_{\mathbb{Q}}[f(X_T)] = 1,$$

and that f is (A, S, T, x) -admissible.

Define the martingale probability \mathbb{Q}^f on (Ω, \mathcal{G}_T) by

$$\frac{d\mathbb{Q}^f}{d\mathbb{Q}} := f(X_T),$$

and define

$$H_t := \mathbb{E}_{\mathbb{Q}}[f(X_T) \mid \mathcal{G}_t], \quad t \in [S, T].$$

Then there exists a unique Borel function

$$h : [S, T] \times \mathcal{L}_A^x \rightarrow [0, \infty]$$

such that, for every $t \in [S, T]$,

$$H_t = h(t, X_t) \quad \mathbb{Q}\text{-a.s.}$$

More precisely,

$$h(t, y) = (P_{t,T}^A f)(y) = \int_{\mathcal{L}_A^x} p_A(t, y; T, z) f(z) d\ell_A^x(z), \quad (t, y) \in (S, T) \times \mathcal{L}_A^x.$$

Moreover, the following hold.

(i) The function h is C^1 in time on (S, T) , and C^∞ along the diffusive directions q_1, \dots, q_r on $(S, T) \times \mathcal{L}_A^x$. It satisfies

$$\partial_t h(t, y) + \frac{1}{2} \sum_{i=1}^r \lambda_i D_{q_i q_i}^2 h(t, y) = 0, \quad (t, y) \in (S, T) \times \mathcal{L}_A^x.$$

Furthermore, the map

$$[S, T] \ni t \longmapsto \mu_t \in \mathcal{M}_+^{\text{loc}}(\mathcal{L}_A^x),$$

defined by

$$\mu_t := h(t, \cdot) \ell_A^x \quad \text{for } t \in [S, T), \quad \mu_T := f(\cdot) \ell_A^x,$$

is continuous. Equivalently, the terminal condition is attained as

$$h(T, \cdot) \ell_A^x = f(\cdot) \ell_A^x \quad \text{in } \mathcal{M}_+^{\text{loc}}(\mathcal{L}_A^x).$$

Finally,

$$h(t, y) > 0 \quad \forall (t, y) \in (S, T) \times \mathcal{L}_A^x.$$

(ii) There exists a d -dimensional \mathbb{Q}^f -Brownian motion W^f such that

$$dX_t = b_t^f dt + \sigma dW_t^f, \quad t \in [S, T],$$

where

$$b_t^f = \sum_{i=1}^r \lambda_i D_{q_i} \log h(t, X_t) q_i, \quad dt \otimes \mathbb{Q}^f\text{-a.e.}$$

Proof. Let $Q = (Q_r, Q_0)$ be an orthogonal matrix whose first r columns are q_1, \dots, q_r , so that

$$Q^\top A Q = \begin{pmatrix} \Lambda_r & 0 \\ 0 & 0 \end{pmatrix}, \quad \Lambda_r := \text{diag}(\lambda_1, \dots, \lambda_r).$$

Let

$$\eta_0 := Q_0^\top x \in \mathbb{R}^{d-r},$$

so that

$$\mathcal{L}_A^x = \{Q_r \xi + Q_0 \eta_0 : \xi \in \mathbb{R}^r\}.$$

Since

$$Q_0^\top A Q_0 = 0,$$

we have $Q_0^\top \sigma = 0$. Hence, for every $t \in [S, T]$,

$$Q_0^\top X_t = Q_0^\top x + Q_0^\top \sigma (W_t - W_S) = \eta_0,$$

so that

$$X_t \in \mathcal{L}_A^x \quad \mathbb{Q}\text{-a.s.}$$

for every $t \in [S, T]$. In particular, since f is supported on \mathcal{L}_A^x , the random variable $f(X_T)$ is well defined.

Define

$$h(t, y) := \mathbb{E}_{\mathbb{Q}}[f(y + \sigma(W_T - W_t))], \quad (t, y) \in [S, T] \times \mathcal{L}_A^x.$$

Since $y \in \mathcal{L}_A^x$ and $\sigma(W_T - W_t) \in E_A$, the point $y + \sigma(W_T - W_t)$ belongs to \mathcal{L}_A^x \mathbb{Q} -a.s. By (A, S, T, x) -admissibility of f ,

$$h(t, y) = \int_{\mathcal{L}_A^x} p_A(t, y; T, z) f(z) d\ell_A^x(z) < \infty \quad \forall (t, y) \in [S, T] \times \mathcal{L}_A^x.$$

Since

$$X_T = X_t + \sigma(W_T - W_t),$$

and $W_T - W_t$ is independent of \mathcal{G}_t , we obtain for every $t \in [S, T)$,

$$+\infty > H_t = \mathbb{E}_{\mathbb{Q}}[f(X_T) \mid \mathcal{G}_t] = \mathbb{E}_{\mathbb{Q}}[f(X_t + \sigma(W_T - W_t)) \mid \mathcal{G}_t] = h(t, X_t),$$

which gives the required representation.

We now study the regularity of h . For

$$y = Q_r \xi + Q_0 \eta_0 \in \mathcal{L}_A^x,$$

define

$$U(t, \xi) := h(t, Q_r \xi + Q_0 \eta_0), \quad (t, \xi) \in [S, T) \times \mathbb{R}^r.$$

Then

$$U(t, \xi) = \mathbb{E}_{\mathbb{Q}}[f(Q_r \xi + Q_0 \eta_0 + \sigma(W_T - W_t))].$$

Since only the Q_r -coordinates are diffusive, U is the classical nondegenerate heat semigroup in \mathbb{R}^r applied to the terminal datum

$$\xi \longmapsto f(Q_r \xi + Q_0 \eta_0).$$

Therefore,

$$U \in C^{1, \infty}([S, T) \times \mathbb{R}^r),$$

and U is the unique classical solution on $[S, T) \times \mathbb{R}^r$ of

$$\partial_t U(t, \xi) + \frac{1}{2} \sum_{i=1}^r \lambda_i \partial_{\xi_i \xi_i} U(t, \xi) = 0, \quad (t, \xi) \in [S, T) \times \mathbb{R}^r,$$

whose associated measure-valued path

$$\nu_t := U(t, \cdot) d\xi, \quad t \in [S, T),$$

extends continuously to $t = T$ in $\mathcal{M}_+^{\text{loc}}(\mathbb{R}^r)$ with terminal value

$$\nu_T = f(Q_r \cdot + Q_0 \eta_0) d\xi.$$

Translating back to the affine leaf \mathcal{L}_A^x , we obtain that h is C^1 in time on (S, T) , C^∞ along the diffusive directions q_1, \dots, q_r , and satisfies

$$\partial_t h(t, y) + \frac{1}{2} \sum_{i=1}^r \lambda_i D_{q_i q_i}^2 h(t, y) = 0, \quad (t, y) \in [S, T) \times \mathcal{L}_A^x.$$

Now define, for $t \in [S, T)$,

$$\mu_t := h(t, \cdot) \ell_A^x, \quad \mu_T := f(\cdot) \ell_A^x.$$

Since ℓ_A^x is the push-forward of the Lebesgue measure on \mathbb{R}^r under the affine map

$$\Xi_x(\xi) := Q_r \xi + Q_0 \eta_0,$$

we have

$$\mu_t = (\Xi_x)_\# \nu_t, \quad t \in [S, T].$$

Hence,

$$t \longmapsto \mu_t$$

belongs to $C([S, T]; \mathcal{M}_+^{\text{loc}}(\mathcal{L}_A^x))$, and this is precisely the terminal condition

$$h(T, \cdot) \ell_A^x = f(\cdot) \ell_A^x \quad \text{in } \mathcal{M}_+^{\text{loc}}(\mathcal{L}_A^x).$$

Uniqueness of h within the class stated in the lemma follows from the uniqueness of U for the corresponding nondegenerate backward heat problem on \mathbb{R}^r .

Moreover, for every $t \in [S, T]$,

$$\mathbb{Q}^f(H_t = 0) = \mathbb{E}_{\mathbb{Q}}[f(X_T) \mathbf{1}_{\{H_t=0\}}] = \mathbb{E}_{\mathbb{Q}}[H_t \mathbf{1}_{\{H_t=0\}}] = 0.$$

Therefore,

$$\int_S^T \mathbb{Q}^f(H_t = 0) dt = 0,$$

and since $H_t = h(t, X_t)$, this yields

$$h(t, X_t) > 0 \quad dt \otimes \mathbb{Q}^f\text{-a.s.}$$

Moreover, since $p_A(t, y; T, z) > 0$ for every $t < T$ and every $y, z \in \mathcal{L}_A^x$, and since

$$\int_{\mathcal{L}_A^x} f(z) p_A(S, x; T, z) d\ell_A^x(z) = 1,$$

the terminal datum is not identically zero. Hence

$$h(t, y) > 0 \quad \forall (t, y) \in (S, T) \times \mathcal{L}_A^x.$$

This proves (i).

We now prove (ii). Set

$$Z_t := Q_r^\top X_t \in \mathbb{R}^r, \quad t \in [S, T].$$

Since $Q_0^\top X_t = \eta_0$, we have

$$X_t = Q_r Z_t + Q_0 \eta_0 \quad \text{for all } t \in [S, T].$$

Next, define the deterministic matrix

$$R := \Lambda_r^{-1/2} Q_r^\top \sigma \in \mathbb{R}^{r \times d}.$$

Since

$$RR^\top = \Lambda_r^{-1/2} Q_r^\top \sigma \sigma^\top Q_r \Lambda_r^{-1/2} = \Lambda_r^{-1/2} Q_r^\top A Q_r \Lambda_r^{-1/2} = I_r,$$

the process

$$\widetilde{W}_t := R(W_t - W_S), \quad t \in [S, T],$$

is an r -dimensional Brownian motion under \mathbb{Q} . Moreover,

$$dZ_t = Q_r^\top dX_t = Q_r^\top \sigma dW_t = \Lambda_r^{1/2} d\widetilde{W}_t.$$

By the representation already proved,

$$H_t = h(t, X_t) = U(t, Z_t), \quad t \in [S, T].$$

Since $U \in C^{1,2}$, we may apply the classical Itô formula to $U(t, Z_t)$ under \mathbb{Q} , obtaining

$$dU(t, Z_t) = \sum_{i=1}^r \sqrt{\lambda_i} \partial_{\xi_i} U(t, Z_t) d\widetilde{W}_t^i.$$

By Girsanov's theorem in \mathbb{R}^r , there exists an r -dimensional \mathbb{Q}^f -Brownian motion \widetilde{W}^f such that

$$dZ_t = \sum_{i=1}^r \lambda_i \partial_{\xi_i} \log U(t, Z_t) e_i dt + \Lambda_r^{1/2} d\widetilde{W}_t^f.$$

Since

$$X_t = Q_r Z_t + Q_0 \eta_0$$

and

$$\partial_{\xi_i} \log U(t, Z_t) = D_{q_i} \log h(t, X_t),$$

this already identifies the intrinsic drift correction along the diffusive directions as

$$\sum_{i=1}^r \lambda_i D_{q_i} \log h(t, X_t) q_i.$$

Multiplying by Q_r , we obtain

$$dX_t = \sum_{i=1}^r \lambda_i D_{q_i} \log h(t, X_t) q_i dt + Q_r \Lambda_r^{1/2} d\widetilde{W}_t^f.$$

We note that, since $\text{rank}(\sigma) = \text{rank}(\sigma^\top) = r$, there exists

$$\bar{Q}_0 \in \mathbb{R}^{d \times (d-r)}$$

whose columns form an orthonormal basis of $\ker(\sigma)$. In particular,

$$\bar{Q}_0^\top \bar{Q}_0 = I_{d-r}, \quad \sigma \bar{Q}_0 = 0.$$

Moreover,

$$Q_r \Lambda_r^{1/2} = \sigma R^\top, \quad R \bar{Q}_0 = 0.$$

Possibly after enlarging the filtered probability space, choose a $(d-r)$ -dimensional \mathbb{Q}^f -Brownian motion B^f , independent of \widetilde{W}^f . Since the rows of R are orthonormal and the columns of \bar{Q}_0 form an orthonormal basis of $\ker(\sigma)$, we have

$$R^\top R + \bar{Q}_0 \bar{Q}_0^\top = I_d.$$

Therefore the process

$$W_t^f := R^\top \widetilde{W}_t^f + \bar{Q}_0 B_t^f$$

is a d -dimensional \mathbb{Q}^f -Brownian motion. Finally,

$$\sigma dW_t^f = \sigma R^\top d\widetilde{W}_t^f + \sigma \bar{Q}_0 dB_t^f = Q_r \Lambda_r^{1/2} d\widetilde{W}_t^f,$$

and hence

$$dX_t = \sum_{i=1}^r \lambda_i D_{q_i} \log h(t, X_t) q_i dt + \sigma dW_t^f.$$

This is the claimed controlled-diffusion representation. \square

We now pass from the global variational identification to the local intervalwise dynamics of the minimiser. The key point is that, once the coarse past and the realisation of the latent volatility environment that determines the intervalwise frozen reference are fixed, the relevant terminal object is the conditional law of $X_{t_{i+1}}$, and the local backward potential is the backward propagation of its density with respect to the one-step transition of the reference law. Throughout this section we therefore work conditionally on the augmented state (\mathbf{x}_i, y_{i+1}) , where $y_{i+1} \in \mathcal{Y}$ denotes the realisation of the latent environment that fixes the frozen covariance on the next coarse interval $(t_i, t_{i+1}]$, as described in Section 3.2; the dependence on y_{i+1} is carried by every i -indexed object below.

Proposition 5 (Local intervalwise representation of the minimiser). *Adopt the setup of Section 3, and let μ satisfy the finite-entropy condition (1) conditionally on the latent realisation. Fix*

$$i \in \{0, \dots, N-1\}, \quad \mathbf{X}_i := (X_0, X_{t_1}, \dots, X_{t_i}), \quad \mathbf{x}_i := (x_0, x_1, \dots, x_i),$$

and a latent realisation $y_{i+1} \in \mathcal{Y}$ determining the intervalwise frozen reference on $(t_i, t_{i+1}]$. Throughout the statement, every i -indexed object depends on the augmented conditioning (\mathbf{x}_i, y_{i+1}) ; we introduce light shorthands by suppressing this conditioning in the indexed symbol whenever it is the running augmented past. Specifically, we set

$$\begin{aligned} \sigma_i &:= \sigma_i(\mathbf{x}_i, y_{i+1}), & A_i &:= A_i(\mathbf{x}_i, y_{i+1}) = \sigma_i \sigma_i^\top, \\ r_i &:= \text{rank } A_i, & \mathcal{L}_i &:= \text{Ran } A_i \subset \mathbb{R}^d, \\ \ell_i &:= \text{canonical Lebesgue measure on } \mathcal{L}_i, & P^{*,i} &:= P^*(\cdot \mid \mathbf{X}_i = \mathbf{x}_i, Y = y_{i+1}), \end{aligned}$$

where \mathcal{L}_i is the active linear subspace of admissible increments (so the active affine leaf at x_i in position space is $x_i + \mathcal{L}_i$), and, for $j = 1, \dots, r_i$,

$$\lambda_{i,j} := \lambda_{i,j}(\mathbf{x}_i, y_{i+1}), \quad q_{i,j} := q_{i,j}(\mathbf{x}_i, y_{i+1}),$$

the strictly positive eigenvalues and associated orthonormal eigenvectors of A_i . We work throughout with the next-interval increment $\Delta X_{i+1} := X_{t_{i+1}} - X_{t_i}$ as the natural variable; the one-step conditional laws are

$$\begin{aligned} \eta_i^* &:= P^*(\Delta X_{i+1} \in \cdot \mid \mathbf{X}_i = \mathbf{x}_i, Y = y_{i+1}), \\ k_i^R &:= R(\Delta X_{i+1} \in \cdot \mid \mathbf{X}_i = \mathbf{x}_i, Y = y_{i+1}), \end{aligned}$$

respectively the conditional law of the next-interval increment under the minimiser and under the reference. Choosing regular conditional probabilities consistently under $P^ = G(\Pi)R$, we have $\eta_i^* \ll k_i^R$ for $P^* \circ (\mathbf{X}_i, Y)^{-1}$ -a.e. (\mathbf{x}_i, y_{i+1}) ; we set the Radon–Nikodym derivative*

$$f_i(\delta) := \frac{d\eta_i^*}{dk_i^R}(\delta), \quad \delta \in \mathbb{R}^d,$$

viewed as a Borel function on the active subspace \mathcal{L}_i and extended by zero outside \mathcal{L}_i . The local backward potential is denoted

$$H_i(t, x) := H_i(t, x; \mathbf{x}_i, y_{i+1}) : [t_i, t_{i+1}) \times \mathcal{L}_i \rightarrow [0, \infty],$$

and the local logarithmic-gradient drift is

$$b_i^*(t, x) := b_i^*(t, x; \mathbf{x}_i, y_{i+1}).$$

Then, for $P^ \circ (\mathbf{X}_i, Y)^{-1}$ -a.e. (\mathbf{x}_i, y_{i+1}) , the following hold (in the shorthand notation just introduced).*

- (a) The function f_i is (A_i, t_i, t_{i+1}, x_i) -admissible in the sense of (3) (formulated on the active increment subspace \mathcal{L}_i).
- (b) Under $P^{*,i}$, there exists a d -dimensional Brownian motion $W^{*,i}$ such that, on $[t_i, t_{i+1})$,

$$dX_t = b_i^*(t, X_t) dt + \sigma_i dW_t^{*,i},$$

where

$$b_i^*(t, x) = \sum_{j=1}^{r_i} \lambda_{i,j} D_{q_{i,j}} \log H_i(t, x) q_{i,j}, \quad dt \otimes P^{*,i}\text{-a.e.}$$

The potential H_i is the unique function given by Lemma 4, namely the unique backward heat potential associated with the frozen interval $[t_i, t_{i+1}]$, the frozen diffusion matrix σ_i , and the terminal tilt f_i on \mathcal{L}_i . In particular,

$$\partial_t H_i(t, x) + \frac{1}{2} \sum_{j=1}^{r_i} \lambda_{i,j} D_{q_{i,j} q_{i,j}}^2 H_i(t, x) = 0, \quad (t, x) \in [t_i, t_{i+1}) \times (x_i + \mathcal{L}_i),$$

with the terminal condition $H_i(t_{i+1}, x_i + \delta) = f_i(\delta)$ for ℓ_i -a.e. $\delta \in \mathcal{L}_i$, and

$$H_i(t, x) > 0 \quad \forall (t, x) \in (t_i, t_{i+1}) \times (x_i + \mathcal{L}_i).$$

Proof. Throughout the proof we use the shorthand notation of the statement; in addition, write

$$R^i := R(\cdot \mid \mathbf{X}_i = \mathbf{x}_i, Y = y_{i+1})$$

for the conditional reference law, and

$$p_i(t, x; t_{i+1}, \delta) := \text{density of } \Delta X_{i+1} = \delta \text{ given } X_t = x \text{ under } R,$$

the intrinsic Gaussian heat kernel on the increment associated with the frozen covariance A_i ; it is supported on $\delta \in \mathcal{L}_i$. At the runtime anchor $p_i(t_i, x_i; t_{i+1}, \delta)$ is the centred Gaussian density on \mathcal{L}_i with covariance $(t_{i+1} - t_i)A_i$.

Fix (\mathbf{x}_i, y_{i+1}) in a full $P^* \circ (\mathbf{X}_i, Y)^{-1}$ -measure set. By construction of the reference law, under R^i one has on $[t_i, t_{i+1}]$

$$dX_t = \sigma_i dW_t^R, \quad X_{t_i} = x_i;$$

in particular, R^i -a.s. $\Delta X_{i+1} \in \mathcal{L}_i$, and the process X evolves on the affine leaf $x_i + \mathcal{L}_i$.

Let $G := d\mu/d\mu_T^R$. Since $P^* = G(\Pi)R$, for every bounded $\mathcal{F}_{t_{i+1}}$ -measurable random variable F , Bayes' formula yields

$$E_{P^{*,i}}[F] = \frac{E_R[F G(\Pi) \mid \mathbf{X}_i = \mathbf{x}_i, Y = y_{i+1}]}{E_R[G(\Pi) \mid \mathbf{X}_i = \mathbf{x}_i, Y = y_{i+1}]}.$$
 (4)

The tower property rewrites this as

$$E_{P^{*,i}}[F] = E_{R^i} \left[F \frac{E_R[G(\Pi) \mid \mathbf{X}_i = \mathbf{x}_i, Y = y_{i+1}, \mathcal{F}_{t_{i+1}}]}{E_R[G(\Pi) \mid \mathbf{X}_i = \mathbf{x}_i, Y = y_{i+1}]} \right].$$

Hence, by the intervalwise Markov property of R conditional on Y , there exists a Borel function $\tilde{f}_i : \mathcal{L}_i \rightarrow [0, \infty]$ such that, for every bounded $\mathcal{F}_{t_{i+1}}$ -measurable F ,

$$E_{P^{*,i}}[F] = E_{R^i} [F \tilde{f}_i(\Delta X_{i+1})].$$
 (5)

We identify \tilde{f}_i with f_i . Testing (5) with $F = \phi(\Delta X_{i+1})$, $\phi \in C_b(\mathbb{R}^d)$, gives

$$\int_{\mathcal{L}_i} \phi(\delta) \eta_i^*(d\delta) = \int_{\mathcal{L}_i} \phi(\delta) \tilde{f}_i(\delta) k_i^R(d\delta).$$

By uniqueness of the Radon–Nikodym derivative, $\tilde{f}_i = f_i k_i^R$ -a.e. Therefore, (5) becomes

$$E_{P^{*,i}}[F] = E_{R^i}[F f_i(\Delta X_{i+1})]$$

for every bounded $\mathcal{F}_{t_{i+1}}$ -measurable F . This shows that $P^{*,i}$ is induced from R^i by the terminal martingale density $f_i(\Delta X_{i+1})$.

We next verify the (A_i, t_i, t_{i+1}, x_i) -admissibility of f_i . With the shorthand introduced above,

$$k_i^R(d\delta) = p_i(t_i, x_i; t_{i+1}, \delta) \ell_i(d\delta).$$

Fix $t \in (t_i, t_{i+1})$ and $x \in x_i + \mathcal{L}_i$. Then

$$\begin{aligned} & \int_{\mathcal{L}_i} p_i(t, x; t_{i+1}, \delta) f_i(\delta) d\ell_i(\delta) \\ &= \int_{\mathcal{L}_i} \frac{p_i(t, x; t_{i+1}, \delta)}{p_i(t_i, x_i; t_{i+1}, \delta)} \eta_i^*(d\delta). \end{aligned}$$

Both kernels act on the same active subspace \mathcal{L}_i and are associated with the same frozen matrix A_i . In intrinsic coordinates on \mathcal{L}_i ,

$$\frac{p_i(t, x; t_{i+1}, \delta)}{p_i(t_i, x_i; t_{i+1}, \delta)} = \left(\frac{t_{i+1} - t_i}{t_{i+1} - t} \right)^{r_i/2} \exp \left(- \frac{\|x_i + \delta - x\|_i^2}{2(t_{i+1} - t)} + \frac{\|\delta\|_i^2}{2(t_{i+1} - t_i)} \right),$$

where $\|v\|_i^2 := \langle A_i^+ v, v \rangle$ is the Mahalanobis norm attached to A_i on \mathcal{L}_i . Expanding the exponent yields a quadratic function of δ whose quadratic part is

$$-\frac{1}{2} \left(\frac{1}{t_{i+1} - t} - \frac{1}{t_{i+1} - t_i} \right) \|\delta\|_i^2,$$

strictly negative since $t \in (t_i, t_{i+1})$. After completing the square, the ratio is bounded in $\delta \in \mathcal{L}_i$ by a Gaussian-type function. Since η_i^* is a probability measure,

$$\int_{\mathcal{L}_i} p_i(t, x; t_{i+1}, \delta) f_i(\delta) d\ell_i(\delta) < \infty,$$

and at $t = t_i$, $x = x_i$, the same integral equals $E_{R^i}[f_i(\Delta X_{i+1})] = 1$. Therefore f_i is (A_i, t_i, t_{i+1}, x_i) -admissible.

We are thus exactly in the setting of Lemma 4, with

$$S = t_i, \quad x = x_i, \quad \sigma = \sigma_i, \quad f = f_i.$$

Applying that lemma yields the existence of a unique backward heat potential H_i on $(t_i, t_{i+1}) \times \mathcal{L}_i$, with terminal datum $f_i \ell_i$, and the controlled-diffusion representation

$$dX_t = \sum_{j=1}^{r_i} \lambda_{i,j} D_{q_{i,j}} \log H_i(t, X_t) q_{i,j} dt + \sigma_i dW_t^{*,i}, \quad t \in (t_i, t_{i+1}),$$

under $P^{*,i}$, for some d -dimensional Brownian motion $W^{*,i}$. This is precisely the claimed representation. \square

Remark 6 (Boundary semantics at $t = t_i$). *Under $P^{*,i}$ the controlled diffusion is initialised at the single point $X_{t_i} = x_i$, so the natural domain of H_i and b_i^* is the open cylinder $(t_i, t_{i+1}) \times \mathcal{L}_i$; the left endpoint $t = t_i$ carries no transverse mass, and only the diagonal evaluation at (t_i, x_i) is meaningful. We therefore set*

$$H_i(t_i, x_i) := \lim_{t \downarrow t_i} H_i(t, x_i) = 1, \quad b_i^*(t_i, x_i) := \lim_{t \downarrow t_i} b_i^*(t, x_i),$$

respectively the bridge normalisation and the starting drift of the controlled diffusion. The same convention applies to the regularised and empirical potentials of Section 4.

Since P^* projects onto μ on the augmented state space, the terminal datum f_i of Proposition 5 is determined entirely by μ , as we now record.

Corollary 7 (Identification of the exact terminal datum under μ). *Adopt the setup and shorthand of Proposition 5, and set*

$$\eta_i^\mu := \mu(\Delta X_{i+1} \in \cdot \mid \mathbf{X}_i = \mathbf{x}_i, Y = y_{i+1}).$$

Let μ_i denote the joint law of (\mathbf{X}_i, Y) on the augmented state space. Then, for μ_i -a.e. (\mathbf{x}_i, y_{i+1}) ,

$$\eta_i^* = \eta_i^\mu, \quad f_i(\delta) = \frac{d\eta_i^\mu}{dk_i^R}(\delta).$$

Proof. On the augmented space, $P^* \circ (X_{t_0}, \dots, X_{t_N}, Y)^{-1} = \mu$, so for every bounded measurable $\varphi : \mathbb{R}^d \rightarrow \mathbb{R}$,

$$E_{P^*}[\varphi(\Delta X_{i+1}) \mid \mathbf{X}_i, Y] = E_\mu[\varphi(\Delta X_{i+1}) \mid \mathbf{X}_i, Y] \quad P^*\text{-a.s.}$$

Hence $\eta_i^* = \eta_i^\mu$ for μ_i -a.e. (\mathbf{x}_i, y_{i+1}) , and substituting in the definition of f_i from Proposition 5 yields the claim. \square

What remains to be estimated. Under the conditioning (\mathbf{x}_i, y_{i+1}) the reference kernel k_i^R is *deterministic*: it is an explicit function of (\mathbf{x}_i, y_{i+1}) through the frozen covariance A_i , available in closed form from the construction of the triangular reference. The terminal datum $f_i = d\eta_i^\mu/dk_i^R$ on the active increment subspace \mathcal{L}_i is therefore an explicit function of the single unknown η_i^μ , the transition kernel of μ on the coarse grid conditional on the latent. Consequently, the local backward potential H_i —the backward heat propagation of the terminal tilt f_i under the frozen reference semigroup—is itself an explicit function of η_i^μ , and the only object that has to be estimated from data is η_i^μ itself.

3.2 Volatility-informed references and intervalwise freezing

Section 3 specialised the entropy projection to the intervalwise frozen Gaussian reference. This subsection places that reference into a broader picture: a volatility-informed *ideal* reference whose covariance varies continuously inside each coarse interval, its frozen approximation along the coarse grid, and—most importantly—the triangular hierarchy of conditionings that makes the whole construction a *single* TR-SBTS entropy projection on an augmented state space, with two equivalent readings.

Ideal vs frozen reference on one interval. Fix a coarse interval $[S, T]$, $\Delta := T - S$. Let h denote the coarse past at S and Y a latent volatility environment. Conditionally on (h, Y) , the ideal reference is the additive Gaussian martingale $dZ_t = \sigma(t, h, Y) dW_t$ with covariance $a_t(h, Y) = \sigma\sigma^\top \in \mathbb{S}_+^d$, possibly random and degenerate but *state-independent* in Z_t ; this conditional Gaussianity is the structural property that makes the entropy projection decompose interval by interval. Set the covariance cumulant

$$\Gamma_t(h, Y) := \int_S^t a_r(h, Y) dr, \quad C_{S,T}(h, Y) := \Gamma_T(h, Y),$$

so that the terminal Gaussian scale and the active affine leaf $x + \text{Ran } C_{S,T}$ are determined by $C_{S,T}$.

The implementable construction uses the one-piece frozen covariance $\bar{a}_{S,T} = C_{S,T}/\Delta$, whose cumulant is the linear interpolation $\bar{\Gamma}_t = \frac{t-S}{\Delta} C_{S,T}$ between 0 and $C_{S,T}$; on a refinement $\mathcal{P} = \{S = s_0 < \dots < s_M = T\}$ one obtains the *piecewise-frozen* cumulant $\Gamma^{\mathcal{P}}$ by linear interpolation of Γ between consecutive gridpoints. The algorithm of this work uses $M = 1$; finer subgrids accommodate finer volatility information when available.

Bridge comparison through the cumulant. The two references share the same terminal covariance $C_{S,T}$, hence the same endpoint Gaussian scale and the same active leaf; they differ only inside the interval. For a fixed endpoint pair (x, z) with $z - x \in \text{Ran } C_{S,T}$, the means of the ideal and piecewise-frozen bridges are $m_t(\cdot; x, z) = x + \Gamma_t C_{S,T}^+(z - x)$ and $m_t^{\mathcal{P}}(\cdot; x, z) = x + \Gamma_t^{\mathcal{P}} C_{S,T}^+(z - x)$, where $C_{S,T}^+$ is the Moore–Penrose inverse on the active leaf. Setting the intrinsic endpoint norm and the normalised cumulant interpolation error

$$r_{S,T}(h, Y; x, z) := |C_{S,T}^{+/2}(z - x)|, \quad \eta_{\mathcal{P}}(h, Y) := \sup_{S \leq t \leq T} \|(\Gamma_t - \Gamma_t^{\mathcal{P}}) C_{S,T}^{+/2}\|,$$

one has the uniform mean-bound $\sup_t |m_t - m_t^{\mathcal{P}}| \leq \eta_{\mathcal{P}} \cdot r_{S,T}$, and the covariance kernels of the two Gaussian bridges are controlled by the same $\eta_{\mathcal{P}}$ through their explicit expressions in terms of Γ and $C_{S,T}^+$.

Proposition 8 (Stability of piecewise-frozen endpoint bridges). *Under conditional Gaussianity of R^a , if $\eta_{\mathcal{P}_n}(h, Y) \rightarrow 0$ in probability and the intrinsic endpoint norms $r_{S,T}(h, Y; x, z)$ are tight under the endpoint laws $\pi^{h,Y}$, then the piecewise-frozen entropy projection $P^{h,Y,\mathcal{P}_n,\star}$ converges in probability, in the weak topology on $C([S, T]; \mathbb{R}^d)$, to its ideal counterpart $P^{h,Y,\star}$.*

Proof. For fixed (h, Y, x, z) , both bridges are Gaussian; means and covariance kernels are continuous functions of Γ , $\Gamma^{\mathcal{P}_n}$ and $C_{S,T}^+$, and the difference is uniformly controlled by $\eta_{\mathcal{P}_n} \cdot r_{S,T}$. Tightness of $r_{S,T}$ localises the argument, and $\eta_{\mathcal{P}_n} \rightarrow 0$ closes the convergence after integration against $\pi^{h,Y}$. \square

The natural sufficient conditions are: continuity of $(t, h, Y) \mapsto a_t(h, Y)$ on compact sets of histories and latent paths (so that $\eta_{\mathcal{P}_n} \rightarrow 0$ for refining subgrids by uniform continuity of $t \mapsto a_t$ on compact strata), and finite entropy of $\pi^{h,Y}$ relative to the Gaussian endpoint law induced by $C_{S,T}$ (so that tightness of $r_{S,T}$ follows from the entropy inequality applied to the Gaussian-Mahalanobis quadratic form). The relevant approximation error is therefore on the cumulative covariance of the reference, not on instantaneous volatilities: at $M = 1$ the one-piece frozen reference already preserves the total covariance $(T - S)\bar{a}_{S,T} = C_{S,T}$, hence the endpoint Gaussian scale and the terminal leaf; finer subgrids refine the path-level approximation of the cumulant.

Disintegration and the triangular hierarchy. The conditional Gaussianity of R^a makes the entropy projection unfold one level at a time. By disintegration of relative entropy on the augmented state space (X, Y) ,

$$H(P^{X,Y} | R^{X,Y}) = H(P^Y | R^Y) + \mathbb{E}_{P^Y}[H(P^{X|Y} | R^{X|Y})],$$

the joint problem decomposes into an inner TR-SBTS problem in X at fixed Y (solved by Section 3) and an outer minimisation in the law of Y ; the latent environment enters the inner reference only through its trajectory, with the same regularity requirements (continuity of a_t , finite endpoint entropy) imposed at every level. The outer problem is itself a TR-SBTS at a higher level of conditioning, with its own conditional reference. Iterating yields a triangular sequence of conditioning levels, in which the conditioning past widens as one ascends; the construction terminates whenever a stable reference is available at the current level. This is the sense in which the present framework is a *triangular-reference* extension of SBTS.

Joint and hierarchical reading of the construction. The construction is a *single* TR-SBTS entropy projection on the augmented state space, but its triangular structure admits two equivalent readings.

Joint reading. The variational constraint is imposed simultaneously across time and across the latent levels: the augmented coarse-grid law of

$$\tilde{X}_t := (X_t, \theta(\Gamma_t)) \in \mathbb{R}^d \times \mathbb{S}^d$$

is fixed, and the conditional reference on each interval depends on the joint past $(\tilde{X}_{t_0}, \dots, \tilde{X}_{t_i})$; the reference is stochastic above the bottom level, generating the intervalwise covariance descriptors $\theta(\Gamma_t)$ conditionally on this joint history. This allows arbitrary cross-dependence between price and volatility paths.

Hierarchical reading. The localised intervalwise subproblems unfold bottom-up via disintegration of entropy: each level is solved conditionally on the trajectory of the level below, and produces a dynamic reference for the level above. In the implementation this dynamic reference is summarised by a covariance descriptor in the PSD cone \mathbb{S}_+^d ; any factorisation enters only at runtime, for simulation, density evaluation, and local geometric normalisation (Section 5.2).

Both readings refer to the same entropy projection, the same minimiser, and the same reference. The analysis of Section 3 and of the present subsection applies unchanged, the only structural ingredient used being state-independence of the reference inside each coarse interval.

Aim. The aim is to build a *dynamic, informed triangular reference* under which the entropy projection is well-posed—not to track the data-generating volatility process exactly. The latter is generally infeasible: in the Heston example of Section 6.2, the volatility is itself a CIR process and admits no exact finite-rank description.

4 Statistical approximation and main convergence theorem

For each frozen interval $[t_i, t_{i+1}]$, the exact local drift is determined by the backward potential H_i of Proposition 5. This section isolates the implementable approximation problem in the order in which it appears at run time: target of estimation, analytic regularisation, empirical Gaussian estimator, statistical assumptions, and final convergence theorem. Detailed proofs are deferred to Appendix A.

4.1 The target of estimation

We adopt throughout this section the shorthand of Proposition 5: A_i , σ_i , \mathcal{L}_i , k_i^R , η_i^μ , f_i , H_i , b_i^* , etc., all carry the implicit conditioning (\mathbf{x}_i, y_{i+1}) . By the closing remarks of Corollary 7, the frozen covariance A_i , the reference kernel k_i^R and the leafwise heat semigroup are deterministic functions of

the conditioning; the only object that has to be estimated from data is the transition kernel of μ on the coarse grid,

$$\eta_i^\mu := \mu(\Delta X_{i+1} \in \cdot \mid \mathbf{X}_i = \mathbf{x}_i, Y = y_{i+1}).$$

Our strategy is three-step:

- (i) *Analytic regularisation*: replace the rank-deficient frozen covariance A_i with its spectral floor A_i^ε and the leafwise heat semigroup with the corresponding full-rank Gaussian semigroup, producing a regularised potential H_i^ε and drift b_i^ε . Under the conditioning, A_i^ε remains a deterministic function of (\mathbf{x}_i, y_{i+1}) ; only the leafwise geometry of A_i is softened, not the conditioning itself.
- (ii) *Empirical substitution*: replace the conditional law η_i^μ inside H_i^ε by its Nadaraya–Watson kernel-weighted empirical surrogate built from M i.i.d. samples, producing an empirical estimator $\widehat{H}_i^{\varepsilon, M}$ and the corresponding drift $\widehat{b}_i^{\varepsilon, M}$.
- (iii) *Diagonal extraction*: drive $(\varepsilon_n, M_n, h_n) \rightarrow (0, \infty, 0)$ along a sequence admissible in the statistical sense, so that $\widehat{H}_i^{\varepsilon_n, M_n} \rightarrow H_i$ on compacta of the open intervalwise cylinder $(t_i, t_{i+1}) \times \mathcal{L}_i$, and the corresponding drifts and transition kernels converge to their exact counterparts.

Steps (i)–(ii) are spelled out in Sections 4.2 and 4.3; step (iii) is Theorem 10 of Section 4.5.

4.2 Coherent regularised objects

Write $r_i := \text{rank } A_i$, $\Delta_i := t_{i+1} - t_i$, and $\lambda_i^{\min,+}$ for the smallest strictly positive eigenvalue of A_i . For $\varepsilon > 0$, the spectral floor of A_i is

$$A_i^\varepsilon := Q \Lambda_\varepsilon Q^\top, \quad \Lambda_\varepsilon := \text{diag}(\max(\lambda_1, \varepsilon), \dots, \max(\lambda_d, \varepsilon)), \quad (6)$$

where $A_i = Q \text{diag}(\lambda_1, \dots, \lambda_d) Q^\top$ is any spectral decomposition; A_i^ε is full-rank, uniformly elliptic, with $A_i^\varepsilon \succeq \varepsilon I$ and $\det A_i^\varepsilon \geq \varepsilon^d$, and is independent of the choice of Q . The associated full-rank backward Gaussian density *on the increment* is

$$p_i^\varepsilon(t, x; t_{i+1}, \delta) := \frac{\exp\left(-\frac{1}{2(t_{i+1}-t)} \langle (A_i^\varepsilon)^{-1}(x_i + \delta - x), x_i + \delta - x \rangle\right)}{(2\pi(t_{i+1}-t))^{d/2} (\det A_i^\varepsilon)^{1/2}}, \quad (7)$$

the density of $\Delta X_{i+1} = \delta$ given $X_t = x$ under the ε -floored reference (so that the position at t_{i+1} lies at $x_i + \delta$).

The *regularised backward potential* is defined as the coherent Doob kernel ratio: for $t_i < t < t_{i+1}$ and $x \in \mathbb{R}^d$,

$$H_i^\varepsilon(t, x) := \int_{\mathbb{R}^d} \Phi_i^\varepsilon(t, x, \delta) \eta_i^\mu(d\delta), \quad \Phi_i^\varepsilon(t, x, \delta) := \frac{p_i^\varepsilon(t, x; t_{i+1}, \delta)}{p_i^\varepsilon(t_i, x_i; t_{i+1}, \delta)}; \quad (8)$$

equivalently,

$$H_i^\varepsilon(t, x) = \mathbb{E}_\mu[\Phi_i^\varepsilon(t, x, \Delta X_{i+1}) \mid \mathbf{X}_i = \mathbf{x}_i, Y = y_{i+1}]. \quad (9)$$

Both transition densities in Φ_i^ε share the same floor A_i^ε ; the ε -dependent normalisation $(2\pi(t_{i+1} - t))^{-d/2}(\det A_i^\varepsilon)^{-1/2}$ cancels in the ratio, and Φ_i^ε collapses to a Gaussian-type function of δ . The corresponding *regularised drift* is the intrinsic logarithmic-gradient quantity

$$b_i^\varepsilon(t, x) := A_i^\varepsilon \nabla_x \log H_i^\varepsilon(t, x). \quad (10)$$

Analytic facts. The analytic properties of H_i^ε and b_i^ε are proved in Proposition 12 of Appendix A. The key ingredient is the $\alpha < \beta$ gap of the kernel ratio ($\alpha := t_{i+1} - t$, $\beta := t_{i+1} - t_i$), which realises Φ_i^ε as a bounded Gaussian-type function of δ and supplies uniform domination on bounded x -sets and on $\{t \leq t_{i+1} - \tau\}$ for every $\tau > 0$. The matched floor leaves the active eigenvalues unchanged, so the coherent ratio on the active affine leaf reduces to the unfloored leafwise ratio, yielding

$$H_i^\varepsilon(t, x) = H_i(t, x), \quad (t, x) \in (t_i, t_{i+1}) \times (x_i + \mathcal{L}_i), \quad \varepsilon \in (0, \lambda_i^{\min,+}), \quad (11)$$

and the global collapse

$$H_i^\varepsilon \longrightarrow H_i \mathbf{1}_{x_i + \mathcal{L}_i} \quad \text{as } \varepsilon \downarrow 0 \quad \text{pointwise on } \mathbb{R}^d, \quad (12)$$

locally uniformly on compacta of $(t_i, t_{i+1}) \times (x_i + \mathcal{L}_i)$. Off the leaf the convergence is driven by the same $\alpha < \beta$ gap: numerator and denominator of Φ_i^ε share the same A_i^ε and both contribute a transverse penalty in $1/\varepsilon$, but the numerator's penalty, evaluated at the shorter time $\alpha = t_{i+1} - t$, is strictly stronger than the denominator's at $\beta = t_{i+1} - t_i$; the net residual $\sim \exp(-\text{dist}(x - x_i, \mathcal{L}_i)^2 / (2\varepsilon\alpha))$ drives $H_i^\varepsilon \rightarrow 0$ exponentially in $1/\varepsilon$. The intrinsic-gradient drift converges accordingly on every compact $K \Subset (t_i, t_{i+1}) \times (x_i + \mathcal{L}_i)$: $b_i^\varepsilon \rightarrow A_i \nabla_x \log H_i = b_i^*$, in the Mahalanobis geometry of A_i . The natural quantities throughout are $A_i^{\varepsilon, 1/2} \nabla H_i^\varepsilon$, $A_i^\varepsilon \nabla \log H_i^\varepsilon$ and the intrinsic Dirichlet energy $|A_i^{\varepsilon, 1/2} \nabla \log H_i^\varepsilon|^2$, not the naked Euclidean gradient.

Boundary semantics at $t = t_i$. At the left endpoint the boundary semantics of Remark 6 apply unchanged. We set

$$H_i^\varepsilon(t_i, x_i) := \lim_{t \downarrow t_i} H_i^\varepsilon(t, x_i) = 1, \quad (13)$$

$$b_i^\varepsilon(t_i, x_i) := \lim_{t \downarrow t_i} b_i^\varepsilon(t, x_i). \quad (14)$$

The first equality follows from (11) together with the Doob normalisation $H_i(t, x_i) \rightarrow 1$; the second limit exists by dominated convergence on the Gaussian-ratio integrand, using the finite intrinsic A_i^+ -Mahalanobis first moment on the active leaf, implied by finite conditional entropy via Donsker–Varadhan (with global finite entropy via the finite-entropy hypothesis (1) and disintegration); for fixed $\varepsilon \in (0, \lambda_i^{\min,+})$ the leaf inequality $|\delta|_{(A_i^\varepsilon)^{-1}} \leq \|(A_i^\varepsilon)^{-1/2}(A_i^+)^{1/2}\|_{\text{op}} |\delta|_{A_i^+}$ transfers this to the regularised A_i^ε -Mahalanobis quantity that actually appears in the integrand.

4.3 Statistical estimator

We use throughout the joint samples $(\mathbf{X}_i^{(m)}, Y^{(m)}, \Delta X_{i+1}^{(m)})_{m=1}^M$ i.i.d. from μ ; the latent realisations $Y^{(m)} \in \mathcal{Y}$ are observed since they are produced by the joint TR-SBTS construction (Section 5.4).

Macro-conditioning variable. For every level ℓ and interval i , package all the finite-dimensional summaries on which the regression conditions into a single macro-variable

$$\mathcal{U}_i^\ell := \left(\underbrace{x_i}_{\text{state}}, \underbrace{(\Delta x_i, \dots, \Delta x_1)}_{\text{past incr.}}, \underbrace{y_{i+1}}_{\text{latent}}, \underbrace{(C_k^{\varepsilon, \ell})_{k \leq i+1}}_{\text{frozen ref.s}} \right), \quad (15)$$

with runtime query value $u_0 \in \mathcal{U}_i^\ell$ and historical sample value $v = U_i^{\ell, (m)} \in \mathcal{U}_i^\ell$. All notations (\mathbf{x}_i, y_{i+1}) , (ξ_i, y) , etc. collapse onto u_0 and v from now on.

Reference-aware pseudo-distance. Define a single query-dependent pseudo-distance on \mathcal{U}_i^ℓ by

$$d_\varepsilon^\ell(u_0, v)^2 := \sum_{a \in \mathcal{A}_i^\ell} d_{a, \varepsilon}(u_0, v)^2, \quad (16)$$

summing over the components of \mathcal{U}_i^ℓ : for a state or increment component z_a , $d_{a, \varepsilon}(u_0, v)^2 = |z_a(u_0) - z_a(v)|_{C_{a, \varepsilon}(u_0)^{-1}}^2$, the Mahalanobis distance in

the runtime-floored covariance; for each frozen-reference component the log-spectral distance

$$d_{a,\varepsilon}^{\text{ref}}(u_0, v) := |\log(C_{a,\varepsilon}(u_0)^{-1/2} C_{a,\varepsilon}(v) C_{a,\varepsilon}(u_0)^{-1/2})|_{\text{op}}. \quad (17)$$

Locality is measured in the geometry in which the process actually moves, i.e. in the metrics induced by the floored references; in particular d_ε^ℓ automatically contains the reference-comparison growth bounded by $\kappa_\varepsilon^\ell(u_0, v) \leq \exp(d_\varepsilon^\ell(u_0, v)/2)$ (Lemma 14).

Single-kernel regression. The Nadaraya–Watson kernel is a univariate function of the macro pseudo-distance:

$$W_h(u_0, v) := K_h(d_\varepsilon^\ell(u_0, v)), \quad \begin{cases} K(d_\varepsilon^\ell/h), & \text{supp } K \subset [0, 1], & (\text{compact}) \\ \exp(-d_\varepsilon^\ell(u_0, v)^2/(2h^2)), & & (\text{Gaussian}) \end{cases} \quad (18)$$

with NW weights and empirical regression

$$\omega_{i,m}^M(u_0) := \frac{W_{h_M}(u_0, U_i^{\ell,(m)})}{\sum_{n=1}^M W_{h_M}(u_0, U_i^{\ell,(n)})}, \quad (19)$$

$$\widehat{\mathbb{E}}_M[\psi(\Delta) \mid u_0] := \sum_{m=1}^M \omega_{i,m}^M(u_0) \psi(\Delta_i^{(m)}).$$

The *empirical regularised potential* replaces η_i^μ in (8) by the NW surrogate $\widehat{\eta}_i^M := \sum_m \omega_{i,m}^M(u_0) \delta_{\Delta X_{i+1}^{(m)}}$:

$$\widehat{H}_i^{\varepsilon,M}(t, x; u_0) := \sum_{m=1}^M \omega_{i,m}^M(u_0) \Phi_i^\varepsilon(t, x, \Delta X_{i+1}^{(m)}), \quad (20)$$

$$\widehat{b}_i^{\varepsilon,M}(t, x; u_0) := A_i^\varepsilon \nabla_x \log \widehat{H}_i^{\varepsilon,M}(t, x; u_0),$$

with Φ_i^ε the kernel-ratio response of (8); at $t = t_i$ the boundary semantics of Remark 6 apply unchanged.

Remark 9 (Geometry of the kernel: d_ε^ℓ is fundamental). *The single-distance form (18) is the fundamental object: the theory is developed in d_ε^ℓ , and all separate Mahalanobis, log-spectral and Euclidean kernels collapse to it. The classical Euclidean estimator with bandwidth in $q_i + q_Y$ is recovered as a sufficient special case: if there is a local chart T_{u_0} of \mathcal{U}_i^ℓ that is bi-Lipschitz with respect to d_ε^ℓ , $c|T_{u_0}(v) - T_{u_0}(u_0)| \leq d_\varepsilon^\ell(u_0, v) \leq C|T_{u_0}(v) - T_{u_0}(u_0)|$ near u_0 , then the effective dimension is $q_{\text{eff}} = \dim T_{u_0}(\mathcal{U}_i^\ell)$ and a positive Euclidean density at u_0 implies the small-ball condition (21). In general the chart is not used; the regression localises directly in d_ε^ℓ .*

4.4 Statistical assumptions

All assumptions are stated in the macro-conditioning variable \mathcal{U}_i^ℓ of (15) and the reference-aware pseudo-distance d_ε^ℓ of (16); we write $B_\varepsilon(u_0, r) := \{v \in \mathcal{U}_i^\ell : d_\varepsilon^\ell(u_0, v) < r\}$ for the associated pseudo-metric balls. The query point is $u_0 \in \mathcal{U}_i^\ell$. For the interior convergence we assume:

- (S1) (LOCAL LOWER MASS) there exist $r_0 > 0$, $c_{u_0} > 0$ and an effective dimension $q_{\text{eff}} > 0$ such that

$$\mu_U(B_\varepsilon(u_0, r)) \geq c_{u_0} r^{q_{\text{eff}}} \quad \forall 0 < r < r_0; \quad (21)$$

- (S2) (CONDITIONAL CONTINUITY) the map $v \mapsto \eta_i^{\mu, \ell}(\cdot | v) := \mu(\Delta X_{i+1} \in \cdot | U_i^\ell = v)$ is weakly continuous on a d_ε^ℓ -neighbourhood of u_0 , and $v \mapsto A_i^\ell(v)$ is operator-norm continuous at u_0 ;

- (S3) (I.I.D. SAMPLE) the historical sample $(U_i^{\ell, (m)}, \Delta X_{i+1}^{(m)})_{m=1}^M$ is i.i.d. with law induced by μ ;

- (S4) (BANDWIDTH) the bandwidth satisfies $h_M \downarrow 0$ and $Mh_M^{q_{\text{eff}}} \rightarrow \infty$;

- (S5) (STRONG BANDWIDTH) for a.s. convergence the stronger $Mh_M^{q_{\text{eff}}} / \log M \rightarrow \infty$ holds.

For the boundary-diagonal statement of Theorem 10(ii) we additionally assume the *local conditional entropy admissibility in the same geometry*:

- (S6) (LOCAL CONDITIONAL ENTROPY ADMISSIBILITY) there exists $\rho > 0$ such that

$$\sup_{v \in B_\varepsilon(u_0, \rho)} H\left(\eta_i^{\mu, \ell}(\cdot | v) \mid k_i^{R, \ell}(\cdot | v)\right) < \infty.$$

The small-ball lower mass (21) is the fundamental positivity condition in d_ε^ℓ ; the kernel-denominator non-collapse and localiser concentration follow as a lemma (Appendix A.6). *Euclidean special case.* If a chart T_{u_0} of \mathcal{U}_i^ℓ is bi-Lipschitz with respect to d_ε^ℓ near u_0 , then $q_{\text{eff}} = \dim T_{u_0}(\mathcal{U}_i^\ell)$ and (S1) follows from strict positivity and continuity of the push-forward density at u_0 ; in the elementary chart with present state, past increments and latent stacked into $\mathbb{R}^{q_i + q_Y}$ one recovers the classical $Mh_M^{q_i + q_Y} \rightarrow \infty$ bandwidth condition. The macro form is the fundamental one; the Euclidean chart is invoked only when verifying (S1) in concrete examples.

4.5 Main statistical convergence theorem

The theorem below combines the fixed- ε statistical step $\widehat{H}_i^{\varepsilon, M} \rightarrow H_i^\varepsilon$ with the deterministic analytic step $H_i^\varepsilon \rightarrow H_i \mathbf{1}_{\mathcal{L}_i}$, and closes the chain by a diagonal extraction in $(\varepsilon_n, M_n, h_n)$.

Theorem 10 (Main statistical convergence). *Adopt the setup and shorthand of Proposition 5. Fix a compact set $K \Subset (t_i, t_{i+1}) \times \mathcal{L}_i$ contained in the backward stratum $\{t \leq t_{i+1} - \tau\}$ for some $\tau > 0$. Then there exist sequences $\varepsilon_n \downarrow 0$, $M_n \rightarrow \infty$, and admissible bandwidths h_{M_n} such that, writing $\widehat{H}_i^{(n)}$ for the empirical regularised potential with parameters $(\varepsilon_n, M_n, h_{M_n})$:*

(i) INTERIOR DRIFT CONVERGENCE. *Under (S1)–(S5), $\sup_{(t,x) \in K} |\widehat{b}_i^{(n)}(t,x) - b_i^*(t,x)| \rightarrow 0$ in probability, with $\widehat{b}_i^{(n)} := A_i^{\varepsilon_n} \nabla_x \log \widehat{H}_i^{(n)}$; a.s. under the stronger (S5) bandwidth.*

(ii) BOUNDARY-DIAGONAL DRIFT CONVERGENCE. *Under (S1)–(S6), the empirical boundary drift defined as the finite-sample diagonal limit $\widehat{b}_i^{(n)}(t_i, x_i) := \lim_{t \downarrow t_i} \widehat{b}_i^{(n)}(t, x_i)$ satisfies $\widehat{b}_i^{(n)}(t_i, x_i) \rightarrow b_i^*(t_i, x_i; u_0)$ in probability; a.s. under (S5).*

(iii) TRANSITION-KERNEL CONVERGENCE. *Under (S1)–(S5), let $K_i^*(t; \cdot)$ be the transition kernel of the exact conditional bridge of Proposition 5, and let $\widehat{K}_i^{(n)}(t; \cdot)$ be the time- t marginal of the empirical bridge mixture $\widehat{\mathcal{K}}_i^{(n)}$ of Appendix A.5 (equation (54)). For every $t \in [t_i, t_{i+1}]$ and every bounded continuous $\varphi : \mathbb{R}^d \rightarrow \mathbb{R}$, $\int_{\mathbb{R}^d} \varphi d\widehat{K}_i^{(n)}(t; \cdot) \rightarrow \int_{\mathbb{R}^d} \varphi dK_i^*(t; \cdot)$ in probability.*

The boundary statement (ii) is the only one requiring the local entropy admissibility (S6); the interior statements (i) and (iii) hold under (S1)–(S5) alone.

Remark 11 (Diagonal extraction). *At fixed $\varepsilon > 0$ the regularised Gaussian kernels are full-rank and uniformly elliptic ($A_i^\varepsilon \succeq \varepsilon I$, $\det A_i^\varepsilon \geq \varepsilon^d$); determinant and inverse-covariance constants depend polynomially on ε but are harmless: at every $\varepsilon > 0$ the statistical error can be made small by choosing M large and h_M small, and the final convergence follows by selecting the diagonal sequence $(\varepsilon_n, M_n, h_n)$ sufficiently slowly. No rank-stability assumption on A_i is required: rank and active leaf enter only in the deterministic geometric limit $\varepsilon \downarrow 0$ via the global collapse $H_i^\varepsilon \rightarrow H_i \mathbf{1}_{\mathcal{L}_i}$. The compactly supported auxiliary estimator $\widehat{H}_i^{\varepsilon, M, K}$ of Appendix A.2 achieves the same*

compact-uniform convergence almost surely under the stronger bandwidth condition $Mh_M^{\text{eff}} / \log M \rightarrow \infty$.

We can now turn to the finite-dimensional conditioning, precomputation, and runtime choices of the implementation.

5 Computational architecture

This section turns the analytic construction of Section 4 into a finite-dimensional, sample-based generator. Three operational ingredients: (i) a finite-dimensional summary of the conditioning past (Section 5.1); (ii) a covariance-descriptor database (Section 5.2); (iii) a coupled bridge step that produces the next state and the next descriptor jointly (Section 5.4).

5.1 Complementary reductions of the conditioning past

The exact intervalwise conditioning variable is the entire past \mathbf{x}_i , whose dimension grows linearly with time; like the original SBTS framework, TR-SBTS is therefore exposed to the curse of dimensionality on the memory used by the kernel regression. We present three *complementary* reductions of the conditioning past, each targeting a different statistical facet of the history, and combine them at the end into a three-estimator architecture.

(a) Block principal component regression. The PCR variant follows the original SBTS recipe: reduce the conditioning to a fixed-dimensional summary by retaining the current state and a finite block of recent increments,

$$x_i, \quad (\Delta x_{i-p_i+1}, \dots, \Delta x_i), \quad \Delta x_k := x_{k+1} - x_k, \quad p_i \leq p_{\max},$$

and mapping each piece through its own PCR projection, $\Pi_X : \mathbb{R}^d \rightarrow E_X$ on the state and $\Pi_\Delta : \mathbb{R}^d \rightarrow E_\Delta$ on the increments:

$$\mathbf{c}_i(x_{0:i}) := (\Pi_X x_i, \Pi_\Delta \Delta x_{i-p_i+1}, \dots, \Pi_\Delta \Delta x_i) \in E_X \times E_\Delta^{p_i}. \quad (22)$$

PCR is understood in a flexible block sense (joint, blockwise, or purely componentwise variance normalisation), with truncation governed by an explained-variance threshold selected by validation. A single set of principal directions is used for the entire runtime regime, making PCR a global second-order summary of the joint distribution of positions and increments on the training set.

(b) Reference-aware Mahalanobis kernel. The reference-aware kernel W_h of (18) is the kernel of §4.3 itself, read here as an increment-by-increment Mahalanobis comparison under the dynamic reference geometry: each past increment Δx_k is compared to its historical counterpart in the floored cumulant $C_k^\varepsilon(\mathbf{u}_{k-1})$. It acts as the Nadaraya–Watson conditioning kernel of the three-estimator architecture below, and is a second-moment statistic of past increments only; first-order conditioning information is supplied by (a) or by the next reduction.

(c) Past-window WLS drift regressor. Given a memory length $L \leq i$, fit a low-dimensional parametric drift model $\mu_k(\theta)$ (linear in past features, locally constant, or a low-order polynomial in time) on the past window $k = i - L + 1, \dots, i$, with the reference Mahalanobis metric $(C_k^\varepsilon)^{-1}$ as innovation weight:

$$\hat{\theta}_i := \operatorname{argmin}_{\theta \in \mathbb{R}^q} \sum_{k=i-L+1}^i \|\Delta x_k - \mu_k(\theta)\|_{(C_k^\varepsilon(\mathbf{u}_{k-1}))^{-1}}^2. \quad (23)$$

The output $\hat{\theta}_i \in \mathbb{R}^q$ has fixed dimension independent of L , so enlarging the memory length stabilises the regressor instead of widening the conditioning vector: there is no curse of dimensionality in L . The memory length L is itself selected by the predictive energy validation of Section 5.5.

Three-estimator architecture. The three reductions (a)–(c) target three distinct facets of the conditioning past and are most usefully combined as:

- (i) a *present anchor*, the runtime state x_i in normalised coordinates (active eigenbasis of the runtime reference, spectrally floored), carrying first-order location information;
- (ii) a *past-drift regressor* $\hat{\theta}_i$ from (23), encoding the first-order temporal trend over the past window with fixed output dimension;
- (iii) a *present/near-future volatility estimator*, the covariance descriptor Σ_i of Section 5.2, carrying the second-order geometric information through the dynamic reference.

The kernel (b) plays the role of the NW conditioning kernel. The PCR option (a) remains available as a global alternative or as an additional block within (i)–(ii). The conditional consistency analysis of Section 4.5 applies unchanged: by Remark 9, the runtime spectrally floored metric is bounded above and below, and the standard NW proof transfers via change of coordinates.

Logweights and terminal surrogate. Each admissible historical candidate $j \in \mathcal{J}_i$ receives a Gaussian logweight; in the PCR variant,

$$\ell_{i,j} := -\frac{1}{2} \|\Pi_X x_i - \Pi_X x_j^{\text{hist}}\|_{\Lambda_X}^2 - \frac{1}{2} \sum_{q=1}^{p_i} \|\Pi_{\Delta} \Delta x_{i-p_i+q} - \Pi_{\Delta} \Delta x_{j,q}^{\text{hist}}\|_{\Lambda_{\Delta,q}}^2, \quad (24)$$

with bandwidth matrices $\Lambda_X, \Lambda_{\Delta,q}$; in the reference-aware variant, the increment bandwidths are replaced by the floored inverse cumulants $C_k^{\varepsilon}(\mathbf{u}_{k-1})^{-1}$ of Section 4.3 (the anchor term retains its isotropic Euclidean form). Mixture weights follow from the stable softmax

$$w_{i,j} := \frac{\exp(\ell_{i,j} - L_i)}{\sum_{m \in \mathcal{J}_i} \exp(\ell_{i,m} - L_i)}, \quad L_i := \max_{m \in \mathcal{J}_i} \ell_{i,m}, \quad (25)$$

giving the empirical terminal surrogate

$$\hat{\nu}_i := \sum_{j \in \mathcal{J}_i} w_{i,j} \eta_{i,j}, \quad \eta_{i,j} := \delta_{\Delta X_{i+1}^{(j)}}. \quad (26)$$

The intrinsic drift of Proposition 5 is then read off the backward heat potential evaluated against $\hat{\nu}_i$; the analytic and stability properties of the coherent kernel ratio are those of Section 4.2.

5.2 Covariance-descriptor database

At each coarse step i the framework attaches an intervalwise *covariance descriptor* $\Sigma_i \in \mathbb{S}_+^d$ —either estimated from data or supplied exogenously (e.g. a daily realised covariance computed from intraday increments)—summarising the triangular reference by its second-order geometry on the interval. Latent kernels of Section 5.4 regress directly on the PSD-valued trajectory in the flat ambient space of symmetric matrices, with regression row

$$\gamma_i := \text{vech}(\Sigma_i) \in \mathbb{R}^{d(d+1)/2}. \quad (27)$$

PSD projection and runtime factorisation. Since regression in \mathbb{S}^d is linear, a generated descriptor may fail to be PSD and is projected onto \mathbb{S}_+^d spectrally: with eigendecomposition $\Sigma_i^{\text{gen}} = Q_i \text{diag}(\lambda_{i,1}, \dots, \lambda_{i,d}) Q_i^{\top}$,

$$\Sigma_i := Q_i \text{diag}(\lambda_{i,1}^+, \dots, \lambda_{i,d}^+) Q_i^{\top}, \quad \lambda^+ := \max(\lambda, 0) \quad (28)$$

(equivalently, the Frobenius projection onto the PSD cone). For simulation, the canonical symmetric square root is used,

$$F_i := \Sigma_i^{1/2} \in \mathbb{S}^d, \quad F_i F_i^{\top} = \Sigma_i; \quad (29)$$

Algorithm 1 Single-component TR-SBTS generation

Require: fitted component model, initial state X_0 , horizon H

- 1: **for** $m = 0, \dots, H - 2$ **do**
 - 2: $\mathbf{c}_m \leftarrow$ conditioning summary of $X_{0:m}$: present anchor x_m in normalised coordinates, past-drift summary $\hat{\theta}_m$ from (23), and/or block-PCR coordinate (22), depending on which reductions of Section 5.1 are active
 - 3: $\ell_{m,\cdot} \leftarrow$ Gaussian logweights (PCR variant (24), reference-aware analogue, or WLS-summary analogue) under the reference-aware Mahalanobis geometry on past increments
 - 4: $w_{m,\cdot} \leftarrow$ softmax($\ell_{m,\cdot}$) via (25)
 - 5: $\hat{\nu}_m \leftarrow \sum_j w_{m,j} \eta_{m,j}$
 - 6: **for** $r = 0, \dots, n_{\text{in}} - 1$ **do**
 - 7: $b_{m,r} \leftarrow A_m^\varepsilon \nabla_x \log H_m(\tau_r, X_m^{(r)}; \hat{\nu}_m)$
 - 8: $X_m^{(r+1)} \leftarrow X_m^{(r)} + b_{m,r} \Delta\tau_r + \sigma_m \sqrt{\Delta\tau_r} \xi_{m,r}$
 - 9: **end for**
 - 10: $X_{m+1} \leftarrow X_m^{(n_{\text{in}})}$
 - 11: register $X_{m+1} - X_m$ in the increment history
 - 12: **end for**
 - 13: **return** (X_0, \dots, X_{H-1})
-

continuity of $\Sigma \mapsto \Sigma^{1/2}$ on the closed PSD cone makes the factorisation numerically stable on rank-deficient matrices. When the projected covariance feeds the reference backend (transition densities of Section 4.2, or reference-aware Mahalanobis kernels of Sections 4.3 and 5.1), it is spectrally floored with the same regularisation parameter ε :

$$\Sigma_i^\varepsilon := Q_i \text{diag}(\max(\lambda_{i,1}^+, \varepsilon), \dots, \max(\lambda_{i,d}^+, \varepsilon)) Q_i^\top, \quad (30)$$

with $\Sigma_i^\varepsilon \succeq \varepsilon I$ and $\det \Sigma_i^\varepsilon \geq \varepsilon^d$. PSD projection enforces admissibility; the ε -floor provides the non-degenerate geometry used in inverses and Mahalanobis distances.

5.3 Coupling through logweights

The state and covariance components are coupled at the level of their empirical terminal mixtures, by mixing the corresponding Gaussian logweights before the softmax of (25) is taken. Let $\ell_{m,j}^X$ and $\ell_{m,j}^F$ be the logweights produced by the two components for the historical candidate j ; the example

adopted in the implementation is

$$\bar{\ell}_{m,j}^X := (1 - \rho_X)\ell_{m,j}^X + \rho_X\ell_{m,j}^F, \quad (31)$$

$$\bar{\ell}_{m,j}^F := (1 - \rho_Y)\ell_{m,j}^F + \rho_Y((1 - \alpha)\ell_{m,j}^X + \alpha\ell_{m,j}^{X,0}(X_m)), \quad (32)$$

with parameters $\rho_X, \rho_Y, \alpha \in [0, 1]$. The state component uses $\bar{\ell}_{m,\cdot}^X$, the covariance component uses $\bar{\ell}_{m,\cdot}^F$, and both are normalised through the same softmax. The parameter ρ_X tunes how much external covariance information is mixed into the state component, while ρ_Y controls the analogous external (primary / present-state) share injected into the covariance component, with $(1 - \rho_Y)$ weighting the covariance-component self-history. The parameter α splits the external state contribution to the covariance component between the running history and the present-step anchor $\ell_{m,j}^{X,0}(X_m)$. No new estimator is introduced; the coupling only changes which historical terminal atoms are emphasised by each component.

5.4 Joint TR-SBTS generation

The full TR-SBTS generator instantiates Algorithm 1 jointly on the augmented process (X_t, Σ_t) of Section 3.2. At each coarse step, the covariance component produces the next covariance descriptor $\Sigma_{m+1} \in \mathbb{S}_+^d$ from the joint past $(X_{0:m}, \Sigma_{0:m})$ through its own bridge step applied to the covariance-descriptor sequence on \mathbb{S}^d ; this bridge step is realised concretely on the symmetric-square-root parametrisation (γ_t) of Section 5.2, and the descriptor Σ_{m+1} thereby produced is read as the operational summary of the triangular reference attached to the upper level on the next coarse interval. The intervalwise covariance driving the state bridge step on $[t_m, t_{m+1}]$ is then Σ_{m+1} , factorised at runtime as $F_{m+1}F_{m+1}^\top = \Sigma_{m+1}$ with $F_{m+1} = \text{mat}(\gamma_{m+1})$ solely for the operational purposes listed in Section 5.2. The state bridge step produces X_{m+1} from the same joint past via the coupled logweights of Section 5.3, and the next coarse boundary is reached. The single-component case is recovered when the covariance component reduces to a fixed externally-supplied descriptor.

5.5 Hyperparameter selection

Free parameters are selected through a three-phase hierarchical ladder built around the predictive energy score of Appendix B; the predictive horizon K is progressively lengthened from one phase to the next.

Phase 1:covariance component. Bandwidth, memory length, and PCR threshold of the covariance component are selected in isolation by maximising the basic predictive energy score on the covariance trajectory $(\Sigma_i)_i$, via the symmetric-square-root sequence $(\gamma_i)_i$. This produces a reliable descriptor generator before any coupling is introduced.

Phase 2:state component. Bandwidth, memory length, and the spectral floor ε of the state component are selected analogously on the state path $(X_i)_i$ at a longer predictive horizon, with the Phase-1 configuration fixed.

Phase 3:coupling. The coupling parameters ρ_X, ρ_Y, α are selected jointly with the enriched coupled score (features combining positions and packed squared increments) at the longest predictive horizon used in the suite.

6 Numerical experiments

We test TR-SBTS along two complementary axes. The first (Section 6.1) probes the *dimensional* robustness of the kernel-PCR conditioning: a diffusion whose true dynamics live on a low-dimensional subspace is embedded in increasingly high ambient dimension, and we ask whether a PCR-truncated TR-SBTS keeps tracking the true subspace once the ambient dimension is much larger than the intrinsic one. The second (deferred to Section 6.2) probes the *stochastic-volatility* case: synthetic paths from a calibrated Heston model are used as ground truth, TR-SBTS is fitted on them, and the per-parameter Heston QMLE distribution recovered from the synthetic paths is compared with the QMLE distribution recovered from the real paths.

6.1 Low-rank dimensional stress

We embed a non-trivial two-dimensional motion in an ambient space of growing dimension and ask whether the SBTS estimator continues to recover its predictive distribution as the codimension grows. The informative motion is a Hopf oscillation on (X_1, X_2) — a stable limit cycle of unit radius with non-linear (cubic) drift, dominantly tangential, so that every cycle phase has a different conditional mean and a globally smoothed kernel cannot match the ground truth. The remaining $d - 2$ coordinates are an independent fast Ornstein–Uhlenbeck process whose contribution to the conditional law of any future state is, in the asymptotic limit $\lambda_\perp \rightarrow \infty$, a pure isotropic Brownian increment over the macro step. The trajectory is generated by an exact transition kernel on a trading-day grid ($dt = 1/250$, 20 calendar years

per run); we sweep $d \in \{4, 8, 16, 32, 64, 128, 256, 512\}$ with three seeds per dimension and keep the training-set size fixed at $M = 4500$, so as d grows the ratio M/d collapses from 1125 to 8.8. The signal subspace is taken canonical, $\text{span}(e_1, e_2)$; under any random orthonormal loading the same conclusions hold up to a fixed rotation, but the canonical choice lets the test scoring be performed on the first two coordinates without a data-driven projection.

The kernel weights are the *quartic compact-support kernel* of [15] (eq. 4.2), $K_h(u) = (1 - \|u\|^2/h^2) \mathbf{1}_{\{\|u\| \leq h\}}$, used as a multiplicative factor at every past time point. This is the architectural choice that exposes the conditioning effect: a Gaussian softmax cancels noise-axis contributions in its own normalisation and masks the curse of dimensionality on this DGP, while a hard support cutoff lets the perpendicular squared-distance accumulate freely and push every candidate outside the support as d grows. We compare two variants: `classic_no_pcr`, which conditions the kernel on the full d -dimensional state, and `classic_pcr`, which conditions it on the validated PCA-truncated state — and the validated truncation lands on $k=2$ at every d , since the position covariance has a clean step at rank 2 by construction. Hyperparameters are validated per dimension on a held-out validation block; the test metric is the one-step predictive multivariate energy score on the test block, sliced to the first two ambient coordinates and normalised by \sqrt{q} so that values are directly comparable across d . With the chosen DGP parameters the score is bounded below by the Bayes-optimal floor $\widetilde{\text{ES}}^* \approx 0.040$ (the entropy of the one-step Brownian transition on the signal subspace) and above by the predict-the-marginal-mean floor of order 0.7; reporting both the absolute score and its excess over the Bayes-optimal floor isolates the curse-of-dimensionality contribution to the predictive error.

Figure 1 summarises the experiment. The PCR variant is essentially flat in d : its excess over the Bayes-optimal floor stays in a narrow $[0.013, 0.039]$ band across two orders of magnitude in the codimension. The no-PCR baseline degrades monotonically; its excess over the same floor grows by roughly a factor of three from $d = 4$ to $d = 512$, with the PCR/no-PCR ratio on the excess climbing to ≈ 4 at the intermediate dimensions and stabilising around 2.5 at the largest. The two variants coincide at $d = 4$, where there are no perpendicular axes to exploit, and diverge as soon as the codimension is comparable to the signal dimension. This is the regime the construction is designed to absorb: a kernel that is contracted on the data manifold by PCR keeps contact with the data at every ambient dimension, while a kernel that sees the full ambient state loses contact as the noise dimension grows.

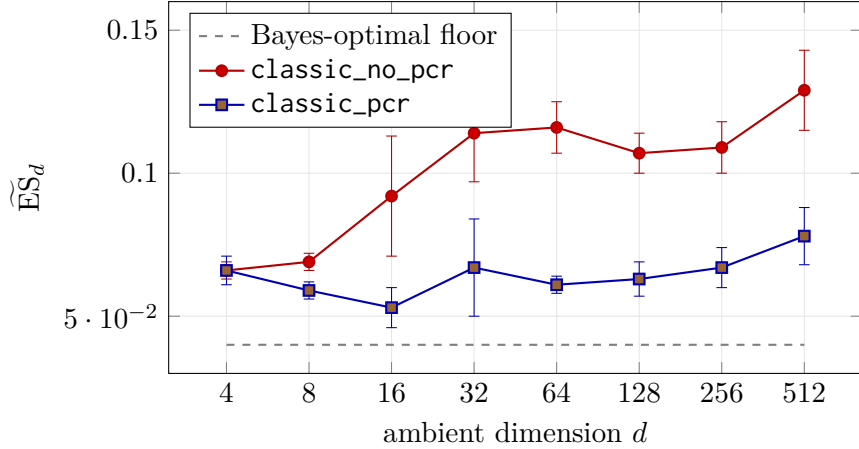


Figure 1: Predictive energy score on the canonical signal subspace as a function of the ambient dimension d . The PCR variant stays within $2\times$ the Bayes-optimal floor at every d ; the no-PCR baseline degrades from $\approx 1.7\times$ the floor at $d = 4$ to $\approx 3.2\times$ at $d = 512$. Error bars are one standard deviation across three independent seeds.

6.2 Heston parameter recovery

The second experiment runs the three-layer TR-SBTS pipeline end-to-end on a canonical stochastic-volatility model. Let (S_t, V_t) solve the standard Heston system

$$\begin{aligned} dS_t &= \mu S_t dt + \sqrt{V_t} S_t dW_t^S, \\ dV_t &= \kappa(\theta - V_t) dt + \xi \sqrt{V_t} dW_t^V, \quad d\langle W^S, W^V \rangle_t = \rho dt, \end{aligned} \quad (33)$$

with parameters $(\kappa, \theta, \xi, \rho)$ drawn per path from a fixed prior and an horizon of $T = 252$ coarse increments at $\Delta t = 1/T$. The observable state is $\zeta_t := (\log S_t, V_t)$. The experiment is a stress test on how informative a TR-SBTS reference constructed *purely from data* — without any parametric Heston assumption inside the model — can be made, when the data is the diffusion of ζ_t itself.

Three layers and what they encode

The pipeline is the three-layer TR-SBTS construction of Section 5.4, instantiated with the following causal interpretation of the layers:

Primary (X-layer). State $X_t \equiv \zeta_t \in \mathbb{R}^2$ — the observable log-price/variance pair. This is the only level whose generated output the user consumes.

Secondary (Y-layer). State $Y_t \in \mathbb{R}^3$, the packed lower triangle of the *cumulative average* of the outer products of past coarse increments of ζ_t ,

$$M_t = \frac{1}{t \Delta t} \sum_{i=1}^t \Delta \zeta_i (\Delta \zeta_i)^\top,$$

packed in lower-triangular form. M_t is a fully causal, parameter-free running estimate of the path’s average covariance rate; the secondary models its time evolution.

Tertiary (Z-layer). State Z_t is a *hybrid-frame parametrisation* of the path’s average covariance ribbon: a finite-dimensional vector whose first component is the dominant principal direction of the path’s cumulative covariance estimator (after normalisation by its X -variance), and whose remaining components are the normalisations of the second and first principal components of that same estimator. The tertiary thus encodes the *geometry* of where the diffusion lives — the path-specific ribbon in Sym_2^+ along which the cumulative covariance accumulates — independently of the magnitude controlled by V_t .

The reference at each level is produced by a deterministic *backward map* from the state of the level immediately below, applied at every closed-loop step. The map at the upper edge (tertiary \rightarrow secondary) sends a hybrid-frame point back into the cone of symmetric PSD matrices, picking out the rank-one covariance ribbon parametrised by that point; the map at the lower edge (secondary \rightarrow primary) is the unpacking of the 3-vector into a 2×2 symmetric matrix used as the primary’s runtime diffusion covariance. Both maps are closed-form and state-independent inside each coarse interval, in line with the intervalwise-frozen reference structure of Section 3.

Data-driven references

The most delicate aspect of the experiment is the choice of references the upper layers expose to the lower ones. Each is read off the data without ever invoking a parametric form of the Heston diffusion:

- The secondary’s training stream is the cumulative-average packed covariance M_t of ζ_t defined above. No smoothing kernel, no half-life, no tuning: the running mean of the squared increments is the most

parsimonious causal estimator of where the increments are diffusing on average up to time t .

- The tertiary’s training stream is the hybrid-frame parametrisation of the path’s terminal cumulative covariance M_T , obtained by a principal-component analysis on ζ and a backward-map reduction into the ribbon coordinates that the secondary will consume as reference.

Both streams are computed per path on the training pool only, and each layer is then fitted by the kernel-regression estimator of Section 4.3 against its own stream as if it were the ground truth. No information about the Heston law enters the model.

Implementation

The model implementing this pipeline is a three-layer TR-SBTS as described in Section 5, run on N_{train} training paths and validated on a held-out pool of N_{val} paths. The closed-loop generation warm-starts on the path’s real history of length $H = 64$ and then evolves the joint (Z, Y, X) state by the joint TR-SBTS generator for the remaining $T - H$ coarse steps. The secondary and tertiary bandwidths, history lengths, and integration controls are selected by a predictive-energy validation on the same pool.

Results

We evaluate the closed-loop synthetic paths through the same per-path Heston-like estimators of $(\kappa, \theta, \xi, \rho)$ that one would apply to the real series, and report their cross-path distributions on the held-out pool. Figure 2 shows, for the selected configuration, the four parameter densities on the synthetic trajectories overlaid on the densities obtained on the held-out real trajectories and on those produced by the SBTS-Classic baseline of [1], which fits a single kernel-regression layer against a frozen, state-independent Brownian reference. The classical baseline recovers the mean-reversion level θ and the long-run drift, but the variance-of-variance ξ and the leverage ρ collapse onto the empirical priors of those parameters, as the frozen Brownian reference carries no information about the path-specific diffusion direction. The TR-SBTS pipeline, by contrast, replaces that frozen reference with the variable, intervalwise reference produced by the tertiary \rightarrow secondary backward map, and as a consequence recovers *also* the geometry-defining pair (ξ, ρ) distributionally; the long-run level θ is recovered within the empirical finite-sample fluctuation of the per-path estimator; the mean-reversion rate

κ is the least informative channel at this horizon and bandwidth, consistent with its weak identifiability from a fixed-length single trajectory. Allowing the reference to vary along the path is what unlocks recovery of the diffusion structure that an isochronous Brownian reference cannot see.

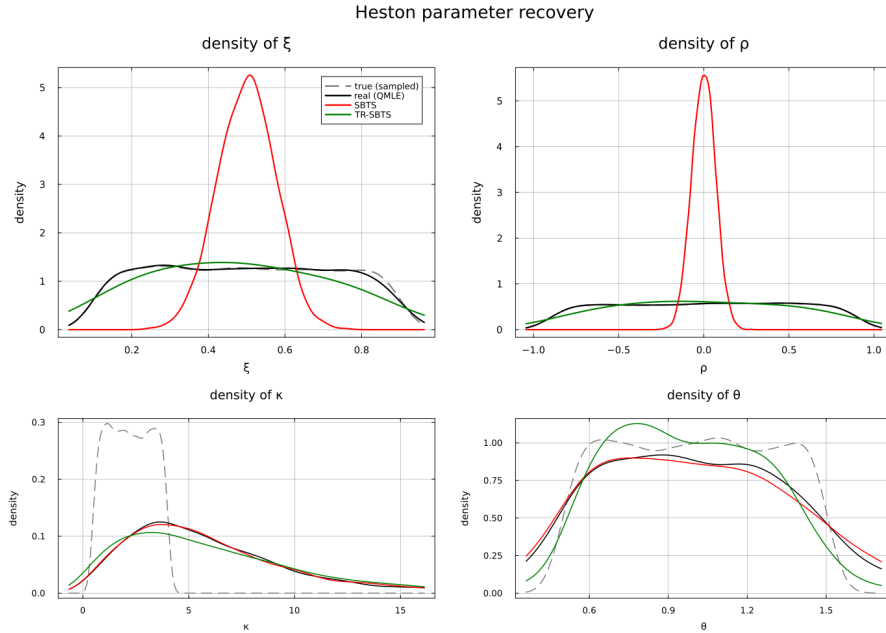


Figure 2: Heston parameter recovery on closed-loop synthetic trajectories. Real held-out paths, TR-SBTS synthetic paths under the selected configuration, and SBTS-Classic baseline. SBTS-Classic recovers θ but collapses (ξ, ρ) onto the empirical priors. TR-SBTS additionally recovers the geometry pair (ξ, ρ) distributionally; the mean-reversion rate κ is the least identifiable channel at this horizon.

Hardware and software environment. The experiments above were performed on a laptop with the following characteristics: Intel(R) Core(TM) i7-8565U CPU at 1.80 GHz (turbo up to 1.99 GHz), 4 physical cores and 8 logical processors, 16 GB of RAM, and an integrated Intel UHD Graphics 620 GPU (no discrete accelerator), running Microsoft Windows 11 Pro (build 10.0.26200). All algorithms were implemented in Julia (version 1.12.3). The core TR-SBTS solver depends only on the Julia standard library; the elementary aggregations used at run time come from the

Statistics 1.11.1 standard module. The synthetic datasets are generated using `DifferentialEquations.jl` 7.17.0, `Distributions.jl` 0.25.123 and `StatsBase.jl` 0.34.9; the Heston experiment additionally uses `Optim.jl` 1.13.3 for the calibration step. All figures are produced with `Plots.jl` 1.41.4. The TR-SBTS solver runs on the CPU only; no GPU acceleration is used.

7 Conclusion and outlook

We have developed *TR-SBTS*, a conservative extension of the Schrödinger Bridge for Time Series framework in which the Brownian prior is replaced by a triangular, intervalwise frozen, and possibly degenerate diffusion reference. The exact entropy-minimisation problem on path space remains the same in spirit: one searches for the path law closest to a reference measure while matching the observed joint law on the coarse time grid. The novelty lies in the choice of reference, which now incorporates an intervalwise volatility structure depending on the coarse past and on a latent volatility environment, but state-independent inside each coarse interval. Iterating this construction over the latent environment yields a triangular hierarchy of conditioning levels, in which each level is itself a TR-SBTS conditional on a higher-level volatility signal.

The construction preserves the transparency of the original SBTS framework. The minimiser is identified explicitly as an h -transform of the reference law, and locally, on each frozen interval, the optimal dynamics are described by backward heat potentials on the affine leaves generated by the active covariance directions, yielding a logarithmic-gradient drift formula that remains meaningful when the frozen covariance is degenerate or has variable rank. Beyond the local drift, the paper records a structural stability result on the freezing approximation itself: the discrepancy between the ideal volatility-informed reference and its intervalwise frozen approximation is controlled by a cumulant interpolation error, and the construction itself is a single entropy projection on the augmented state space, with the variational constraint imposed jointly across time and the latent levels and unfolded hierarchically by the disintegration of entropy, allowing arbitrary cross-dependence between price and volatility paths (Proposition 8). On the statistical side, the conditional regression object that must be estimated is isolated and convergence of regularised kernel estimators is established for the corresponding heat potentials, heat drifts, and conditional transition kernels. The accompanying implementation realises this construction on finite samples through a finite-dimensional conditioning map—either PCR-based or reference-aware, the

latter inducing a runtime local Mahalanobis geometry on the conditioning increments through the frozen covariance cumulants themselves—together with a coupled state–covariance bridge step in which each latent level produces a dynamic reference for the level above, summarised by a covariance descriptor; the symmetric square-root factorisation enters only at runtime for simulation, density evaluation, and local geometric normalisation.

Several directions remain open.

Jumps. The present formulation is continuous-path. A natural extension combines the intervalwise frozen diffusion reference with a jump component, in the spirit of Schrödinger bridges with jumps. This would let the model treat stochastic volatility and discontinuous path behaviour within a single framework, and is empirically relevant for financial and energy time series where abrupt moves, heavy tails, and regime switches are central.

Conditional generation. The explicit Brownian noise injected at each inner step, together with the path-dependent bridge mechanism, makes the framework structurally suited to conditional generation under pathwise events—barrier- or drawdown-type constraints, scenario reconstruction on rare-event subsets, and more generally the simulation of trajectories subject to path-dependent conditions. We intend to pursue this direction in future work.

Neural estimators. The kernel-based estimator used here is interpretable but exposed to bandwidth sensitivity and to the curse of dimensionality. A controlled introduction of neural components into the bridge mechanism, preserving the analytic stability guarantees and the transparency of the path-space construction, is a natural direction of investigation.

Multi-resolution data. The cumulant stability result of Section 3.2 is itself a multi-resolution statement: refining the volatility grid inside each coarse interval recovers the continuous volatility limit (Proposition 8). The same principle extends to settings in which the volatility process is observed or updated at a finer rate than the state, and more generally to interacting processes with non-identical observation grids, where each component contributes information when it is observed while the latent continuous-time interpolation keeps the joint dynamics coherent.

Acknowledgements

The author thanks Arakne S.r.l. for providing the working environment in which this research was carried out and for the original suggestion to look into the SBTS framework.

The author also thanks Jacopo Stortini for sustained collaboration on the volatility-related components of the construction throughout its development, and for serving as a critical interlocutor whose questions led to several methodological refinements.

The author is particularly indebted to Professor Alessio Porretta, whose analytical training and sustained guidance underpin the approach taken here. The choice to handle the local conditional dynamics through a backward heat-equation regularisation, rather than via direct drift estimation, traces back to his methodological influence, as does the introduction to the surrounding literature on mean-field Schrödinger bridges and finite-entropy Girsanov theory.

Finally, the author thanks Professor Lidia Aceto for several stimulating exchanges that proved decisive in reorienting the numerical approach in a non-trivial direction, and for the perspective that her expertise in numerical analysis brought to bear on the ill-conditioned aspects of the problem.

A Technical proof of the statistical approximation theorem

This appendix contains the proof of the statistical approximation Theorem 10. The argument is split into three layers. First, we replace the degenerate leafwise heat kernel by its spectrally floored full-rank extension. Second, we prove consistency for compactly supported regression kernels. Third, we transfer the result to the Gaussian kernels used in the implementation by a truncation argument.

A.1 Spectral regularisation of the leafwise backward kernel

Proposition 12 (Spectral regularisation of the leafwise backward kernel). *Adopt the setup of Section 3, let μ satisfy the finite-entropy condition (1), and fix $i \in \{0, \dots, N - 1\}$.*

For μ_i -a.e. (\mathbf{x}_i, y_{i+1}) the following hold.

- (i) SMOOTHNESS. *For every $\varepsilon > 0$, the regularised kernel $p_i^\varepsilon(\cdot, \cdot; t_{i+1}, \cdot)$ of (7) is smooth and strictly positive on $[t_i, t_{i+1}) \times \mathbb{R}^d \times \mathbb{R}^d$, and the*

regularised potential H_i^ε of (8) is smooth in x on \mathbb{R}^d and continuous in t on $[t_i, t_{i+1})$.

(ii) GLOBAL COLLAPSE. As $\varepsilon \downarrow 0$,

$$H_i^\varepsilon(t, x) \longrightarrow H_i(t, x) \mathbf{1}_{\mathcal{L}_i}(x) \quad \text{pointwise on } (t_i, t_{i+1}) \times \mathbb{R}^d, \quad (34)$$

locally uniformly on compact subsets of $(t_i, t_{i+1}) \times \mathcal{L}_i$ (where the limit is the exact leafwise potential H_i) and on every compact set in $(t_i, t_{i+1}) \times \mathbb{R}^d$ disjoint from $(t_i, t_{i+1}) \times \mathcal{L}_i$ (where the limit is 0).

(iii) DRIFT CONVERGENCE ON COMPACTA. As $\varepsilon \downarrow 0$, for every compact $K \subseteq (t_i, t_{i+1}) \times \mathcal{L}_i$,

$$\sup_{(t,x) \in K} |A_i^\varepsilon \nabla_x \log H_i^\varepsilon(t, x) - b_i^*(t, x)| \longrightarrow 0, \quad (35)$$

in the intrinsic Mahalanobis geometry of A_i .

(iv) DRIFT CONVERGENCE AT THE BOUNDARY (t_i, x_i) . For every $\varepsilon > 0$ sufficiently small, the diagonal limit

$$b_i^\varepsilon(t_i, x_i) := \lim_{t \downarrow t_i} A_i^\varepsilon \nabla_x \log H_i^\varepsilon(t, x_i) \quad (36)$$

exists, and $b_i^\varepsilon(t_i, x_i) \rightarrow b_i^*(t_i, x_i)$ as $\varepsilon \downarrow 0$, where $b_i^*(t_i, x_i)$ is the starting drift of Proposition 5.

Proof. Fix (\mathbf{x}_i, y_{i+1}) in a full μ_i -measure set for which Corollary 7 and Proposition 5 hold. Write $A := A_i$, $r := r_i$, $k := d - r$, and $L := \mathcal{L}_i = \text{Ran } A$ (linear subspace of admissible increments). Let P, P^\perp denote the orthogonal projections onto L and $\ker A$, and set

$$\Pi x := x_i + P(x - x_i), \quad d_\perp(x) := |P^\perp(x - x_i)|, \quad \alpha := t_{i+1} - t, \quad \beta := t_{i+1} - t_i,$$

so that $0 < \alpha < \beta$ on (t_i, t_{i+1}) . By Corollary 7, η_i^μ is supported on L ; throughout, $\delta \in L$ denotes the increment variable.

Step 1: factorisation along leaf-tangent and leaf-transverse parts.

Since the conditioning pair (\mathbf{x}_i, y_{i+1}) is fixed, the active threshold $\lambda_i^{\min,+} > 0$ is a.s. strictly positive and ε eventually falls below it; we conduct the analysis on this eventual range $\varepsilon \in (0, \lambda_i^{\min,+})$, the only regime that matters in the limit $\varepsilon \downarrow 0$. There the floor leaves the active eigenvalues unchanged and replaces the kernel directions by ε . Since $\delta \in L$ and $x_i + \delta - x_i = \delta$ has no

transverse component, while $x_i + \delta - x = \delta - P(x - x_i) - P^\perp(x - x_i)$ splits into active and transverse parts; writing $\delta' := \delta - P(x - x_i)$,

$$\begin{aligned} \langle (A_i^\varepsilon)^{-1}(x_i + \delta - x), x_i + \delta - x \rangle &= \langle A_i^+ \delta', \delta' \rangle + \frac{d_\perp(x)^2}{\varepsilon}, \\ \langle (A_i^\varepsilon)^{-1} \delta, \delta \rangle &= \langle A_i^+ \delta, \delta \rangle. \end{aligned}$$

With $\det A_i^\varepsilon = (\det A) \varepsilon^k$ the ε -dependent normalisation $(2\pi(\cdot))^{-d/2} (\det A_i^\varepsilon)^{-1/2}$ cancels between numerator and denominator. Combining the remaining factors,

$$\Phi_i^\varepsilon(t, x, \delta) := \frac{p_i^\varepsilon(t, x; t_{i+1}, \delta)}{p_i^\varepsilon(t_i, x_i; t_{i+1}, \delta)} = \exp\left(-\frac{d_\perp(x)^2}{2\alpha\varepsilon}\right) \frac{p_i(t, \Pi x; t_{i+1}, \delta)}{p_i(t_i, x_i; t_{i+1}, \delta)}, \quad \delta \in L, \quad (37)$$

where p_i is the unfloored leafwise heat kernel of A_i as a density on the increment. Integrating (37) against $\eta_i^\mu(d\delta)$ yields the global factorisation

$$H_i^\varepsilon(t, x) = \exp\left(-\frac{d_\perp(x)^2}{2\alpha\varepsilon}\right) H_i(t, \Pi x). \quad (38)$$

Step 2: Gaussian-ratio domination via the $\alpha < \beta$ gap. For δ ranging in \mathbb{R}^d (not only on L), completing the square in δ in the joint quadratic form of numerator and denominator gives

$$\Phi_i^\varepsilon(t, x, \delta) = \left(\frac{\beta}{\alpha}\right)^{d/2} \exp\left(-\frac{1}{2}\left(\frac{1}{\alpha} - \frac{1}{\beta}\right) \|\delta - m_{t,x}\|_{(A_i^\varepsilon)^{-1}}^2 + R_{t,x}^\varepsilon\right), \quad (39)$$

with $m_{t,x} := \left(\frac{1}{\alpha} - \frac{1}{\beta}\right)^{-1} \frac{1}{\alpha}(x - x_i)$ and $R_{t,x}^\varepsilon$ collecting the δ -independent residual (which embeds the transverse exponential of (37)). The crucial point is the gap $\alpha < \beta$: the *numerator* p_i^ε diffuses over the residual time α while the *prior* $p_i^\varepsilon(t_i, x_i; \cdot)$ diffuses over the full interval β , so the combined quadratic coefficient $\frac{1}{\alpha} - \frac{1}{\beta} > 0$ is strictly positive. Since $(A_i^\varepsilon)^{-1} \succeq (\|A_i\| + \varepsilon)^{-1} I$, the quadratic form in δ of (39) is strictly negative-definite uniformly on $\{t \leq t_{i+1} - \tau\}$ and on bounded x -sets, yielding the Gaussian-ratio bound

$$\Phi_i^\varepsilon(t, x, \delta) \leq C_{\tau,B} \exp(-c_{\tau,B} \|\delta - m_{t,x}\|_{(A_i^\varepsilon)^{-1}}^2),$$

with constants independent of small ε on the active eigenspace. This is the dominated integrand used throughout the appendix.

Step 3: smoothness, on-leaf identity, off-leaf decay. Smoothness of p_i^ε on $[t_i, t_{i+1}) \times \mathbb{R}^d \times \mathbb{R}^d$ is immediate from the explicit Gaussian form, for every $\varepsilon > 0$. Smoothness of H_i^ε in x on \mathbb{R}^d follows by differentiation under the integral, justified by the Gaussian-ratio domination of Step 2.

On the leaf $x \in L$ one has $\Pi x = x$ and $d_\perp(x) = 0$, so (38) reduces to $H_i^\varepsilon(t, x) = H_i(t, x)$ eventually (as soon as $\varepsilon < \lambda_i^{\min,+}$) on $(t_i, t_{i+1}) \times L$; in particular this gives the locally-uniform-on-compacta convergence stated in (ii). Off the leaf, $d_\perp(x) > 0$ and (38) gives

$$H_i^\varepsilon(t, x) \leq C \exp(-d_\perp(x)^2/(2\alpha\varepsilon)) \rightarrow 0$$

as $\varepsilon \downarrow 0$, uniformly on every compact set where $d_\perp \geq \rho > 0$. Combining the two regimes yields the global pointwise collapse (34).

Step 4: active directional derivatives. Differentiating (8) in x along an eigenvector $q_{i,j}$ inserts a polynomial-in- $(\delta - (x - x_i))$ factor against the same dominated integrand of (39); dominated convergence under the Gaussian-ratio bound of Step 2 yields, for every compact $K \Subset (t_i, t_{i+1}) \times (x_i + \mathcal{L}_i)$,

$$\sup_{(t,x) \in K} |D_{q_{i,j}} H_i^\varepsilon(t, x) - D_{q_{i,j}} H_i(t, x)| \rightarrow 0, \quad j = 1, \dots, d. \quad (40)$$

Step 5: drift convergence on compacta. Strict positivity of H_i on $(t_i, t_{i+1}) \times L$ and the uniform-on-compact convergence of both H_i^ε and its active directional derivatives (40) give $A_i^\varepsilon \nabla_x \log H_i^\varepsilon \rightarrow A_i \nabla_x \log H_i$ on compact subsets of $(t_i, t_{i+1}) \times L$. The eigenvalue weights are bounded by $\max(\lambda_{i,j}, \varepsilon) \leq \|A_i\| + \varepsilon$ uniformly in ε ; the kernel-direction contributions are multiplied by A_i^ε and absorbed by the off-leaf collapse of Step 3. This establishes (35).

Step 6: drift convergence at (t_i, x_i) . By Step 1, eventually (i.e. as soon as $\varepsilon < \lambda_i^{\min,+}$) $x_i \in L$ gives $d_\perp(x_i) = 0$, so $H_i^\varepsilon(t, x_i) = H_i(t, x_i)$ and $A_i^\varepsilon \nabla_x \log H_i^\varepsilon(t, x_i) = b_i^*(t, x_i)$ for every $t \in (t_i, t_{i+1})$. It therefore suffices to show that the diagonal limit $\lim_{t \downarrow t_i} b_i^*(t, x_i)$ exists; the value $b_i^\varepsilon(t_i, x_i)$ in (36) then equals that limit for all sufficiently small ε , yielding $b_i^\varepsilon(t_i, x_i) \rightarrow b_i^*(t_i, x_i)$ as $\varepsilon \downarrow 0$.

Differentiating the coherent ratio gives $\nabla_x \log \Phi_i^\varepsilon(t, x, \delta) = \frac{1}{\alpha} (A_i^\varepsilon)^{-1} (\delta - (x - x_i))$; hence the kernel-ratio average representation, at $x = x_i$,

$$A_i^\varepsilon \nabla_x \log H_i^\varepsilon(t, x_i) = \frac{1}{\alpha} \frac{\int_{\mathcal{L}_i} \delta \Phi_i^*(t, x_i, \delta) \eta_i^\mu(d\delta)}{\int_{\mathcal{L}_i} \Phi_i^*(t, x_i, \delta) \eta_i^\mu(d\delta)}, \quad (41)$$

where, by Step 1 with $d_\perp(x_i) = 0$, $\Phi_i^\varepsilon(t, x_i, \delta)$ reduces on \mathcal{L}_i to the unfloored leafwise ratio

$$\Phi_i^*(t, x_i, \delta) := \left(\frac{\beta}{\alpha}\right)^{r_i/2} \exp\left(-\frac{1}{2}\left(\frac{1}{\alpha} - \frac{1}{\beta}\right) \|\delta\|_{A_i^+}^2\right), \quad \delta \in \mathcal{L}_i,$$

independent of ε . For any $\delta_0 \in (0, \beta)$ and $t \in (t_i, t_i + \delta_0]$, the $\alpha < \beta$ gap of Step 2 still holds (with shrinking but strictly positive coefficient $\frac{1}{\alpha} - \frac{1}{\beta}$), so the Gaussian exponential is bounded by 1; the prefactor $(\beta/\alpha)^{r_i/2}$ is uniformly bounded by a constant C_{δ_0} . Hence $\Phi_i^*(t, x_i, \delta) \leq C_{\delta_0}$ uniformly in $(t, \delta) \in (t_i, t_i + \delta_0] \times \mathcal{L}_i$, and $\Phi_i^*(t, x_i, \delta) \rightarrow 1$ pointwise as $t \downarrow t_i$.

The denominator of (41) converges to 1 by dominated convergence (dominated by C_{δ_0}). For the numerator we use that η_i^μ has finite first A_i^+ -Mahalanobis moment: by the finite-entropy hypothesis (1) and disintegration, $H(\eta_i^\mu | k_i^R) < \infty$ for μ_i -a.e. (\mathbf{x}_i, y_{i+1}) , and the Donsker–Varadhan variational inequality applied to the Gaussian–Mahalanobis test function gives $\int_{\mathcal{L}_i} |\delta|_{A_i^+} \eta_i^\mu(d\delta) < \infty$. Hence $C_{\delta_0} |\delta|$ is η_i^μ -integrable, and dominated convergence yields

$$\int_{\mathcal{L}_i} \delta \Phi_i^*(t, x_i, \delta) \eta_i^\mu(d\delta) \longrightarrow \int_{\mathcal{L}_i} \delta \eta_i^\mu(d\delta) \quad \text{as } t \downarrow t_i.$$

Combining with $\alpha \rightarrow \beta = t_{i+1} - t_i$, the right-hand side of (41) converges to

$$\frac{1}{t_{i+1} - t_i} \int_{\mathcal{L}_i} \delta \eta_i^\mu(d\delta) =: b_i^*(t_i, x_i),$$

the starting drift of Proposition 5. The limit is independent of ε for all sufficiently small ε ; this establishes (36). \square

A.2 Compact-kernel estimator and local Gaussian domination

We now introduce the auxiliary regression scheme used in the proof. This scheme is not yet the Gaussian one used in the implementation. It is a compactly supported Nadaraya–Watson scheme with M -dependent kernel profiles. The support may expand in the rescaled variable, but the effective conditioning neighbourhood shrinks because $h_M R_M \rightarrow 0$. This form is needed later to compare with truncated Gaussian weights.

Fix $i \in \{0, \dots, N-1\}$ and a conditioning pair (\mathbf{x}_i, y_{i+1}) with $\mathbf{x}_i = (x_0, \dots, x_i)$ and $y_{i+1} \in \mathcal{Y}$ in the full μ_i -measure regular set where Corollary 7 and Proposition 5 hold and where the eigenstructure of A_i is locally continuous. Write

$$\mathbf{X}_i := (X_{t_0}, \dots, X_{t_i}), \quad q_i := \dim(\mathbf{X}_i) = (i+1)d, \quad q_Y := \dim \mathcal{Y},$$

so the augmented past (\mathbf{X}_i, Y) lives in $\mathbb{R}^{q_i+q_Y}$. Throughout this appendix the compact-kernel estimator is written in the Euclidean chart of the macro-variable \mathcal{U}_i^ℓ (Remark 9), in which the effective dimension is $q_{\text{eff}} = q_i + q_Y$; the abstract small-ball formulation of (S1) gives the same conclusions on replacing $q_i + q_Y$ by q_{eff} in all bandwidth and denominator estimates. Let

$$(\mathbf{X}_i^{(m)}, Y^{(m)}, \Delta X_{i+1}^{(m)}), \quad \Delta X_{i+1}^{(m)} := X_{t_{i+1}}^{(m)} - X_{t_i}^{(m)}, \quad m = 1, \dots, M,$$

be i.i.d. samples from μ on the augmented state space, with the realised next-interval increment as response and the latent realisation $Y^{(m)}$ observed.

Let $K_M : \mathbb{R}^{q_i+q_Y} \rightarrow [0, \infty)$ be a sequence of continuous regression profiles on the augmented past. We assume

$$\int_{\mathbb{R}^{q_i+q_Y}} K_M(u) du = 1, \quad \text{supp } K_M \subset B(0, R_M), \quad R_M \uparrow \infty,$$

together with a radial integrable envelope: there exists a bounded measurable $\bar{K} : [0, \infty) \rightarrow [0, \infty)$ such that

$$0 \leq K_M(u) \leq \bar{K}(|u|^2) \quad \text{for all } u \in \mathbb{R}^{q_i+q_Y}, \quad M, \quad \int_{\mathbb{R}^{q_i+q_Y}} \bar{K}(|u|^2) du < \infty.$$

Let $h_M \downarrow 0$ be a bandwidth sequence with $h_M R_M \rightarrow 0$. The rescaled kernel and Nadaraya–Watson weights localising on the augmented past at the runtime point (\mathbf{x}_i, y_{i+1}) are

$$K_{M, h_M}(u) := h_M^{-(q_i+q_Y)} K_M(u/h_M),$$

$$\omega_{i,m}^{M,K}(\mathbf{x}_i, y_{i+1}) := \frac{K_{M, h_M}((\mathbf{x}_i, y_{i+1}) - (\mathbf{X}_i^{(m)}, Y^{(m)}))}{\sum_{n=1}^M K_{M, h_M}((\mathbf{x}_i, y_{i+1}) - (\mathbf{X}_i^{(n)}, Y^{(n)}))}.$$

Throughout, a generic conditioning vector for the principal past is denoted $\boldsymbol{\xi}_i = (\xi_0, \dots, \xi_i) \in (\mathbb{R}^d)^{i+1}$ with last component ξ_i . The *compact-kernel empirical regularised backward potential* is defined by

$$\hat{H}_i^{\varepsilon, M, K}(t, x) := \sum_{m=1}^M \omega_{i,m}^{M,K}(\mathbf{x}_i, y_{i+1}) \Phi_i^\varepsilon(t, x, \Delta X_{i+1}^{(m)}), \quad (42)$$

where

$$\Phi_i^\varepsilon(t, x, z) := \frac{p_i^\varepsilon(t, \mathbf{x}_i; t_{i+1}, z)}{p_i^\varepsilon(t_i, \mathbf{x}_i; t_{i+1}, z)}$$

is the coherently regularised kernel-ratio response of (8), with the same spectrally floored covariance A_i^ε in numerator and denominator. The estimator (42) is the Nadaraya–Watson estimator of the conditional expectation

$$H_i^\varepsilon(t, x) = \mathbb{E}_\mu[\Phi_i^\varepsilon(t, x, X_{t_{i+1}}; \mathbf{x}_i, y_{i+1}) \mid \mathbf{X}_i = \mathbf{x}_i, Y = y_{i+1}], \quad (43)$$

which is (9) written under μ .

Statistical assumptions for the compact-kernel argument. The Nadaraya–Watson regression localises on the macro-conditioning variable U_i^ℓ of (15) at the runtime query point u_0 , in the geometry of the pseudo-distance d_ε^ℓ of (16); $B_\varepsilon(u_0, r) := \{v : d_\varepsilon^\ell(u_0, v) < r\}$. The assumptions (S1)–(S6) of Section 4.4 apply. For ease of reference:

- (S1) *Local lower mass.* There exist $r_0, c_{u_0}, q_{\text{eff}} > 0$ with $\mu_U(B_\varepsilon(u_0, r)) \geq c_{u_0} r^{q_{\text{eff}}}$ for $0 < r < r_0$;
- (S2) *Conditional continuity.* $v \mapsto \eta_i^{\mu, \ell}(\cdot | v)$ weakly continuous near u_0 ; $v \mapsto A_i^\ell(v)$ operator-norm continuous at u_0 ;
- (S3) *i.i.d. sample.* $(U_i^{\ell, (m)}, \Delta X_{i+1}^{(m)})_{m=1}^M$ i.i.d.;
- (S4) *Bandwidth.* $h_M \downarrow 0$, $Mh_M^{q_{\text{eff}}} \rightarrow \infty$; for compact-kernel truncation $R_M \uparrow \infty$ with $h_M R_M \rightarrow 0$;
- (S5) *Strong bandwidth.* $Mh_M^{q_{\text{eff}}} / \log M \rightarrow \infty$ for a.s. statements;
- (S6) *Local conditional entropy admissibility.* For some $\rho > 0$,

$$\sup_{v \in B_\varepsilon(u_0, \rho)} H(\eta_i^{\mu, \ell}(\cdot | v) | k_i^{R, \ell}(\cdot | v)) < \infty.$$

The reference-comparison factor of Lemma 14 satisfies $\kappa_\varepsilon^\ell \leq \exp(d_\varepsilon^\ell/2)$ since d_ε^ℓ already contains the reference log-spectral distance (17).

Consequence of (S6): local first moment of the increment. By Donsker–Varadhan applied to the intrinsic Mahalanobis quadratic test against the frozen reference,

$$\sup_{v \in C_\rho(u_0)} \int |\delta|_{C_i^\ell(v)+} \eta_i^{\mu, \ell}(d\delta | v) < \infty; \quad (44)$$

the reference-comparison estimate (48) transports this intrinsic control to the runtime/query geometry,

$$\begin{aligned} & \sup_{v \in C_\rho(u_0)} \int |\delta|_{C_{i, \varepsilon}^\ell(u_0)-1} \eta_i^{\mu, \ell}(d\delta | v) \\ & \leq \left(\sup_{v \in C_\rho(u_0)} \kappa_\varepsilon^\ell(u_0, v) \right) \sup_{v \in C_\rho(u_0)} \int |\delta|_{C_i^\ell(v)+} \eta_i^{\mu, \ell}(d\delta | v) < \infty. \end{aligned} \quad (45)$$

On the active leaf the Euclidean first-moment bound follows from $|\delta| \leq \lambda_{\max}(A_i(v))^{1/2} |\delta|_{C_i^\ell(v)+}$:

$$\sup_{v \in C_\rho(u_0)} \int |\delta| \eta_i^\mu(d\delta | v) < \infty. \quad (46)$$

This bound is used only for the empirical *initial-boundary* drift estimator below; the variational construction of Proposition 5 does not need it. At fixed $\varepsilon \in (0, \lambda_i^{\min,+})$, the regularised covariance $A_i^\varepsilon \succeq \varepsilon I$ with $\det A_i^\varepsilon \geq \varepsilon^d$, so the finite- ε Gaussian estimators of this appendix are well defined and uniformly nondegenerate; the rank r_i and the active leaf \mathcal{L}_i are fixed by the conditioning and enter only in the $\varepsilon \downarrow 0$ geometric step (Proposition 12).

Lemma 13 (Kernel denominator and localisation from the small-ball lower mass). *Under (S1), $D_h(u_0) := \int W_h(u_0, v) \mu_U(dv)$ satisfies $D_h(u_0) \gtrsim h^{q_{\text{eff}}}$ as $h \downarrow 0$, so that $MD_{h_M}(u_0) \rightarrow \infty$ under (S4) and a.s. under (S5). Moreover the normalised kernel measures concentrate at u_0 : for every $\rho > 0$,*

$$\frac{\int_{\{d_\varepsilon(u_0, v) > \rho\}} W_h(u_0, v) \mu_U(dv)}{D_h(u_0)} \rightarrow 0 \quad \text{as } h \downarrow 0. \quad (47)$$

Proof. For the compact case, the kernel is positive on a neighbourhood of the origin in each factor, so for some $c, c' > 0$, $W_h(u_0, v) \geq c \mathbf{1}_{B_\varepsilon(u_0, c'h)}(v)$; hence $D_h(u_0) \geq c \mu_U(B_\varepsilon(u_0, c'h)) \geq cc_{u_0}(c'h)^{q_{\text{eff}}}$. For the Gaussian case, $W_h(u_0, v) \geq \exp(-c'^2/2) \mathbf{1}_{B_\varepsilon(u_0, c'h)}(v)$, giving the same lower bound up to constants. In both cases the numerator in (47) is bounded by $\sup W_h$ times either the kernel-tail mass (compact: zero past $c''h$; Gaussian: $e^{-\rho^2/(2h^2)}$), so the ratio is at most $e^{-\rho^2/(2h^2)}/(ch^{q_{\text{eff}}}) \rightarrow 0$. \square

Lemma 14 (Reference-aware localisation and Mahalanobis comparison). *For every increment $\delta \in \text{Ran } C_i^\ell(v)$,*

$$|\delta|_{C_{i,\varepsilon}^\ell(u_0)^{-1}} \leq \kappa_\varepsilon^\ell(u_0, v) |\delta|_{C_i^\ell(v)+}, \quad \kappa_\varepsilon^\ell(u_0, v) \leq \exp\left(\frac{1}{2} d_{\text{ref},\varepsilon}^\ell(u_0, v)\right). \quad (48)$$

In particular, on the kernel-localised set $\{d_{\text{ref},\varepsilon}^\ell(u_0, v) \leq r\}$ the historical/intrinsic Mahalanobis norm $|\delta|_{C_i^\ell(v)+}$ controls the runtime/query Mahalanobis norm $|\delta|_{C_{i,\varepsilon}^\ell(u_0)^{-1}}$ with constant $e^{r/2}$; compact reference-aware kernels give uniform comparability on their support, and Gaussian reference-aware kernels penalise the comparison-factor growth.

Proof. Write $\delta = C_i^\ell(v)^{1/2}\zeta$ for some $\zeta \in \mathbb{R}^d$. Then

$$|\delta|_{C_{i,\varepsilon}^\ell(u_0)^{-1}} = |C_{i,\varepsilon}^\ell(u_0)^{-1/2}C_i^\ell(v)^{1/2}\zeta| \leq \kappa_\varepsilon^\ell(u_0, v) |\zeta| = \kappa_\varepsilon^\ell(u_0, v) |\delta|_{C_i^\ell(v)^+}.$$

The bound $\kappa_\varepsilon^\ell \leq \exp(d_{\text{ref},\varepsilon}^\ell/2)$ is the spectral form of the quadratic-form sandwich (17), using $C_i^\ell(v) \preceq C_{i,\varepsilon}^\ell(v)$. \square

The next lemma is the core technical estimate of the appendix: it controls the integrand pointwise on compact internal cylinders, and compact-uniform convergence follows by Ascoli–Arzelà.

Lemma 15 (Gaussian-ratio domination). *For every $\varepsilon \in (0, \lambda_i^{\min,+})$, every compact $J \Subset (t_i, t_{i+1})$, $B \Subset (x_i + \mathcal{L}_i)$, there exist a compact neighbourhood $C \Subset C_i$ of (\mathbf{x}_i, y_{i+1}) , a measurable centre map $(t, x, \boldsymbol{\xi}_i) \mapsto m_{t,x,\boldsymbol{\xi}_i} \in \mathbb{R}^d$, and constants $c, C_{J,B} > 0$ such that*

$$\begin{aligned} \Phi_i^\varepsilon(t, x, \delta; \boldsymbol{\xi}_i) &\leq C_{J,B} \exp(-c \|\delta - m_{t,x,\boldsymbol{\xi}_i}\|_{(A_i^\varepsilon)^{-1}}^2) \\ &\quad \forall t \in J, x \in B, \boldsymbol{\xi}_i \in C, \delta \in \mathbb{R}^d. \end{aligned} \quad (49)$$

The same bound holds for every active directional derivative $D_{q_{i,j}} \Phi_i^\varepsilon$, $j = 1, \dots, r_i$.

Proof. Write $\alpha := t_{i+1} - t$, $\beta := t_{i+1} - t_i$, so $0 < \alpha \leq \beta - \tau$ on J for some $\tau > 0$. Both densities in Φ_i^ε share the same covariance $A_i^\varepsilon(\boldsymbol{\xi}_i)$ and the same ε -dependent normalisation $(2\pi)^{-d/2}(\det A_i^\varepsilon)^{-1/2}$; the latter is δ -independent and cancels in the ratio up to the factor $(\beta/\alpha)^{d/2}$. The remaining exponent in δ is

$$-\frac{1}{2\alpha} \|x_i + \delta - x\|_{(A_i^\varepsilon)^{-1}}^2 + \frac{1}{2\beta} \|\delta\|_{(A_i^\varepsilon)^{-1}}^2,$$

a strictly negative-definite quadratic form in δ since $\alpha < \beta$. Completing the square yields a centre $m_{t,x,\boldsymbol{\xi}_i}$ and residual $R_{t,x,\boldsymbol{\xi}_i}^\varepsilon$ such that

$$\Phi_i^\varepsilon(t, x, \delta; \boldsymbol{\xi}_i) = \left(\frac{\beta}{\alpha}\right)^{d/2} \exp\left(-\frac{1}{2}\left(\frac{1}{\alpha} - \frac{1}{\beta}\right) \|\delta - m_{t,x,\boldsymbol{\xi}_i}\|_{(A_i^\varepsilon)^{-1}}^2 + R_{t,x,\boldsymbol{\xi}_i}^\varepsilon\right).$$

On $J \times B$ and on a sufficiently small compact $C \Subset C_i$ of (\mathbf{x}_i, y_{i+1}) , continuity of $(\boldsymbol{\xi}_i, t, x) \mapsto m_{t,x,\boldsymbol{\xi}_i}$ and of $A_i(\boldsymbol{\xi}_i)$ gives a uniform upper bound on the residual, and the $\alpha < \beta$ gap gives $\frac{1}{\alpha} - \frac{1}{\beta} \geq \tau/(\beta(\beta - \tau)) > 0$. The quadratic decay rate c on the active eigenspace is bounded below uniformly in $\varepsilon \in (0, \lambda_i^{\min,+})$ since $(A_i^\varepsilon)^{-1} \succeq (\|A_i\| + \varepsilon)^{-1}I$ there, while the transverse coefficient $1/(\varepsilon\alpha)$ only adds decay; setting $c := \frac{1}{2}(\frac{1}{\alpha} - \frac{1}{\beta})$ and absorbing $(\beta/\alpha)^{d/2}$, $\exp(R)$ and continuity prefactors into a finite $C_{J,B}$ proves (49).

The directional derivative $D_{q_{i,j}} \log \Phi_i^\varepsilon$ along $q_{i,j}$ is $\alpha^{-1} \langle (A_i^\varepsilon)^{-1} (\delta - (x - x_i)), q_{i,j} \rangle$; chain rule inserts a polynomial-in- $(\delta - (x - x_i))$ prefactor against the same Gaussian envelope, absorbed into the exponential domination at the price of slightly smaller c and larger $C_{J,B}$ via $|P(u)| e^{-c|u|^2} \leq C' e^{-c'|u|^2}$ for every polynomial P and $0 < c' < c$. \square

Lemma 16 (Asymptotic nondegeneracy of the regression denominator). *Assume (S1), (S3), (S4). Then*

$$\frac{1}{M} \sum_{m=1}^M K_{M,h_M}(\mathbf{x}_i - \mathbf{X}_i^{(m)}) \longrightarrow \pi_i(\mathbf{x}_i)$$

in probability; under (S5), almost surely. In particular, since $\pi_i(\mathbf{x}_i) > 0$, $\sum_{m=1}^M K_{M,h_M}(\mathbf{x}_i - \mathbf{X}_i^{(m)}) \geq M(\pi_i(\mathbf{x}_i) - \eta)$ eventually for every $\eta \in (0, \pi_i(\mathbf{x}_i))$, in the same stochastic mode.

Proof. The bias term is

$$\int_{\mathbb{R}^{q_i+q_Y}} K_M(u) \pi_i(\mathbf{x}_i - h_M u) du \longrightarrow \pi_i(\mathbf{x}_i),$$

by continuity of π_i , $\int K_M = 1$, and dominated convergence against \bar{K} using $h_M R_M \rightarrow 0$. The variance is bounded by $\|\bar{K}\|_\infty h_M^{-(q_i+q_Y)}$, so

$$\text{Var}\left(\frac{1}{M} \sum_m K_{M,h_M}(\mathbf{x}_i - \mathbf{X}_i^{(m)})\right) = O(1/(M h_M^{q_i+q_Y})) \longrightarrow 0.$$

The almost-sure version follows from exponential inequalities for bounded empirical processes under (S5) and Borel–Cantelli. \square

A.3 Pointwise and compact-uniform consistency

We now combine standard pointwise Nadaraya–Watson consistency with the Gaussian domination of Lemma 15 to obtain uniform convergence on every compact subset of the open intervalwise cylinder.

Proposition 17 (Pointwise consistency). *Assume (S1)–(S4) and fix $\varepsilon \in (0, \lambda_i^{\min,+})$. For every fixed $(t, x) \in (t_i, t_{i+1}) \times \mathcal{L}_i$,*

$$\hat{H}_i^{\varepsilon, M, K}(t, x) \longrightarrow H_i^\varepsilon(t, x)$$

in probability as $M \rightarrow \infty$. Under (S5), the convergence is almost sure. The same conclusion holds for the directional derivative $D_{q_{i,j}} \hat{H}_i^{\varepsilon, M, K}$, $j = 1, \dots, d$, towards $D_{q_{i,j}} H_i^\varepsilon$, along every eigenvector of A_i .

Proof. Write the empirical potential as a Nadaraya–Watson estimator on the augmented past of the conditional expectation (43). For fixed (t, x) and ε the response

$$(\boldsymbol{\xi}_i, y) \mapsto \Phi_{t,x}^\varepsilon(\boldsymbol{\xi}_i, y) := \mathbb{E}_\mu[\Phi_i^\varepsilon(t, x, X_{t_{i+1}}) \mid \mathbf{X}_i = \boldsymbol{\xi}_i, Y = y]$$

is continuous at $(\boldsymbol{\xi}_i, y) = (\mathbf{x}_i, y_{i+1})$, since $\eta_i^\mu(\cdot \mid \boldsymbol{\xi}_i, y)$ depends weakly continuously on $(\boldsymbol{\xi}_i, y)$ by (S2) and the Gaussian-ratio response Φ_i^ε is dominated by Lemma 15 via the $\alpha < \beta$ gap of the coherent kernel ratio. The denominator is asymptotically nondegenerate by Lemma 16. Standard Nadaraya–Watson consistency for compactly supported regression kernels under (S3)–(S4) (cf. [10]) yields $\widehat{H}_i^{\varepsilon, M, K}(t, x) \rightarrow H_i^\varepsilon(t, x)$ in probability, and almost surely under (S5). Differentiating Φ_i^ε in x along any eigenvector $q_{i,j}$, $j = 1, \dots, d$, inserts a polynomial-in- $(z - x)$ factor against the same dominated Gaussian-ratio integrand of Lemma 15. The same Nadaraya–Watson argument applies to give pointwise convergence of $D_{q_{i,j}} \widehat{H}_i^{\varepsilon, M, K}$ for every $j = 1, \dots, d$. \square

Proposition 18 (Compact-uniform consistency). *Assume (S1)–(S4) and fix $\varepsilon \in (0, \lambda_i^{\min,+})$. For every compact*

$$K = J \times B \Subset (t_i, t_{i+1}) \times \mathcal{L}_i,$$

$$\sup_{(t,x) \in K} |\widehat{H}_i^{\varepsilon, M, K}(t, x) - H_i^\varepsilon(t, x)| \longrightarrow 0 \quad \text{in probability.}$$

Under (S5), the convergence is almost sure. The same uniform convergence holds for every directional derivative $D_{q_{i,j}}$, $j = 1, \dots, d$, along the eigenvectors of A_i , both active and kernel directions included.

Proof. By Lemma 15, the integrand defining $\widehat{H}_i^{\varepsilon, M, K}(t, x)$ is, on the event where every sample with nonzero NW-weight satisfies $\mathbf{X}_i^{(m)} \in C$, bounded by $C_{J,B} e^{-c|\Delta X_{i+1}^{(m)}|^2}$ uniformly for $(t, x) \in K$. Combined with the denominator lower bound of Lemma 16, this yields a uniform bound

$$\sup_{(t,x) \in K} |\widehat{H}_i^{\varepsilon, M, K}(t, x)| \leq \tilde{C}_{J,B}$$

in the relevant stochastic mode, for all sufficiently large M . The same bound holds for the exact H_i^ε .

For equicontinuity in $(t, x) \in K$, the explicit Gaussian form of p_i^ε shows that, for any $(t, x), (t', x') \in J \times B$,

$$\begin{aligned} |p_i^\varepsilon(t, x; t_{i+1}, x_i + \delta) - p_i^\varepsilon(t', x'; t_{i+1}, x_i + \delta)| \\ \leq L_{J,B} (|t - t'| + |x - x'|) e^{-c'|\delta|^2}, \end{aligned}$$

for constants $L_{J,B}, c' > 0$ uniform on $J \times B$ and $\delta \in \mathbb{R}^d$ with $\xi_i + \delta \in \mathcal{L}_i^{\xi_i, y}$, for $(\xi_i, y) \in C$; on this neighbourhood the regularised covariance $A_i^\varepsilon(\xi_i, y)$ is uniformly elliptic by (S2). The same domination (49) thus controls the difference, and summing against the NW weights gives

$$|\widehat{H}_i^{\varepsilon, M, K}(t, x) - \widehat{H}_i^{\varepsilon, M, K}(t', x')| \leq \widetilde{L}_{J,B} (|t - t'| + |x - x'|)$$

in the same stochastic mode, for all large M . The exact H_i^ε satisfies the same Lipschitz estimate on K .

The family $\{(t, x) \mapsto \widehat{H}_i^{\varepsilon, M, K}(t, x)\}_M$ is therefore eventually equibounded and equi-Lipschitz on the compact metric space K . Ascoli–Arzelà applied to subsequences identifies the only possible limit, by Proposition 17, with H_i^ε , and the whole sequence converges uniformly on K in the stated stochastic mode.

For the active derivatives $D_{q_{i,j}}$, the same argument applies: the differentiated kernel $D_{q_{i,j}} p_i^\varepsilon(t, x; t_{i+1}, \nu)$ acquires a polynomial-in- $(\nu - x)$ factor against the Gaussian, which is dominated by (49), and a Lipschitz estimate on $(t, x) \in K$ follows from joint smoothness of the Gaussian density. Compact-uniform convergence on K then follows by the same Ascoli–Arzelà argument applied to the derivative estimator. \square

A.4 Gaussian-kernel transfer and drift consistency

The Gaussian weights of (18) have unbounded support; we transfer the compact-kernel consistency by a truncation argument, after reducing the reference-aware product kernel to an isotropic Gaussian chart.

Reduction to the isotropic Gaussian chart. Conditionally on the runtime conditioning, define the linear map $T : \mathbb{R}^{q_i + q_Y} \rightarrow \mathbb{R}^{q_i + q_Y}$ by $(x_i, \Delta x_i, \dots, \Delta x_1, y) \mapsto (x_i, C_i^\varepsilon(\mathbf{u}_{i-1})^{-1/2} \Delta x_i, \dots, C_1^\varepsilon(\mathbf{u}_0)^{-1/2} \Delta x_1, \Sigma_Y^{-1/2} y)$, with Σ_Y an isotropising covariance on \mathcal{Y} . The same query-determined transformation is applied to every sample. In the transformed chart, the reference-aware kernel (18) becomes a scalar multiple of the isotropic Gaussian Γ_h ; the query-dependent Jacobian is m -independent and cancels in the Nadaraya–Watson ratio (19), so the weights $\omega_{i,m}^{M,G}$ coincide with the classical isotropic Gaussian NW weights in the transformed chart. The spectral floor and continuity of $A_k(\cdot, \cdot)$ on the regular set bound the singular values of T above and below by deterministic constants (depending on ε and on the conditioning neighbourhood, but not on rank stability of the unfloored A_k). It is therefore enough to argue in the isotropic chart; we keep the notation

$\mathbf{x}_i, \mathbf{X}_i^{(m)}, y_{i+1}, Y^{(m)}$ for the conditioning variables, with the understanding that Γ_h below is the isotropic Gaussian kernel after this change of coordinates.

Set $q := q_i + q_Y$ and

$$\Gamma(u) := (2\pi)^{-q/2} e^{-|u|^2/2}, \quad \Gamma^{(R)}(u) := \frac{\Gamma(u) \mathbf{1}_{\{|u| \leq R\}}}{Z_R}, \quad Z_R := \int_{|v| \leq R} \Gamma(v) dv.$$

The scaled truncated and genuine Gaussian regression kernels are

$$\Gamma_{h,R}(u) := h^{-q} \Gamma^{(R)}(u/h), \quad \Gamma_h(u) := h^{-q} \Gamma(u/h).$$

The truncation $\Gamma^{(R_M)}$ satisfies the compact-kernel assumptions (S3) with R_M the truncation radius and \bar{K} the radial Gaussian envelope.

Let $\omega_{i,m}^{M,R_M}(\mathbf{x}_i, y_{i+1})$ and $\omega_{i,m}^{M,G}(\mathbf{x}_i, y_{i+1})$ be the Nadaraya–Watson weights built from Γ_{h_M, R_M} and Γ_{h_M} , respectively, and let $\hat{H}_i^{\varepsilon, M, R_M}$ and $\hat{H}_i^{\varepsilon, M, G}$ be the corresponding empirical potentials.

Lemma 19 (Nondegeneracy of the Gaussian regression denominator). *Assume (S1), $h_M \downarrow 0$, $Mh_M^{q_i+q_Y} \rightarrow \infty$. Then $M^{-1} \sum_{m=1}^M \Gamma_{h_M}(\mathbf{x}_i - \mathbf{X}_i^{(m)}) \rightarrow \pi_i(\mathbf{x}_i, y_{i+1})$ in probability, and almost surely under (S5).*

Proof. For the lower bound, fix $\eta \in (0, \pi_i(\mathbf{x}_i, y_{i+1}))$ and choose R with $Z_R \pi_i(\mathbf{x}_i, y_{i+1}) \geq \pi_i(\mathbf{x}_i, y_{i+1}) - \eta/2$. The inequality $\Gamma(u) \geq Z_R \Gamma^{(R)}(u)$ gives $D_M^G(\mathbf{x}_i) \geq Z_R D_M^{(R)}(\mathbf{x}_i)$, and Lemma 16 applied to the fixed compactly supported kernel $\Gamma^{(R)}$ yields the lower bound. The matching upper bound follows from the standard Parzen–Rosenblatt estimate for the Gaussian kernel under the bandwidth conditions. \square

Under the coherent ratio formulation of (8), the empirical estimator integrates Φ_i^ε directly: the same floored covariance $A_i^\varepsilon(\mathbf{x}_i, y_{i+1})$ appears in numerator and denominator and the volume factor $(\det A_i^\varepsilon)^{-1/2}$ cancels, so no sample-specific volume term has to be controlled. What still has to be finite, with high probability over the sample cloud, is the *runtime* Mahalanobis evaluated on the sample increment, $|\delta_m|_{(A_i^\varepsilon(\mathbf{x}_i, y_{i+1}))^{-1}}$. To control it, define the *sample-conditioned intrinsic increment norm*

$$r_i(\boldsymbol{\xi}_i, \delta) := |C_i(\boldsymbol{\xi}_i)^{+/2} \delta|, \quad C_i(\boldsymbol{\xi}_i) := (t_{i+1} - t_i) A_i(\boldsymbol{\xi}_i), \quad (50)$$

where $C_i(\boldsymbol{\xi}_i)^{+/2}$ is the principal symmetric square root of the Moore–Penrose pseudo-inverse of $C_i(\boldsymbol{\xi}_i)$; $r_i(\boldsymbol{\xi}_i, \delta)$ is the intrinsic norm of δ under the sample’s own frozen reference. The finite-entropy hypothesis (1) controls $r_i(\boldsymbol{\xi}_i, \delta_m)$

with high probability via entropy disintegration relative to the sample-conditioned reference density $q_i(\delta \mid \boldsymbol{\xi}_i) := p_i(t_i, \xi_i; t_{i+1}, \xi_i + \delta \mid \boldsymbol{\xi}_i)$ (the unfloored leafwise density of ΔX_{i+1} under R given $\mathbf{X}_i = \boldsymbol{\xi}_i$), and the runtime Mahalanobis is equivalent to $r_i(\boldsymbol{\xi}_i, \cdot)$ on the localised sample cloud by continuity of $(\boldsymbol{\xi}_i, y) \mapsto A_i(\boldsymbol{\xi}_i, y)$ at (\mathbf{x}_i, y_{i+1}) and equivalence of norms on the finite-dimensional matrix space \mathbb{S}^d .

Proposition 20 (High-probability intrinsic localisation for Gaussian weights). *Assume (S1)–(S4) and the finite-entropy hypothesis (1). Fix $\varepsilon \in (0, \lambda_i^{\min,+})$ and a compact $K \subseteq (t_i, t_{i+1}) \times (x_i + \mathcal{L}_i)$. For every $\rho > 0$ there exist $R < \infty$ and M_0 such that, with*

$$\begin{aligned} \mathcal{I}_M(R) := \{m \leq M : |(\mathbf{X}_i^{(m)}, Y^{(m)}) - (\mathbf{x}_i, y_{i+1})| \leq h_M R_M, \\ r_i(\mathbf{X}_i^{(m)}, \Delta X_{i+1}^{(m)}) \leq R\}, \\ \sup_{(t,x) \in K} \left| \sum_{m \notin \mathcal{I}_M(R)} \omega_{i,m}^{M,G}(\mathbf{x}_i, y_{i+1}) \Phi_i^\varepsilon(t, x, \Delta X_{i+1}^{(m)}) \right| \leq \rho \end{aligned} \quad (51)$$

holds with probability $\geq 1 - \rho$ for all $M \geq M_0$. The same holds for $D_{q_{i,j}} \Phi_i^\varepsilon$, $j = 1, \dots, r_i$.

Proof. Decompose $\mathcal{I}_M(R)^c = \mathcal{B}_M(R) \cup \mathcal{A}_M(R)$ into the endpoint-cost tail $\mathcal{B}_M(R) := \{m : r_i > R\}$ and the conditioning-far set $\mathcal{A}_M(R) := \{m : |(\mathbf{X}_i^{(m)}, Y^{(m)}) - (\mathbf{x}_i, y_{i+1})| > h_M R_M, r_i \leq R\}$, and bound each.

Endpoint-cost tail. Entropy disintegration along the past gives

$$H(\mu \mid \mu_T^R) = H(\mu_i \mid \mu_i^R) + \int H(\eta_i^\mu(\cdot \mid \boldsymbol{\xi}_i) \mid k_i^R(\cdot \mid \boldsymbol{\xi}_i)) \mu_i(d\boldsymbol{\xi}_i). \quad (52)$$

By (1) and Markov, $E_\rho := \{\boldsymbol{\xi}_i : H(\eta_i^\mu \mid k_i^R) \leq L_\rho\}$ satisfies $\mu_i(E_\rho) \geq 1 - \rho$ for some $L_\rho < \infty$. On E_ρ , under the intrinsic parametrisation $\delta \mapsto C_i(\boldsymbol{\xi}_i)^{+/2} \delta$ the reference k_i^R is standard r_i -Gaussian with tail $k_i^R(r_i > R \mid \boldsymbol{\xi}_i) \leq C_{r_i} e^{-R^2/(2r_i)}$; Donsker–Varadhan transfers the tail to η_i^μ :

$$\sup_{\boldsymbol{\xi}_i \in E_\rho} \eta_i^\mu(r_i > R \mid \boldsymbol{\xi}_i) \leq \frac{L_\rho + \log 2}{R^2/(2r_i) - \log C_{r_i}} \xrightarrow{R \rightarrow \infty} 0. \quad (53)$$

For $R = R(\rho, L_\rho)$ large enough this is $\leq \rho^2$; Markov on $\#\mathcal{B}_M(R)/M$ bounds its empirical mass by ρ w.h.p.

Conditioning-far set. On $\mathcal{A}_M(R)$, Lemma 15 bounds Φ_i^ε uniformly (constants $c, C_{J,B}$ of the lemma absorb the runtime ε -dependence); by Lemma 19 and the Gaussian tail $\Gamma_{h_M}(u) \leq e^{-R_M^2/2} \|\Gamma_{h_M}\|_\infty$ for $|u| > h_M R_M$, $\omega_{i,m}^{M,G} \leq$

$2e^{-R_M^2/2} \|\Gamma_{h_M}\|_\infty / (M\pi_i(\mathbf{x}_i, y_{i+1}))$ for large M ; the factor $e^{-R_M^2/2} \rightarrow 0$ kills the contribution.

Runtime vs. sample Mahalanobis. The bound from Lemma 15 on Φ_i^ε is in the runtime norm $\|\cdot\|_{(A_i^\varepsilon(\mathbf{x}_i, y_{i+1}))^{-1}}$, while $r_i(\boldsymbol{\xi}_i^{(m)}, \delta_m)$ controls the sample norm. On the localised cloud, operator-norm continuity of $(\boldsymbol{\xi}_i, y) \mapsto A_i^\varepsilon(\boldsymbol{\xi}_i, y)$ by (S2) and equivalence of norms on \mathbb{S}^d give $\|A_i^\varepsilon(\boldsymbol{\xi}_i, y) - A_i^\varepsilon(\mathbf{x}_i, y_{i+1})\| \rightarrow 0$, so the two intrinsic norms are equivalent up to a multiplicative factor approaching 1; the sample bound $r_i \leq R$ transfers to a runtime bound $\|\delta_m\|_{(A_i^\varepsilon(\mathbf{x}_i, y_{i+1}))^{-1}} \leq R(1 + o(1))$ on the event of the two preceding steps.

Combining yields (51). The active-derivative case is identical: differentiating Φ_i^ε along $q_{i,j}$ inserts a polynomial-in- $(\delta - (x - x_i))$ factor absorbed into the same Gaussian envelope of Lemma 15. \square

Remark 21 (Sample-reference compatibility). *Bound (51) is the statistical analogue of the intrinsic endpoint tightness of Section 3.2: the endpoint displacement of the sample is measured in the geometry of its own covariance cumulant, and finite entropy (52) transfers the Gaussian endpoint tails of the frozen reference to the target conditional law. Under the coherent ratio formulation, the volume factor cancels in numerator and denominator and only the intrinsic r_i -tail and the sample-to-runtime Mahalanobis equivalence on the localised cloud are needed.*

Proposition 22 (Compact-uniform consistency of the Gaussian estimator). *Under (S1)–(S4), the finite-entropy hypothesis (1), $\varepsilon \in (0, \lambda_i^{\min,+})$ fixed, and $R_M \uparrow \infty$ with $h_M R_M \rightarrow 0$: for every compact $K \Subset (t_i, t_{i+1}) \times (x_i + \mathcal{L}_i)$,*

$$\sup_{(t,x) \in K} |\widehat{H}_i^{\varepsilon, M, G}(t, x) - H_i^\varepsilon(t, x)| \rightarrow 0 \quad \text{in probability,}$$

and the same uniform convergence holds for every active directional derivative $D_{q_{i,j}}$, $j = 1, \dots, r_i$. The truncated auxiliary estimator $\widehat{H}_i^{\varepsilon, M, R_M}$ converges almost surely on its own under (S5).

Proof. The truncated profile $K_M := \Gamma^{(R_M)}$ satisfies the compact-kernel assumptions of Section A.2; by Proposition 18, $\widehat{H}_i^{\varepsilon, M, R_M} \rightarrow H_i^\varepsilon$ uniformly on K in probability under (S4), a.s. under (S5).

For the passage to the full Gaussian estimator, with $S_M := \sum_m \Gamma_{h_M}(\mathbf{x}_i - \mathbf{X}_i^{(m)})$ and $T_M := \sum_m \Gamma_{h_M}(\mathbf{x}_i - \mathbf{X}_i^{(m)}) \mathbf{1}_{\{|\mathbf{X}_i^{(m)} - \mathbf{x}_i| > h_M R_M\}}$ (suppressing the Y -component, identical by the chart reduction),

$$\sum_{m=1}^M |\omega_{i,m}^{M, R_M} - \omega_{i,m}^{M, G}| = \frac{2T_M}{S_M}.$$

By Lemma 19 $S_M/M \rightarrow \pi_i > 0$; the Gaussian tail with $R_M \rightarrow \infty$ gives $T_M/M \rightarrow 0$. On the event of Proposition 20 the integrand is uniformly bounded by Lemma 15, whence

$$\sup_{(t,x) \in K} |\widehat{H}_i^{\varepsilon, M, R_M} - \widehat{H}_i^{\varepsilon, M, G}| \leq C_{J,B} \frac{2T_M}{S_M} \rightarrow 0.$$

The active-derivative case is identical: the differentiated integrand is Gaussian-dominated by Lemma 15 via the polynomial-prefactor absorption. \square

Compact-uniform drift convergence.

Proposition 23 (Compact-uniform drift convergence). *Under (S1)–(S4), the finite-entropy hypothesis (1), and $\varepsilon \in (0, \lambda_i^{\min,+})$ fixed, for every compact $K \Subset (t_i, t_{i+1}) \times (x_i + \mathcal{L}_i)$,*

$$\sup_{(t,x) \in K} |A_i^\varepsilon \nabla_x \log \widehat{H}_i^{\varepsilon, M, G}(t, x) - A_i^\varepsilon \nabla_x \log H_i^\varepsilon(t, x)| \rightarrow 0 \quad \text{in probability,}$$

and almost surely under (S5) for the truncated auxiliary estimator.

Proof. Write $\widehat{H} := \widehat{H}_i^{\varepsilon, M, G}$ and $H := H_i^\varepsilon$. Strict positivity of H on K gives $\inf_K H \geq \delta_K > 0$; by Proposition 22, $\widehat{H} \rightarrow H$ and $D_{q_{i,j}} \widehat{H} \rightarrow D_{q_{i,j}} H$ uniformly on K , so $\inf_K \widehat{H} \geq \delta_K/2$ for all large M in the stated stochastic mode. The identity

$$\begin{aligned} D_{q_{i,j}} \log \widehat{H} - D_{q_{i,j}} \log H &= \frac{D_{q_{i,j}} \widehat{H} - D_{q_{i,j}} H}{\widehat{H}} + D_{q_{i,j}} H \left(\frac{1}{\widehat{H}} - \frac{1}{H} \right), \\ \left| \frac{1}{\widehat{H}} - \frac{1}{H} \right| &\leq \frac{2}{\delta_K^2} |\widehat{H} - H|, \end{aligned}$$

combined with the uniform compact-uniform convergence of both \widehat{H} and $D_{q_{i,j}} \widehat{H}$ and with smoothness of H on the open cylinder, gives $\sup_K |D_{q_{i,j}} \log \widehat{H} - D_{q_{i,j}} \log H| \rightarrow 0$. Summing the spectral-floor expansion $A_i^\varepsilon \nabla_x \log H = \sum_j \max(\lambda_{i,j}, \varepsilon) D_{q_{i,j}} \log H_{q_{i,j}}$ with deterministically bounded coefficients $\max(\lambda_{i,j}, \varepsilon) \leq \|A_i\| + \varepsilon$ yields the claim. \square

By Proposition 12, the regularised drift converges to the exact leafwise drift on every compact $K \Subset (t_i, t_{i+1}) \times (x_i + \mathcal{L}_i)$ as $\varepsilon \downarrow 0$: $A_i^\varepsilon \nabla_x \log H_i^\varepsilon \rightarrow b_i^*$. A diagonal extraction in $(\varepsilon_n, M_n, h_{M_n})$ combines this with Proposition 23 to give the compact-uniform drift convergence of part (i) of Theorem 10.

A.5 Transition-kernel convergence via endpoint laws

For the transition-kernel statement of part (ii) of Theorem 10, weak convergence of the empirical conditional endpoint law is proved directly via Nadaraya–Watson consistency and transferred to the induced intervalwise kernel by continuity of the frozen Gaussian bridge.

Let

$$\widehat{\eta}_i^M(\cdot) := \sum_{m=1}^M \omega_{i,m}^{M,G}(\mathbf{x}_i, y_{i+1}) \delta_{\Delta X_{i+1}^{(m)}}$$

be the weighted empirical law of the next-interval increment induced by the Gaussian Nadaraya–Watson weights.

Proposition 24 (Weak convergence of the empirical endpoint law). *Assume (S1)–(S4). For every bounded continuous $\phi : \mathbb{R}^d \rightarrow \mathbb{R}$,*

$$\int_{\mathbb{R}^d} \phi(\delta) \widehat{\eta}_i^M(d\delta) \longrightarrow \int_{\mathbb{R}^d} \phi(\delta) \eta_i^\mu(d\delta) \quad \text{in probability.}$$

Hence $\widehat{\eta}_i^M(\cdot) \Rightarrow \eta_i^\mu(\cdot)$ weakly on \mathbb{R}^d , in probability. For compactly supported auxiliary weights, the same conclusion holds almost surely under (S5).

Proof. For $\phi \in C_b(\mathbb{R}^d)$, the regression function $(\boldsymbol{\xi}_i, y) \mapsto \mathbb{E}_\mu[\phi(\Delta X_{i+1}) \mid \mathbf{X}_i = \boldsymbol{\xi}_i, Y = y]$ is continuous on C_i by (S2). Standard NW consistency for Gaussian kernels under (S4) and Lemma 19 give the claimed convergence (a.s. under (S5)); weakness follows since the test class $C_b(\mathbb{R}^d)$ determines weak convergence. \square

For each augmented conditioning $(\boldsymbol{\xi}_i, y) \in C_i$ and each endpoint $z \in \mathcal{L}_i^{\boldsymbol{\xi}_i, y}$, let $R_i^{\boldsymbol{\xi}_i, y, y_i, z}$ denote the law on path space $C([t_i, t_{i+1}]; \mathbb{R}^d)$ of the frozen Gaussian bridge associated with $A_i(\boldsymbol{\xi}_i, y)$, from y_i at time t_i to z at time t_{i+1} . The map $(\boldsymbol{\xi}_i, y, z) \mapsto R_i^{\boldsymbol{\xi}_i, y, y_i, z}$ is continuous on the compatible endpoint set $\{(\boldsymbol{\xi}_i, y, z) : (\boldsymbol{\xi}_i, y) \in C_i, z \in \mathcal{L}_i^{\boldsymbol{\xi}_i, y}\}$, by joint continuity of the frozen Gaussian bridge in its conditioning, initial endpoint, and terminal endpoint.

The empirical path kernel induced by the Gaussian Nadaraya–Watson weights is the sample-conditioned bridge mixture

$$\widehat{\mathcal{K}}_i^M(\cdot) := \sum_{m=1}^M \omega_{i,m}^{M,G}(\mathbf{x}_i, y_{i+1}) R_i^{\mathbf{X}_i^{(m)}, Y^{(m)}, X_{t_i}^{(m)}, \Delta X_{i+1}^{(m)}}, \quad (54)$$

and the target intervalwise path kernel is

$$\mathcal{K}_i^*(\cdot) := \int_{\mathbb{R}^d} R_i^{\mathbf{x}_i, y_{i+1}, x_i, x_i + \delta}(\cdot) \eta_i^\mu(d\delta),$$

the integration ranging over the realised next-interval increment δ so that $x_i + \delta \in \mathcal{L}_i \eta_i^\mu$ -a.s. The intervalwise transition kernel $\widehat{K}_i^M(t, \mathbf{x}_i, y_{i+1}; \cdot)$ at intermediate time $t \in [t_i, t_{i+1}]$ is the time- t marginal of $\widehat{\mathcal{K}}_i^M$, and similarly for K_i^* .

Lemma 25 (Bridge-mixture continuity and sample/runtime equivalence). *For every $\Phi \in C_b(C([t_i, t_{i+1}]; \mathbb{R}^d))$, the scalar response*

$$\Psi_\Phi(\boldsymbol{\xi}_i, y, \delta) := \int \Phi(\omega) R_i^{\boldsymbol{\xi}_i, y, \boldsymbol{\xi}_i, \boldsymbol{\xi}_i + \delta}(d\omega)$$

is bounded by $\|\Phi\|_\infty$ and jointly continuous in $(\boldsymbol{\xi}_i, y, \delta)$ on the compatible increment set, by continuity of A_i on the regular set and weak continuity of the frozen Gaussian bridge in its endpoints. Consequently:

(a) (Bridge-mixture continuity.) *If $\eta_n \Rightarrow \eta_\infty$ on \mathbb{R}^d , then*

$$\int R_i^{\mathbf{x}_i, y_{i+1}, \mathbf{x}_i, \mathbf{x}_i + \delta} \eta_n(d\delta) \Rightarrow \int R_i^{\mathbf{x}_i, y_{i+1}, \mathbf{x}_i, \mathbf{x}_i + \delta} \eta_\infty(d\delta)$$

on $C([t_i, t_{i+1}]; \mathbb{R}^d)$.

(b) (Sample/runtime equivalence.) *On any sample cloud with $(\mathbf{X}_i^{(m)}, Y^{(m)}) \rightarrow (\mathbf{x}_i, y_{i+1})$ (in particular the localised cloud*

$$\{m : |(\mathbf{X}_i^{(m)}, Y^{(m)}) - (\mathbf{x}_i, y_{i+1})| \leq h_M R_M\}, \quad h_M R_M \rightarrow 0),$$

$$\Psi_\Phi(\mathbf{X}_i^{(m)}, Y^{(m)}, \Delta X_{i+1}^{(m)}) - \Psi_\Phi(\mathbf{x}_i, y_{i+1}, \Delta X_{i+1}^{(m)}) \rightarrow 0$$

uniformly in m , and the regression function

$$(\boldsymbol{\xi}_i, y) \mapsto \mathbb{E}_\mu[\Psi_\Phi(\boldsymbol{\xi}_i, y, \Delta X_{i+1}) \mid \mathbf{X}_i = \boldsymbol{\xi}_i, Y = y]$$

is continuous at (\mathbf{x}_i, y_{i+1}) by (S2) and dominated convergence.

Proposition 26 (Weak convergence of transition kernels). *Assume (S1)–(S4). For every bounded continuous functional $\Phi : C([t_i, t_{i+1}]; \mathbb{R}^d) \rightarrow \mathbb{R}$,*

$$\int \Phi d\widehat{\mathcal{K}}_i^M(\cdot) \rightarrow \int \Phi d\mathcal{K}_i^*(\cdot) \quad \text{in probability.}$$

In particular, for every intermediate time $t \in [t_i, t_{i+1}]$ and every bounded continuous $\varphi : \mathbb{R}^d \rightarrow \mathbb{R}$,

$$\int_{\mathbb{R}^d} \varphi(y) \widehat{K}_i^M(t, \mathbf{x}_i; dy) \rightarrow \int_{\mathbb{R}^d} \varphi(y) K_i^*(t, \mathbf{x}_i; dy) \quad \text{in probability.}$$

For compactly supported auxiliary weights, the same conclusion holds almost surely under (S5).

Proof. For $\Phi \in C_b(C([t_i, t_{i+1}]; \mathbb{R}^d))$, by (54) and Lemma 25,

$$\int \Phi d\widehat{\mathcal{K}}_i^M = \sum_{m=1}^M \omega_{i,m}^{M,G}(\mathbf{x}_i, y_{i+1}) \Psi_\Phi(\mathbf{X}_i^{(m)}, Y^{(m)}, \Delta X_{i+1}^{(m)})$$

is the NW estimator on the augmented past of $\mathbb{E}_\mu[\Psi_\Phi(\mathbf{X}_i, Y, \Delta X_{i+1}) \mid \mathbf{X}_i = \mathbf{x}_i, Y = y_{i+1}]$. The regression function is continuous at (\mathbf{x}_i, y_{i+1}) (Lemma 25(b)), Ψ_Φ is bounded, and Lemma 19 gives denominator non-degeneracy; standard NW consistency under (S4) (a.s. under (S5)) yields convergence to $\int \Psi_\Phi(\mathbf{x}_i, y_{i+1}, \delta) \eta_i^\mu(d\delta) = \int \Phi d\mathcal{K}_i^*$. The marginal statement is the case $\Phi(\omega) := \varphi(\omega_t)$. \square

A.6 Initial-boundary drift and diagonal consistency

The interior arguments above give convergence on compacta $K \Subset (t_i, t_{i+1}) \times (x_i + \mathcal{L}_i)$ of the open cylinder, where the strict time gap $\alpha < \beta$ provides the Gaussian-ratio domination of Lemma 15. At the initial diagonal point (t_i, x_i) , $\alpha \uparrow \beta$, the exponential penalisation disappears, and the response becomes the unbounded increment ΔX_{i+1} ; we collect here the dominated- and Donsker–Varadhan-based arguments needed at the boundary. Set $\alpha := t_{i+1} - t$, $\beta := t_{i+1} - t_i$. The leafwise kernel ratio at $x = x_i$ reduces to $\Phi_i^*(t, x_i, \delta) = (\beta/\alpha)^{r_i/2} \exp(-\frac{1}{2}(\frac{1}{\alpha} - \frac{1}{\beta})\|\delta\|_{A_i^+}^2)$ for $\delta \in \mathcal{L}_i$.

Lemma 27 (Analytic boundary drift). *For every conditioning point u_0 at which the conditional entropy $H(\eta_i^\mu(\cdot \mid u_0) \mid k_i^R(\cdot \mid u_0))$ is finite — the full μ_i -measure set provided by disintegration (52) of the global finite-entropy assumption (1) — and for every $\varepsilon \in (0, \lambda_i^{\min,+})$,*

$$\lim_{t \downarrow t_i} b_i^\varepsilon(t, x_i; u_0) = \frac{1}{t_{i+1} - t_i} \mathbb{E}_\mu[\Delta X_{i+1} \mid \mathbf{U}_i = u_0] =: b_i^*(t_i, x_i; u_0),$$

and the limit is independent of ε . No local admissibility assumption (S6) is needed for this analytic step.

Proof. Differentiating the coherent ratio at $x = x_i$ gives the kernel-ratio average

$$b_i^\varepsilon(t, x_i; u_0) = \frac{1}{\alpha} \frac{\int \delta \Phi_i^*(t, x_i, \delta) \eta_i^\mu(d\delta \mid u_0)}{\int \Phi_i^*(t, x_i, \delta) \eta_i^\mu(d\delta \mid u_0)}.$$

For $\alpha \in [\beta/2, \beta]$ the gap $\frac{1}{\alpha} - \frac{1}{\beta} \geq 0$, the exponential is bounded by 1 and the prefactor by $2^{r_i/2}$; hence $\Phi_i^*(t, x_i, \delta) \leq 2^{r_i/2}$ uniformly in (t, δ) and

$\Phi_i^*(t, x_i, \delta) \rightarrow 1$ pointwise as $\alpha \uparrow \beta$ (the convergence is *not* monotone: only pointwise plus dominated convergence is used). The denominator tends to 1.

The numerator requires an $\eta_i^\mu(\cdot | u_0)$ -integrable dominant for $|\delta|$. Since $\eta_i^\mu(\cdot | u_0)$ is supported on the active leaf $\mathcal{L}_i(u_0)$ of $A_i(u_0)$ (Corollary 7), it suffices to control $|\delta|$ on that leaf. By the Donsker–Varadhan variational inequality applied to the intrinsic Mahalanobis quadratic test against the reference $k_i^R(\cdot | u_0)$, finite conditional entropy at u_0 implies the *intrinsic* A_i^+ -Mahalanobis first moment on the active leaf

$$\int_{\mathcal{L}_i(u_0)} |\delta|_{C_i(u_0)^+} \eta_i^\mu(d\delta | u_0) < \infty, \quad C_i(u_0) := \Delta_i A_i(u_0).$$

The Euclidean implication uses the leaf inequality

$$|\delta| \leq \lambda_{\max}(A_i(u_0))^{1/2} |\delta|_{C_i(u_0)^+} \quad \forall \delta \in \mathcal{L}_i(u_0),$$

which gives $\int |\delta| \eta_i^\mu(d\delta | u_0) < \infty$. Hence $2^{r_i/2} |\delta|$ is an integrable dominant; dominated convergence and $\alpha \rightarrow \beta$ yield $b_i^\varepsilon(t, x_i; u_0) \rightarrow \beta^{-1} \int \delta \eta_i^\mu(d\delta | u_0)$. The argument is ε -independent: on the leaf Φ_i^* is the unfloored leafwise ratio. \square

Lemma 28 (Compact reference-aware boundary drift). *Under (S1)–(S6), with the compact choice $W_h(u_0, v) = K(d_\varepsilon^\ell(u_0, v)/h)$ and $\text{supp } K \subset [0, 1]$, the empirical regularised boundary drift admits the finite-sample limit*

$$\begin{aligned} \widehat{b}_i^{M,K}(t_i, x_i) &:= \lim_{t \downarrow t_i} \widehat{b}_i^{\varepsilon, M, K}(t, x_i) \\ &= \frac{1}{\beta} \frac{\sum_{m=1}^M W_{h_M}(u_0, \mathbf{U}_i^{(m)}) \Delta X_{i+1}^{(m)}}{\sum_{m=1}^M W_{h_M}(u_0, \mathbf{U}_i^{(m)})}, \quad \beta = t_{i+1} - t_i, \end{aligned}$$

independent of ε , and $\widehat{b}_i^{M,K}(t_i, x_i) \rightarrow b_i^*(t_i, x_i; u_0)$ in probability; a.s. under (S5).

Proof. Diagonal limit. As $t \downarrow t_i$, $\Phi_i^\varepsilon(t, x_i, \delta) \rightarrow 1$ uniformly in the sample increments (dominated by $2^{r_i/2}$; cf. Lemma 27); the Φ_i^ε factors cancel between numerator and denominator, leaving the NW estimator of ΔX_{i+1} at u_0 with kernel W_{h_M} . *Denominator non-collapse.* Lemma 13 gives $MD_{h_M}(u_0) \rightarrow \infty$ and concentration of $W_{h_M}(u_0, \cdot)/D_{h_M}(u_0)$ at u_0 . *Local uniform integrability.* On the compact support $\{d_\varepsilon(u_0, v) \leq h_M\}$, in particular $d_{\text{ref}, \varepsilon}^\ell(u_0, v) \leq h_M$, and Lemma 14 gives $\kappa_\varepsilon^\ell(u_0, \cdot) \leq e^{h_M/2}$; together with (S6) and Donsker–Varadhan ((44)–(46)), this yields local uniform integrability of ΔX_{i+1} under

the normalised kernel measure. *Numerator.* Continuity of $v \mapsto \int \delta \eta_i^\mu(d\delta | v)$ at u_0 (from (S2)) plus the uniform integrability above give NW consistency of the numerator. *Conclusion.* The ratio converges to $\beta^{-1} \int \delta \eta_i^\mu(d\delta | u_0) = b_i^*(t_i, x_i; u_0)$. \square

Lemma 29 (Gaussian reference-aware boundary drift). *Under (S1)–(S6), with the Gaussian choice $W_h(u_0, v) = \exp(-d_\varepsilon^\ell(u_0, v)^2/(2h^2))$, the empirical boundary drift satisfies*

$$\widehat{b}_i^{M,G}(t_i, x_i) := \lim_{t \downarrow t_i} \widehat{b}_i^{\varepsilon, M, G}(t, x_i) \longrightarrow b_i^*(t_i, x_i; u_0) \quad \text{in probability,}$$

a.s. under (S5).

Proof. The diagonal limit and the cancellation of the Φ_i^ε factors are as in Lemma 28, leaving the Gaussian NW estimator with product kernel W_{h_M} and reference factor $\Gamma_h^{\text{ref}}(u_0, v) = \exp(-r(u_0, v)^2/(2h^2))$, $r(u_0, v) := d_{\text{ref}, \varepsilon}^\ell(u_0, v)$.

Reference factor absorbs the comparison factor. The growth of $\kappa_\varepsilon^\ell(u_0, v)^2 \leq e^{r(u_0, v)}$ is uniformly absorbed by the Gaussian penalty:

$$\Gamma_h^{\text{ref}}(u_0, v) \kappa_\varepsilon^\ell(u_0, v)^2 \leq \exp\left(-\frac{r(u_0, v)^2}{2h^2} + r(u_0, v)\right) \leq \exp\left(\frac{h^2}{2}\right), \quad (55)$$

by maximising the exponent over $r \geq 0$. Hence the reference factor times the comparison factor is uniformly bounded by $\exp(h_M^2/2) \rightarrow 1$.

Normalised kernel concentration. The normalised localiser $\nu_h^{u_0}(dv) := W_h(u_0, v) \mu_U(dv)/D_h(u_0)$ concentrates at u_0 by Lemma 13: for every $\rho > 0$, $\nu_h^{u_0}(\{d_\varepsilon > \rho\}) \rightarrow 0$ as $h \downarrow 0$.

Inner region $\{d_\varepsilon(u_0, v) \leq \rho\}$. For ρ small enough this is contained in the (S6)-neighbourhood $C_\rho(u_0)$; Donsker–Varadhan gives (45), a uniform first-moment bound in the runtime/query Mahalanobis norm $|\cdot|_{C_{i, \varepsilon}^\ell(u_0)}^{-1}$, and the Euclidean implication on the active leaf is (46). The NW numerator restricted to this region is thus uniformly integrable against $\nu_h^{u_0}$ and converges by weak continuity of $v \mapsto \int \delta \eta_i^\mu(d\delta | v)$ at u_0 to $\int \delta \eta_i^\mu(d\delta | u_0)$.

Outer region $\{d_\varepsilon(u_0, v) > \rho\}$: direct exponential tail. The integrand in the numerator is dominated by $\kappa_\varepsilon^\ell(u_0, v) m_{\text{intr}}(v)$ with $m_{\text{intr}}(v) := \int |\delta|_{C_i^\ell(v)+} \eta_i^\mu(d\delta | v)$. Using $d_{\text{ref}, \varepsilon}^\ell(u_0, v) \leq d_\varepsilon(u_0, v)$ and the reference-comparison estimate (48),

$$W_h(u_0, v) \kappa_\varepsilon^\ell(u_0, v) \lesssim \exp\left(-\frac{d_\varepsilon(u_0, v)^2}{2h^2} + \frac{1}{2}d_\varepsilon(u_0, v)\right) \leq \exp\left(-\frac{\rho^2}{4h^2}\right) \quad \text{on } \{d_\varepsilon > \rho\},$$

for h small enough that $\frac{d_\varepsilon^2}{2h^2} - \frac{1}{2}d_\varepsilon \geq \frac{d_\varepsilon^2}{4h^2}$ when $d_\varepsilon > \rho$. The intrinsic moment is globally integrable under μ_U :

$$\int m_{\text{intr}}(v) \mu_U(dv) = \mathbb{E}_\mu \left[\int |\delta|_{C_i(U_i)+} \eta_i^\mu(d\delta | U_i) \right] < \infty, \quad (56)$$

since under the conditioned reference $k_i^R(\cdot | v)$ the intrinsic Mahalanobis norm $|\delta|_{C_i^\ell(v)^+}$ has uniform-in- v exponential moments by construction, and finite global entropy (1) transfers these moments via Donsker–Varadhan to η_i^μ with a global bound. Combining with the denominator lower bound $D_h(u_0) \gtrsim h^{q_{\text{eff}}}$ of Lemma 13,

$$\begin{aligned} \frac{\int_{\{d_\varepsilon > \rho\}} W_h(u_0, v) \kappa_\varepsilon^\ell(u_0, v) m_{\text{intr}}(v) \mu_U(dv)}{D_h(u_0)} &\leq \frac{\exp(-\rho^2/(4h^2))}{c h^{q_{\text{eff}}}} \int m_{\text{intr}} d\mu_U \longrightarrow 0 \end{aligned}$$

as $h \downarrow 0$. The outer contribution to the NW numerator therefore vanishes.

Conclusion. Adding the inner and outer estimates, the NW numerator converges to $\int \delta \eta_i^\mu(d\delta | u_0)$; the denominator stays bounded below by Lemma 13; the ratio tends to $b_i^*(t_i, x_i; u_0)$ in probability, a.s. under (S5). \square

The interior consistency of Proposition 23 together with Lemmas 27–29 gives convergence on every compact subset of the open intervalwise cylinder and at the single boundary diagonal point (t_i, x_i) , where the empirical boundary drift is defined as the finite-sample diagonal limit $\widehat{b}_i^M(t_i, x_i) := \lim_{t \downarrow t_i} \widehat{b}_i^{\varepsilon, M}(t, x_i)$.

A.7 Proof of the main statistical convergence theorem

Proof of Theorem 10. Fix i , the query $u_0 = (\mathbf{x}_i, y_{i+1})$, and a compact $K \Subset (t_i, t_{i+1}) \times (x_i + \mathcal{L}_i)$ in the backward stratum $\{t \leq t_{i+1} - \tau\}$.

Interior drift convergence (part (i)). Under (S1)–(S5), decompose

$$A_i^\varepsilon \nabla_x \log \widehat{H}_i^{\varepsilon, M, G} \xrightarrow{M \rightarrow \infty} A_i^\varepsilon \nabla_x \log H_i^\varepsilon \xrightarrow{\varepsilon \downarrow 0} A_i \nabla_x \log H_i = b_i^*, \quad (57)$$

the first arrow by Proposition 23 (statistical step at fixed ε), the second by Proposition 12 (analytical step in ε). Picking any $\varepsilon_n \downarrow 0$, Proposition 22 at each ε_n provides $M_n \rightarrow \infty$ and admissible $h_{M_n} \downarrow 0$ with compact-uniform $\frac{1}{n}$ -control of $\widehat{H}_i^{(n)}$ and its active gradient in the stated stochastic mode; composing the two arrows in (57) gives $\sup_K |\widehat{b}_i^{(n)} - b_i^*| \rightarrow 0$ in probability (a.s. under (S5)). The strict interior $\alpha < \beta$ gap furnishes the Gaussian-ratio domination of Lemma 15 and no boundary admissibility is invoked.

Boundary-diagonal drift convergence (part (ii)). Under (S1)–(S6), the diagonal-limit value at (t_i, x_i) is supplied directly by the boundary Section A.6: the analytic limit by Lemma 27 (which uses only finite conditional

entropy at u_0 , automatic from disintegration (52) for μ_i -a.e. u_0), and the empirical limit by either Lemma 28 (compact-kernel regression) or Lemma 29 (Gaussian-kernel regression), both using (S6) for the local entropy admissibility and (S1) for the small-ball denominator non-collapse via Lemma 13. Both deliver $\widehat{b}_i^{(n)}(t_i, x_i) \rightarrow b_i^*(t_i, x_i; u_0)$ in probability, a.s. under (S5), with the empirical boundary drift defined as the finite-sample diagonal limit $\widehat{b}_i^{(n)}(t_i, x_i) := \lim_{t \downarrow t_i} \widehat{b}_i^{\varepsilon_n, M_n}(t, x_i)$.

Transition-kernel convergence (part (iii)). Under (S1)–(S5), Proposition 26 at the diagonal triple $(\varepsilon_n, M_n, h_{M_n})$ gives, for every $t \in [t_i, t_{i+1}]$ and every $\varphi \in C_b(\mathbb{R}^d)$, $\int \varphi d\widehat{K}_i^{(n)}(t, u_0; \cdot) \rightarrow \int \varphi dK_i^*(t, u_0; \cdot)$ in probability: the asserted weak convergence of transition kernels. \square

Remark 30 (Uniformity with respect to the conditioning point). *If (\mathbf{x}_i, y_{i+1}) ranges in a compact set $C \subseteq C_i$ where π_i is bounded away from 0 and the eigenstructure of A_i is continuous, the Gaussian-domination constants of Lemma 15 can be chosen uniformly in $(\mathbf{x}_i, y_{i+1}) \in C$, and the same diagonal triple $(\varepsilon_n, M_n, h_{M_n})$ delivers the conclusions of Theorem 10 uniformly on C .*

Remark 31 (Reference-weighted Hilbert structure). *The natural global Hilbert structure on the active subspace \mathcal{L}_i of increments is not $L^2(\mathcal{L}_i, dl_i)$ but the reference-weighted space $L^2(k_i^R)$ with $k_i^R(d\delta) := p_i(t_i, x_i; t_{i+1}, \delta) dl_i(\delta)$: if $f_i \in L^2(k_i^R)$, the backward reference semigroup is contractive in the corresponding norm, and Gaussian smoothing gives active-gradient estimates in the same weighted spaces on compact subintervals of (t_i, t_{i+1}) . The consistency theorem above does not rely on this stronger global integrability: it uses only compact convergence for the heat drift and weak convergence of the transition kernels.*

B Predictive validation: energy score and conditional kernel score

This appendix describes the predictive validation score used to select and compare model configurations. The score is designed to test the conditional predictive law generated by the model. The model is first given a real past trajectory as memory; it then generates several possible future continuations, which are compared with the realised future of the validation path.

Let

$$Z_1, \dots, Z_n \in \mathbb{R}^q$$

be the validation path in the coordinates used by the model. In the white-only case one may simply take $Z_i = X_i$. In a joint state-volatility model, Z_i may instead denote the same-grid joint state, for instance

$$Z_i = (X_i, Y_i),$$

where Y_i is the volatility-factor state. The definition below is independent of this choice.

Fix a memory length $p_{\text{mem}} \geq 1$, a predictive horizon $K \geq 1$, a number $L \geq 1$ of Monte Carlo predictive continuations, and a validation stride $s \geq 1$. For every admissible validation index i , define the real memory block

$$\mathcal{H}_i := (Z_{i-p_{\text{mem}}+1}, \dots, Z_i) \in (\mathbb{R}^q)^{p_{\text{mem}}},$$

and the realised future block

$$Z_{i+1:i+K} := (Z_{i+1}, \dots, Z_{i+K}) \in (\mathbb{R}^q)^K.$$

We identify the future block with its time-major vectorisation

$$z_i^{\text{obs}} := \text{vec}_{\text{time}}(Z_{i+1}, \dots, Z_{i+K}) \in \mathbb{R}^{Kq}.$$

Conditionally on the real memory \mathcal{H}_i , the fitted generative model produces L independent predictive continuations

$$\widehat{Z}_{i,1:K}^{(\ell)} = (\widehat{Z}_{i,1}^{(\ell)}, \dots, \widehat{Z}_{i,K}^{(\ell)}), \quad \ell = 1, \dots, L.$$

For $K > 1$, the continuation is generated autoregressively. After each generated step, the model memory is shifted and the generated value is inserted as the newest state. Equivalently, setting

$$\widehat{\mathcal{H}}_{i,0}^{(\ell)} := \mathcal{H}_i,$$

one samples recursively

$$\widehat{Z}_{i,r}^{(\ell)} \sim \widehat{P}_{\theta}(\cdot \mid \widehat{\mathcal{H}}_{i,r-1}^{(\ell)}), \quad r = 1, \dots, K,$$

and then updates

$$\widehat{\mathcal{H}}_{i,r}^{(\ell)} = \text{shift}(\widehat{\mathcal{H}}_{i,r-1}^{(\ell)}, \widehat{Z}_{i,r}^{(\ell)}).$$

We again use the time-major vectorisation

$$\widehat{z}_i^{(\ell)} := \text{vec}_{\text{time}}(\widehat{Z}_{i,1}^{(\ell)}, \dots, \widehat{Z}_{i,K}^{(\ell)}) \in \mathbb{R}^{Kq}.$$

Energy score and aggregation

The per-window score is the multivariate energy score

$$\widehat{\text{ES}}_i := \frac{1}{L} \sum_{\ell=1}^L \|\widehat{z}_i^{(\ell)} - z_i^{\text{obs}}\| - \frac{1}{2L^2} \sum_{\ell=1}^L \sum_{\ell'=1}^L \|\widehat{z}_i^{(\ell)} - \widehat{z}_i^{(\ell')}\|, \quad (58)$$

and the global score is the empirical mean over admissible validation windows \mathcal{I} :

$$\widehat{\text{ES}} := \frac{1}{|\mathcal{I}|} \sum_{i \in \mathcal{I}} \widehat{\text{ES}}_i. \quad (59)$$

Conditional transition-kernel score

The energy score (58)–(59) tests the *global* generative quality of the model on increments. We complement it with a Gaussian-kernel score that targets a different object: the quality of the approximation of the *conditional* transition kernel itself, $K_i^\mu(u, \cdot) := \mathcal{L}_\mu(\Delta X_{i+1} \mid \mathbf{U}_i = u)$, of which $\widehat{K}_i^{(n)}(u, \cdot)$ is the NW estimator of Theorem 10. The two scores play complementary roles: the energy score evaluates marginal/aggregate generative fit, the conditional kernel score evaluates the statistical operator that the method estimates.

Given a conditioning query u_q from the validation set, let

$$\widehat{K}_i^{\text{train}}(u_q, \cdot) := \sum_{m=1}^M w_m(u_q) \delta_{Z_m}$$

denote the empirical transition kernel produced by the runtime regression weights $w_m(u_q) := \omega_{i,m}^{M,G}(u_q)$ of Section 4.3 on the training set, $Z_m := \Delta X_{i+1}^{(m)}$ being the future increment associated with the m -th training sample. Let z_q denote the realised validation increment at u_q . The Gaussian-kernel conditional score at u_q is

$$S_k(u_q, z_q) := \sum_{m,\ell=1}^M w_m(u_q) w_\ell(u_q) k(Z_m, Z_\ell) - 2 \sum_{m=1}^M w_m(u_q) k(Z_m, z_q), \quad (60)$$

with characteristic Gaussian kernel

$$k(a, b) := \exp\left(-\frac{|S^{-1}(a-b)|^2}{2\sigma_k^2}\right), \quad (61)$$

S the normalisation operator on the increment coordinates and $\sigma_k > 0$ a kernel bandwidth. The global validation score is the robust upper quantile over a validation query set \mathcal{Q} ,

$$\mathcal{S}_k^{(\alpha)} := \text{Quantile}_\alpha \{S_k(u_q, z_q) : u_q \in \mathcal{Q}\}, \quad \alpha \in (0, 1), \quad (62)$$

typically $\alpha = 0.9$. $S_k(u_q, z_q)$ is a kernel discrepancy between $\widehat{K}_i^{\text{train}}(u_q, \cdot)$ and the realised validation transition; the characteristic Gaussian kernel metrises weak convergence of probability measures, so the score provides a practical validation criterion for the statistical approximation of the conditional transition operator itself.

Enriched score for coupled (X, Y) validation

For coupled validation we use the same global score template applied to features that combine positions with a packed squared-increment descriptor. Let $K \geq 1$ be the predictive horizon as above and let $\Delta_r^{\otimes 2} X \in \mathbb{R}^{d_X^2}$ denote the time- r packed squared-increment block, i.e. the vectorisation of $\Delta X_r \Delta X_r^\top$. Define a per-step feature

$$\phi_r(X) := \begin{pmatrix} X_r \\ [\Delta^{\otimes 2} X]_r \end{pmatrix} \in \mathbb{R}^{d_X + d_{\text{inc}, X}}, \quad d_{\text{inc}, X} := d_X^2,$$

with an analogous definition for Y . Stack-rescale by component standard deviations

$$\phi_r(X) := \begin{pmatrix} (\sigma_{\text{pos}} \sqrt{d_X})^{-1} X_r \\ (\sigma_{\text{inc}} \sqrt{d_{\text{inc}}})^{-1} [\Delta^{\otimes 2} X]_r \end{pmatrix} \in \mathbb{R}^{d_X + d_{\text{inc}}},$$

where σ_{pos} and σ_{inc} are the root-mean-square standard deviations of, respectively, the position components and the packed squared-increment components over the training set. The coupled enriched comparison vector is

$$\tilde{z}_i := \text{vec}_{\text{time}} \left([\phi_r(X), \phi_r(Y)]_{r=1, \dots, K} \right) \in \mathbb{R}^{K(d_X + d_{\text{inc}, X} + d_Y + d_{\text{inc}, Y})},$$

and the enriched global score $\widehat{\text{ES}}_{\text{enriched}}$ is obtained by substituting \tilde{z}_i and $\tilde{z}_i^{(\ell)}$ for z_i^{obs} and $\hat{z}_i^{(\ell)}$ in (58)–(59).

C Entropic reference selection and validation

The construction of Sections 3.2 and 5.4 requires, at each latent level, a reference family under which the data-generating law has finite relative entropy on every coarse interval. We use a single finite-sample surrogate of that condition in two roles: selecting a reference family for a given latent level, and validating the closed-loop emission of the level.

Per-step empirical Gaussian negative log-likelihood. Fix a coarse step $[t, t + \Delta t]$ and consider, at the relevant latent level, a candidate zero-mean Gaussian reference for the level’s state increment $\Delta\zeta_t \in \mathbb{R}^d$,

$$R_{\Sigma, \Delta t}(d\zeta) = \mathcal{N}(0, \Sigma \Delta t)(d\zeta), \quad \Sigma \in \text{Sym}_d^+,$$

with density $r_{\Sigma, \Delta t}$: the entropic surrogate is evaluated against the local-martingale part of the reference, whose drift is identically zero. Given an observed increment $\Delta\zeta_{p,t}^{\text{obs}}$ on a training path p , the per-step Gaussian negative log-likelihood under $R_{\Sigma, \Delta t}$ is

$$\begin{aligned} \mathcal{S}_t^{(p)}(\Sigma) &:= -\log r_{\Sigma, \Delta t}(\Delta\zeta_{p,t}^{\text{obs}}) \\ &= \frac{1}{2} \log \det(\Sigma \Delta t) + \frac{1}{2} (\Delta\zeta_{p,t}^{\text{obs}})^\top (\Sigma \Delta t)^{-1} \Delta\zeta_{p,t}^{\text{obs}} + \frac{d}{2} \log(2\pi). \end{aligned} \quad (63)$$

The first Σ -dependent term in (63) is the log-volume of the reference; the second is the squared Mahalanobis norm of the observed increment in the metric induced by Σ . The Σ -independent additive constant $\frac{d}{2} \log(2\pi)$ cancels in any comparison between candidates evaluated on the same $\Delta\zeta_{p,t}^{\text{obs}}$.

When the candidate family produces rank-deficient covariances by construction (for instance a directional rank-one parametrisation), (63) is evaluated on the spectrally floored covariance $\Sigma_t^{(f), \varepsilon}$ of (30), so the inverse exists and the perpendicular component of $\Delta\zeta_{p,t}^{\text{obs}}$ enters as the leaf-aware penalty $\frac{1}{2} \|\Delta\zeta_{p,t}^{\text{obs}, \perp}\|^2 / (\varepsilon \Delta t)$ discussed in Section 5.2. Comparison across families with different ranks accordingly uses the same ε -floor on all candidates.

Selecting a reference family for a latent level. Let $\{\Sigma_t^{(f)}\}_f$ be a finite family of candidate frozen reference trajectories indexed by a hyperparameter f (smoothing length, history window, rank constraint, parametric form). For each training path p , aggregate (63) along the path’s step set \mathcal{T}_p :

$$\bar{\mathcal{S}}_p(\Sigma^{(f)}) := \frac{1}{|\mathcal{T}_p|} \sum_{t \in \mathcal{T}_p} \mathcal{S}_t^{(p)}(\Sigma_t^{(f), \varepsilon}).$$

The selection rule is the cross-path q_α -quantile of these path-wise scores,

$$\hat{f} := \arg \min_f q_\alpha \left(\{\bar{\mathcal{S}}_p(\Sigma^{(f)})\}_p \right), \quad \alpha \in (0, 1), \quad (64)$$

typically with $\alpha = 0.9$. The quantile suppresses tail paths on which any candidate would be a poor description and orders families by how well their reference explains the bulk of the observed increments; no closed-loop generation is required at this stage.

Forward entropic validation of a generated latent level. For a held-out validation path p , let $\Sigma_{p,t}^{\text{gen}} \in \text{Sym}_d^+$ denote the closed-loop generation of the level on p , PSD-projected and spectrally floored at the common ε via (28)–(30). The per-path entropic-adherence score is the same NLL aggregate as for selection, applied now to the closed-loop generated reference,

$$\bar{\mathcal{S}}_p^{\text{val}}(\Sigma^{\text{gen}}) := \frac{1}{|\mathcal{T}_p|} \sum_{t \in \mathcal{T}_p} \mathcal{S}_t^{(p)}(\Sigma_{p,t}^{\text{gen},\varepsilon}), \quad (65)$$

the empirical Gaussian negative log-likelihood of the observed increment under the level’s own generated reference, averaged over the validation step set. The cross-path scalar score is the q_α -quantile of $\{\bar{\mathcal{S}}_p^{\text{val}}\}_p$, with the same α and the same ε -floor used at selection.

The two scores (64)–(65) share a single objective: the empirical entropy of the data-generating law under the level’s Gaussian model. Selection applies it to candidate frozen references, validation applies it to the closed-loop generated reference on held-out paths, and no intermediate proxy enters between the two stages.

References

- [1] Alexandre Alouadi, Baptiste Barreau, Laurent Carlier, and Huy en Pham. Robust time series generation via schr odinger bridge: a comprehensive evaluation. In *Proceedings of the 6th ACM International Conference on AI in Finance*, pages 906–914, 2025.
- [2] Alexandre Alouadi, Gr egoire Loeper, C elien Marsala, Othmane Mazhar, and Huy en Pham. SBBTS: A unified schr odinger-bass framework for synthetic financial time series, 2026.
- [3] Martin Arjovsky, Soumith Chintala, and L eon Bottou. Wasserstein generative adversarial networks. In *Proceedings of the 34th International Conference on Machine Learning*, volume 70, pages 214–223, 2017.
- [4] Valentin De Bortoli, James Thornton, Jeremy Heng, and Arnaud Doucet. Diffusion schr odinger bridge with applications to score-based generative modeling, 2021.
- [5] Hans B uhler, Blanka Horvath, Terry Lyons, Imanol Perez Arribas, and Ben Wood. A data-driven market simulator for small data environments, 2020.

- [6] Andrew Campbell, Valentin De Bortoli, Arnaud Doucet, and Yuyang Shi. Diffusion schrödinger bridge matching. In *Advances in Neural Information Processing Systems*, pages 62183–62223, 2023.
- [7] Yongxin Chen, Tryphon T. Georgiou, and Michele Pavon. Stochastic control liaisons: Richard sinkhorn meets gaspard monge on a schrödinger bridge. *SIAM Review*, 63(2):249–313, 2021.
- [8] Ilya Chevyrev and Andrey Kormilitzin. *A Primer on the Signature Method in Machine Learning*, pages 3–64. Springer Nature Switzerland, 2026.
- [9] Vedant Choudhary, Sebastian Jaimungal, and Maxime Bergeron. FuN-Vol: A multi-asset implied volatility market simulator using functional principal components and neural SDEs, 2023.
- [10] Wenquan Cui and Meng Wei. Strong consistency of kernel regression estimate. *Open Journal of Statistics*, 3:179–182, 2013.
- [11] Marco Cuturi. Sinkhorn distances: lightspeed computation of optimal transport. In *Proceedings of the 27th International Conference on Neural Information Processing Systems*, pages 2292–2300, 2013.
- [12] Paolo Da Pra. A stochastic control approach to reciprocal diffusion processes. *Applied Mathematics and Optimization*, 23(1):313–329, 1991.
- [13] Ian Goodfellow, Jean Pouget-Abadie, Mehdi Mirza, Bing Xu, David Warde-Farley, Sherjil Ozair, and Aaron Courville. Generative adversarial networks. *Advances in Neural Information Processing Systems*, 3, 2014.
- [14] Nikita Gushchin, Sergei Kholkin, Evgeny Burnaev, and Alexander Korotin. Light and optimal schrödinger bridge matching. In *Proceedings of the 41st International Conference on Machine Learning*, volume 235, pages 17100–17122, 2024.
- [15] Mohamed Hamdouche, Pierre Henry-Labordere, and Huyên Pham. Generative modeling for time series via schrödinger bridge. *arXiv*, 2023.
- [16] Jonathan Ho, Ajay Jain, and Pieter Abbeel. Denoising diffusion probabilistic models, 2020.
- [17] Danilo Jimenez Rezende and Shakir Mohamed. Variational inference with normalizing flows. In *Proceedings of the 32nd International Conference on Machine Learning*, pages 1530–1538, 2015.

- [18] Patrick Kidger, James Foster, Xuechen Li, Harald Oberhauser, and Terry Lyons. Neural SDEs as infinite-dimensional GANs. In *Proceedings of the 38th International Conference on Machine Learning*, volume 38, pages 5453–5463, 2021.
- [19] Diederik P Kingma and Max Welling. Auto-encoding variational bayes, 2013.
- [20] Christian Léonard. Girsanov theory under a finite entropy condition. *Lecture Notes in Mathematics – Springer-Verlag*, 2046, 2011.
- [21] Christian Léonard. A survey of the schrödinger problem and some of its connections with optimal transport, 2013.
- [22] Stefano De Marco, Huyên Pham, and Davide Zanni. Schrödinger bridges with jumps for time series generation, 2026.
- [23] Yang Song, Jascha Sohl-Dickstein, Diederik Kingma, Abhishek Kumar, Stefano Ermon, and Ben Poole. Score-based generative modeling through stochastic differential equations, 2020.
- [24] Magnus Wiese, Robert Knobloch, Ralf Korn, and Peter Kretschmer. Quant GANs: deep generation of financial time series. *Quantitative Finance*, 20:1–22, 2020.
- [25] Tianlin Xu, Li Wenliang, Michael Munn, and Beatrice Acciaio. COT-GAN: Generating sequential data via causal optimal transport, 2020.
- [26] Jinsung Yoon, Daniel Jarrett, and Mihaela Schaar. Time-series generative adversarial networks. In *Advances in Neural Information Processing Systems*, 2019.